IMPROVED NUMERICAL SIMULATION OF WORMHOLE PROPAGATION IN CARBONATE CORE DURING ACID STIMULATION

BY

LATEEF A. KAREEM

A Thesis Presented to the
DEANSHIP OF GRADUATE STUDIES

KING FAHD UNIVERSITY OF PETROLEUM & MINERALS
DHAHRAN, SAUDI ARABIA

In Partial Fulfillment of the
Requirements for the Degree of

MASTER OF SCIENCE

In

PETROLEUM ENGINEERING DEPARTMENT

MAY, 2013

KING FAHD UNIVERSITY OF PETROLEUM & MINERALS

DHAHRAN- 31261, SAUDI ARABIA

DEANSHIP OF GRADUATE STUDIES

This thesis, written by **Lateef A. Kareem** under the direction his thesis advisor and approved by his thesis committee, has been presented and accepted by the Dean of Graduate Studies, in partial fulfillment of the requirements for the degree of **MASTER OF SCIENCE IN PETROLEUM ENGINEERING.**

Dr. Abdullah S. Sultan
(Advisor)

18 JUL 2013
for

Dr. Abdullah S. Sultan
Department Chairman

Dr. Abeeb A. Awotunde
(Member)

Dr. Salam A. Zummo
Dean of Graduate Studies

Dr. Rajai Alassar
(Member)

21/7/13
Date

I dedicate this research work to my mum, my dad and my wife

ACKNOWLEDGMENTS

My profound gratitude goes to almighty Allah for the gift of life and thinking faculty. The immensity of support I got from my advisor Dr. Abdullah S, Sultan; committee members (Dr Abeeb A, Awotunde and Dr Rajai Alassar), in terms of guidance and patience cannot be over emphasized. They allow me to come up with my creativity and pull me through when I got stuck

I will like to extend my appreciation to Sarmad Zafar Khan Sherwani, Najmudeen Sibaweihi, Khaled Zidan, Hassaan Ahmed, Abdulafeez Adebiyi, Abiola Obembe and the rest of Nigerian Community at KFUPM for their supports.

Special thanks to my brother Muhammad Tajudeen Iwalewa who took the time to convince the admission committee, and to Dr. Darren Malekzadeh and Dr. Sidqi A. Abu-Khamsin who saw to it that I was admitted into the deanship program.

I cannot but thank King Fahd University of Petroleum and Minerals for providing the scholarship opportunity and Schlumberger for supporting this research work under the project CPM (2298).

Finally, I cannot thank my dad-Alh. Najeem A. Kareem, my mum-Mrs Rainat A. Kareem, my wife-Mrs Ojora A. Mardiyyat, and my brother-Muhammad Tajudeen Iwalewa enough for their patience, love and supports. They are the best.

TABLE OF CONTENTS

LIST OF TABLES

LIST OF FIGURES

ABSTRACT

Full Name : Lateef A. Kareem

Thesis Title : Improved Numerical Simulation of Wormhole Propagation in Carbonate Core during Acid Stimulation

Major Field : Petroleum Engineering

Date of Degree : May 2013

The ever-increasing global demand of oil and gas over the years has put engineers on their toes to continue to improve upon current oil and gas production technology. The need to improve productivity and maintain the reservoir energy for sustained long-term production led to the development of acid stimulation, acid fracturing and hydraulic fracturing technologies. Acid and hydraulic fracturing are used to alter the flow geometry and in so doing reduce the reservoir resistance to production of the formation fluid, while acid stimulation is used to improve the near wellbore permeability.

Acid stimulation in carbonate reservoir unlike sandstone results in the development of wormholes. These wormholes are highly conductive channels in the near wellbore region and helps in reducing the resistance of the near wellbore to fluid flow. Over the years, researchers have investigated the development, propagation and control of wormholes with the aim to minimize the cost and improve the effectiveness of acid stimulation process.

In this work, we developed an improved simulator for wormhole propagation in carbonate core during acid stimulation. The objective was to use the physics of the flow in porous media, chemistry of HCl-Carbonate interaction and porosity-permeability variation relation for carbonate reservoir in the simulation of wormholes. We redesigned

the convection-advection-reaction equation in porous medium to accommodate changes in porosity and permeability during the stimulation treatment and introduce a new resistance-weighting scheme for numerical evaluation of velocity field from pressure fields.

Using the simulator so developed, we simulated acidization of core 15 and 12 (diameter 1.5 inches and length 2.4 inches). We reproduced the acidization curve for injection rates between 0.5cc/min and 10cc/min. We were observed that changes in the local acid molecule transfer rate results in shift in the acidization curve. Finally, we found that initial permeability of the core also affects the amount of pore volume of acid injected to breakthrough.

ملخص الرسالة

الاسم الكامل: لطيف أدلولي كريم

عنوان الرسالة: نموذج محسن للمحاكاة الرقمية للقنوات الدودية خلال عملية تحفيز الصخور الكربونية باستخدام الأحماض

التخصص: هندسة البترول

تاريخ الدرجة العلمية: مايو 2013

وقد وضع الطلب العالمي المتزايد على النفط والغاز المهندسين خلال السنوات الاخيرة على اهبة الاستعداد لتحسين التكنولوجيا الحالية المتعلقة بإنتاج النفط و الغاز. كما أن الحاجة إلى تحسين الإنتاجية والمحافظة على الطاقة للانتاج المستدام على المدى الطويل أدى إلى تطوير عمليات تحفيز الآبار النفطية باستخدام الاحماض، وتقنيات التكسير الهيدروليكي. وتستخدم الأحماض والتكسير الهيدروليكي لتغيير طريقة تدفق النفط حلو البئر، وبذلك تقلل من مقاومة المكمن للسوائل المتدفقة، في حين يتم استخدام حمض التحفيز لتحسين النفاذية.

التحفيز بالأحماض في المكامن الكربونية له نتائج عكس الحجر الرملي حيث يسهم في فتح و تطوير الثقوب المسماة بالقنوات الدودية. هذه الثقوب هي قنوات تصل بين جوف البئر والمنطقة المحيطة بها و تساعد في الحد من مقاومة تدفق السوائل حول جوف البئر القريب. على مر السنين، حقق الكثير من الباحثين دراسات لفهم ومراقبة طريقة انتشار القنوات الدودية بهدف تقليل التكلفة وتحسين فعالية عملية التحفيز الحمضي.

في هذا العمل، درسنا المعادلات الرياضية لوضع نموذج يساعد في تحسين محاكاة انتشار الثقوب الدودية في الصخور الكربونية خلال عملية التحفيز الحمضي. وكان الهدف هو وضع نموذج رياضي يجمع بين استخدام العوامل الفيزيائية للتدفق في الصخور الكربونية التي يسهل اختراقها، والعوامل الكيميائية التي تنتج عن تفاعل حمض الهيدروكلوريك، وكذلك اختلافات درجات المسامية و النفاذية في المكامن الكربونية لمحاكاة من القنوات الدودية. وقد تم اعادة ترتيب المعادلات المتعلقة بالتدفق والانتشار في الصخور المسامية لاستيعاب

التغيرات في الخصائص المسامية والنفاذية خلال معالجة الصخور بالحمض، كما تم إدخال نظام مقاومة للترجيح جديدة لتقييم العددية والتنبؤ بسرعة المائع بالاعتماد على الضغط.

باستخدام جهاز المحاكاة المطور في هذا العمل، تمت محاكاة نمو القنوات الدودية في العينات رقم 15 و 12 (قطر 1.5 بوصة وطول 2.4 بوصة). وقد تم ايجاد المنحى المتعلق بمعدلات الحقن بين 0.5 سم^3/دقيقة و10 سم^3/دقيقة وقد لاحظنا أن التغيرات في نقل جزيء الحمض ينتج تحول في منحنى المعدل المحل.

وأخيرا، وجدنا أن نفاذية الصخور تؤثر أيضا على كمية حجم المسام والقنوات التي يتم تكوينها من عملية حقن الصخور بالحمض .

1. CHAPTER 1

INTRODUCTION

Over the years, petroleum engineers have used acid stimulation to improve the productivity/injectivity of production/injection wells and our general understanding of the wormhole phenomenon in carbonate reservoir has evolved. Wormholes are highly conductive channels that develop during acid stimulation of carbonate cores. Experimental investigations revealed that wormholes are results of bulk of injecting acid passing through and connecting very limited number of existing pores in the core [1].

Previous experimental studies have shown that the competition between the rate of material transfer and reaction at the rock surface is the deciding factor in the rate of propagation, diameter and length of wormholes [2, 3]. This competition is represented by a dimensionless quantity called Damkohler number:

$$\boldsymbol{D_a = \frac{rate\ of\ reaction}{convective\ mass\ transfer\ rate} = \pi\ \frac{dLK_r}{q}} \qquad (\mathbf{1.1})$$

Where q is the fluid flow-rate, d and L are the diameter and the length of the wormhole-modeling cylindrical channel (these are determined from seepage experiments), and K_r is the reduced rate of the chemical reaction determined from the corresponding kinetic experiments. A Damkohler number of 1 represents equal mass transfer and reaction rate.

A Damkohler number greater than one signifies faster reaction rate while a value of Damkohler number less than one is for a rate of reaction slower than rate of mass transfer.

Generally, experiments have shown that higher rate of injection helps to reduce the Damkohler number and increase the propagation of wormholes. It is also know that higher rate of injection can lead to higher volume of injection over the same amount of time. The need to minimize the cost of acid stimulation via reduction of acid volume requirement underscored the need to develop a means to study the treatment under several procedures for optimization of the criteria.

Experimental investigations of wormhole propagation have deepened our knowledge of the phenomenon but minimizing the cost of acid stimulation means, we must develop other means of investigation that eliminates the cost of setting up experiments. This gives birth to the use of simulation (computational investigation) in the study of wormholes and stimulation treatment design.

Computational investigations of wormhole propagation involving the use of numerical solution of system of discretized differential equations are widely documented. Examples include mechanistic model [1], stochastic model with biased randomness [4] and quantitative model [5]. Others are network model [6], dynamic model [7], numerical model [8], semi-empirical model [9] and numerical simulation .

1.1 Statement of the Problem

The great complexity of naturally couple system of differential equations that accurately describes the worm-holing phenomenon has led previous researcher to adopt wholesale simplifications of the problem [10]. Examples of these gross simplifications include the use of cylindrical wormhole shape [1], disregard of rock-acid chemical interaction [4, 6], use of homogenous core assumption [5, 7]. Others include the use of dimensionless parameters (neglects spatial variation of porosity and permeability) [8, 11] and neglect of porosity and permeability variation [12]. These simplifications led to the inability of previous works to accurately describe the propagation of the wormhole.

1.2 Objective

1. To develop a robust mathematics of worm-holing phenomenon that account for convection and diffusion of acid, acid mineral interaction, variation of porosity and permeability with time and location.
2. To correct errors of past study regarding the use of the convection equation in porous medium
3. To correct errors of past studies regarding the effect of convection on diffusion
4. To develop a 4D (3D spatial + 1D time) Numerical Wormhole Simulator.
5. To validate the numerical model with real experimental observations.

2. CHAPTER 2

LITERATURE REVIEW

2.1 Wormhole.

Wormholes are fractal-like networks of interconnected pores that develop during the acid stimulation of carbonate reservoirs. This interconnection of pores form highly conductive channels that continues to funnel freshly injected acids away from the rest of the core (carbonate reservoir) and so continues to grow at a much higher rate that the rest of the core receiving less amount of fresh acid. Understanding the patters as well as factors that affect its development and propagation can determine the success of an acid treatment of a reservoir [2, 13]. To achieve this, experimental and computational studies were conducted with the aim to unravel the nature of wormholes as well as factors that control its development and growth.

2.2 Experimental studies of wormhole propagation.

Experimental studies have shown that the nature and pattern of wormholes are largely dependent on the initial distribution of vugs (pockets of high porosity and permeability section) in the core (reservoir) under study [14, 15]. Other factors that affect the geometry

of the wormholes are the rate of the reactions, rate of acid injection and the amount of acid injected.

Experimental studies have been moderately successful in providing insights into the behavior of wormholes but the difficulties of conducting large number of experiments needed for create a data pool for a more rigorous study of the phenomenon has led to the shift towards computational study of problem.

2.3 Computational studies of wormhole propagation

Computational studies of the worm-holing phenomenon have recorded less success when compared with the experimental study. This is due to the simplified mathematical description of the very complex dynamics of the problem. During the last decade, attentions have shifted towards numerical simulation, which allows us to develop approximates solution to complex but adequate mathematical description that would otherwise remain unsolvable. A broad classification of computational studies is as follows:

- ✓ Analytical Models
- ✓ Semi-empirical Models
- ✓ Stochastic Models
- ✓ Numerical Models

2.3.1 Analytic Models

Analytical models produce exact solution to poor mathematical description of the physical problems. While these models are largely unrepresentative of the worm-holing behavior, they represent the first attempt at solving the problem without recourse to the laboratory. The failure of these models lies in their gross simplification of the problem to allow for analytical solution of the system of equations developed. Under this category, mechanistic wormhole model[1, 16], Daccord's model [17], dynamic model [18], analytical model [19], well-wormhole model [20] and volumetric model were developed.

Table 2-1: List of some Analytical Models

Model types	Ref	Models
Mechanistic wormhole model	[1]	$x = \frac{Q_T}{q_L}\left[1 - \exp\left(-\frac{q_L \beta C_o t}{\rho \pi r_o^2}\right)\right]$ (2.1)
		$r = \left\{r_o^2 + \frac{q_L \beta C_o}{\rho \pi}\left[t + \frac{\rho \pi r_o^2}{q_L \beta C_o}\ln\left(1 - \frac{q_L}{Q_T}x\right)\right]\right\}^{0.5}$ (2.2)
	[16]	$u = \frac{k\left(g_f D - p_R\right)}{r_w \mu\left(\ln\left(\frac{r_e}{r_w} - s\right)\right)}$ (2.3)
Daccord's model	[17]	$r_e(V) = \left(\frac{bN_{ac}V}{\pi h \emptyset} N_{Pe}^{-1/3}\right)^{1/d_f}$ (2.4)

2.3.2 Semi-Empirical Models.

Semi-empirical models represent hybrids of the experimental and analytical models. Although better than the purely analytical models, these models also fall short of

adequately reproducing the wormholes when implemented. The most prominent of this category are semi-empirical model [9], exponential decay model [5] and network model [4, 6, 21].

Table 2-2: List of some Semi-Empirical Models

Model types	Ref	Models	
Semi-empirical model	[9]	$V_i(R) = \frac{Q}{2\pi Rh \cdot \emptyset}$	(2.5)
		$B(V_i) = \left(1 - \exp\left(-W_B \cdot V_i^2\right)\right)^2$	(2.6)
		$V_{wh}(R_{wh}) = W_B \cdot V_i(R_{wh})^{2/3} \cdot B\left(V_i(R_{wh})\right)$	(2.7)
Exponential decay model	[5]	$N(r) = N(r_o)\left(\frac{r}{r_o}\right)^{d-1}$	(2.8)
		$D(r) = D(r_o)\left(\frac{r}{r_o}\right)^{\varepsilon}$	(2.9)
Network model	[21]	$M_{eff}(r) = \frac{N(r)D^2(r)}{4rH}[M_w(r) - M_m] + M_m$	(2.10)
		$M_m = \frac{K_m K_{mro}}{\mu_o}$	(2.11)
		$M_w(r) = \begin{cases} \frac{K_w K_{wro}}{\mu_o} & if\ \lvert\nabla P\rvert < \frac{4\tau_o}{D(r)} \\ \frac{D^2(r)}{32\mu_{slurry}} & if\ \lvert\nabla P\rvert \geq \frac{4\tau_o}{D(r)} \end{cases}$	(2.12)

2.3.3 Stochastic Models.

These models are developed with the aim to produce the wormhole without respecting the physics of flow through porous media or the chemistry of rock acid interaction that naturally determines the behaviors and formation of wormholes. A typical example here

is the use the of the diffusivity equation to force bias the random-stochastic model [4] without the use of the information about the acid-rock chemical interaction. Under this category, we have biased stochastic model [4, 17], probabilistic active walker model [6] and diffusion limited aggregation model[13].

2.3.4 Numerical Models.

These represent the most successful computational attempt at modeling wormholes. Numerical models allow for the fields of inputs against single values used in other models described above. The use of input fields allows for the actual representation of the most important parameters (vugs-porosity and permeability field) in the determination of wormholes. Despite this freedom, earlier works on numerical simulation of wormholes have used dimensionless form of the parameters, which like the previous methods does not allow for multiplicity of inputs. Past works on numerical simulation of wormholes include numerical model [8], simulation and comparison of models [11] , simulation of wormholes in vuggy carbonate reservoirs [12] and very recently 3-D simulation of carbonate acidization [22].

The limitations of past numerical simulation include:

1. The use of dimensionless numbers- Acid numbers and Damkholer numbers that uses a single value of permeability, porosity against local values of the heterogeneity parameters at each grid centers [8, 9].

2. The non-inclusion of the reactive term in the advection convection equation, assumption of zero rate of change of local porosity, and the elimination of Darcy effect (permeability)on the pressure drop as exemplified in [12],
3. The use of Darcy equation of motion to model the flow that is partly in the matrix and partly in the wormhole is inadequate [8, 9, 11, 22, 23]. This flow can me better modeled with the brinkman flow equation.

3. CHAPTER 3

METHODOLOGY

3.1 Development of the Mathematical Formulations

Numerical models are developed to provide an approximate solution to the exact mathematical description of the physical system, hence it is surprising however that previous attempts to provide numerical models for this problem have generally made assumption that simplifies the problem and neglects the most important reason for which the model was developed-heterogeneity.

3.1.1 Equation of Continuity

Using the Cartesian volume element shown in **Error! Reference source not found.**,
Where

$\Delta x, \Delta y\ and\ \Delta z$ are the dimensions of the element,

$u_x, u_y, and\ u_z$ are the velocities of fluid into the element at point $x, y\ and\ z$ respectively,

$u_{x+\Delta x}, u_{y+\Delta y}, and\ u_{z+\Delta z}$ are the velocities of fluid out of the element at point $x + \Delta x$,

$y + \Delta y\ and\ z + \Delta z$, respectively,

Δt is the change in time t

ρ_A is the density of the fluid, and

$\emptyset_t, and\ \emptyset_{t+\Delta t}$ are the porosities of the element at time t and $t + \Delta t$

During a period Δt,

$$\begin{aligned} &Mass\ of\ fluid\ inflow\ into\ the\ element + Source \\ &= Mass\ of\ fluid\ outflow\ from\ the\ element \\ &+ Accumulated\ mass \end{aligned} \tag{3.1}$$

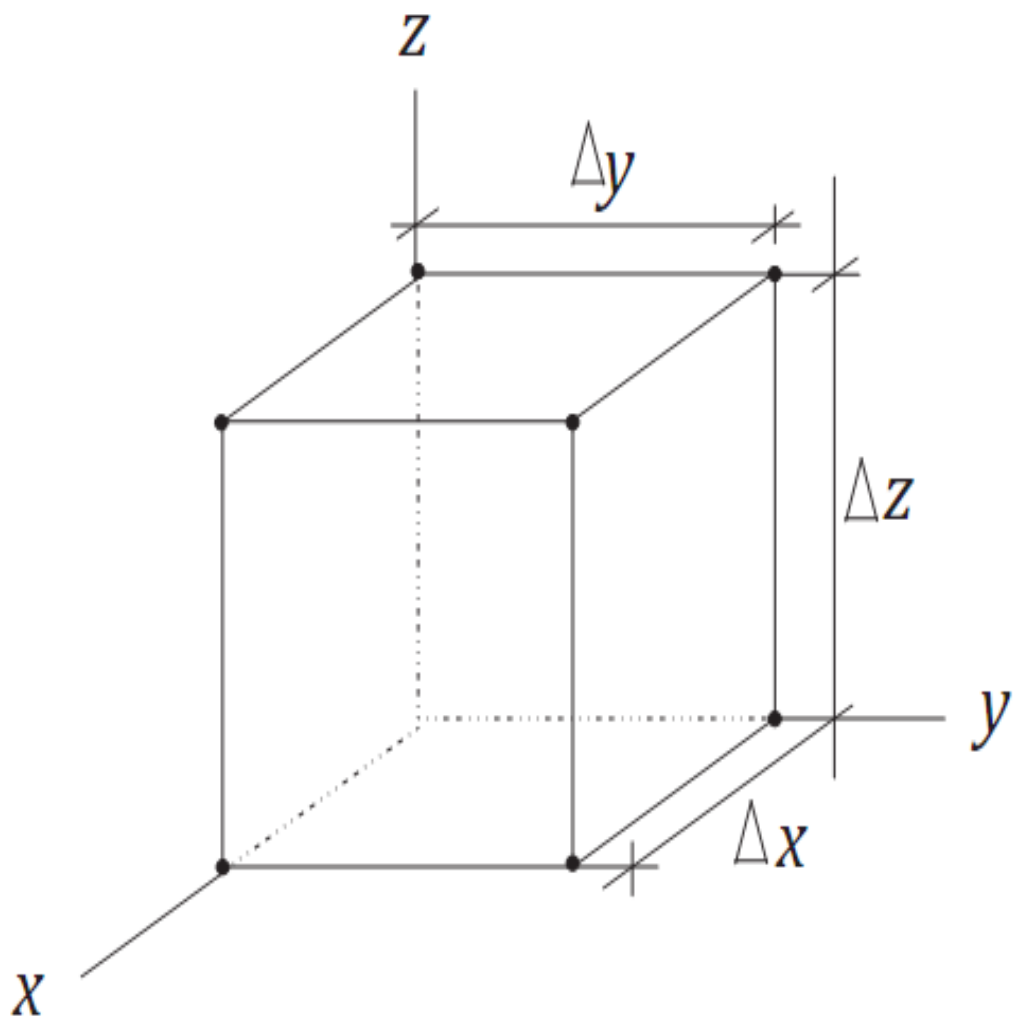

Figure 3-1: The 3D elemental control volume

$$Mass\ of\ fluid\ inflow\ into\ the\ element$$

$$= \Delta t \left(\rho_A u_x \Delta y \Delta z|_x + \rho_A u_y \Delta x \Delta z\big|_y + \rho_A u_z \Delta x \Delta y|_z \right) \tag{3.2}$$

$$Mass\ of\ fluid\ outflow\ from\ the\ element$$

$$= \Delta t \left(\rho_A u_x \Delta y \Delta z|_{x+\Delta x} + \rho_A u_y \Delta x \Delta z\big|_{y+\Delta y} + \rho_A u_z \Delta x \Delta y|_{z+\Delta z} \right) \tag{3.3}$$

$$Source = 0\ (No\ mass\ production\ or\ loss\ within\ the\ cell) \tag{3.4}$$

$$Accumulation = \Delta x \Delta y \Delta z((\rho_A \emptyset)|_{t+\Delta t} - (\rho_A \emptyset)|_t) \tag{3.5}$$

Hence

$$\begin{aligned} &Mass\ of\ fluid\ inflow\ into\ the\ element \\ &\qquad - Mass\ of\ fluid\ outflow\ from\ the\ element \\ &\qquad = \ Accumulated\ mass \end{aligned} \tag{3.6}$$

$$\begin{aligned} &\Delta t \left(\rho_A u_x \Delta y \Delta z|_x + \rho_A u_y \Delta x \Delta z\big|_y + \rho_A u_z \Delta x \Delta y|_z \right) \\ &\qquad - \Delta t \left(\rho_A u_x \Delta y \Delta z|_{x+\Delta x} + \rho_A u_y \Delta x \Delta z\big|_{y+\Delta y} + \rho_A u_z \Delta x \Delta y|_{z+\Delta z} \right) \\ &\qquad = \Delta x \Delta y \Delta z((\rho_A \emptyset)|_{t+\Delta t} - (\rho_A \emptyset)|_t) \end{aligned} \tag{3.7}$$

Dividing through with $\Delta x \Delta y \Delta z \Delta t$ and rearranging,

$$\begin{aligned} &\frac{\rho_A u_x|_x - \rho_A u_x|_{x+\Delta x}}{\Delta x} + \frac{\rho_A u_y\big|_y - \rho_A u_y\big|_{y+\Delta y}}{\Delta y} + \frac{\rho_A u_z|_z - \rho_A u_z|_{z+\Delta z}}{\Delta z} \\ &\qquad = \frac{(\rho_A \emptyset)|_{t+\Delta t} - (\rho_A \emptyset)|_t}{\Delta t} \end{aligned} \tag{3.8}$$

Assuming a constant fluid density (incompressible fluid) and letting all differential elements approach zero,

$$-\frac{\partial u_x}{\partial x} - \frac{\partial u_y}{\partial y} - \frac{\partial u_z}{\partial z} = \frac{\partial \emptyset}{\partial t} \tag{3.9}$$

3.1.2 Equation of Motion

Flow equation in porous medium is generally governed by Darcy law, however the acid mineral interaction creates wormholes in which flow is non-Darcy and hence has to be modeled by Navier-Stokes equation. Hence we combine these equations to accurately depict the hydraulics of acid stimulation of carbonate core.

Darcy law

$$u_x = \frac{k_{xx}}{\mu}\frac{\partial p}{\partial x} \tag{3.10}$$

$$u_y = \frac{k_{yy}}{\mu}\frac{\partial p}{\partial y} \tag{3.11}$$

$$u_z = \frac{k_{zz}}{\mu}\frac{\partial p}{\partial z} \tag{3.12}$$

Where k_{xx}, k_{yy} , k_{zz} represent the permeability in the direction x y and z respectively

μ is the viscosity of the fluid and

p is the pressure

Navier-Stokes equation

$$\rho_A\left(\frac{\partial u_x}{\partial t} + u_x\frac{\partial u_x}{\partial x} + u_y\frac{\partial u_x}{\partial y} + u_z\frac{\partial u_x}{\partial z}\right) + \frac{\partial p}{\partial x} = \mu\left[\frac{\partial^2 u_x}{\partial x^2} + \frac{\partial^2 u_x}{\partial y^2} + \frac{\partial^2 u_x}{\partial z^2}\right] + \rho g_x \tag{3.13}$$

$$\rho_A\left(\frac{\partial u_y}{\partial t} + u_x\frac{\partial u_y}{\partial x} + u_y\frac{\partial u_y}{\partial y} + u_z\frac{\partial u_y}{\partial z}\right) + \frac{\partial p}{\partial y} = \mu\left[\frac{\partial^2 u_y}{\partial x^2} + \frac{\partial^2 u_y}{\partial y^2} + \frac{\partial^2 u_y}{\partial z^2}\right] + \rho g_y \tag{3.14}$$

$$\rho_A\left(\frac{\partial u_z}{\partial t}+u_x\frac{\partial u_z}{\partial x}+u_y\frac{\partial u_z}{\partial y}+u_z\frac{\partial u_z}{\partial z}\right)+\frac{\partial p}{\partial z}=\mu\left[\frac{\partial^2 u_z}{\partial x^2}+\frac{\partial^2 u_z}{\partial y^2}+\frac{\partial^2 u_z}{\partial z^2}\right]+\rho g_z \quad (3.15)$$

By combining these equations, neglecting gravity and taking out the nonlinear terms to reducing computational load, we derive the transient brinkman's equation of flow.

$$\rho_A\left(\frac{\partial u_x}{\partial t}\right)+\frac{\partial p}{\partial x}=-\frac{\mu}{k_{xx}}u_x+\mu\left[\frac{\partial^2 u_x}{\partial x^2}+\frac{\partial^2 u_x}{\partial y^2}+\frac{\partial^2 u_x}{\partial z^2}\right] \quad (3.16)$$

$$\rho_A\left(\frac{\partial u_y}{\partial t}\right)+\frac{\partial p}{\partial y}=-\frac{\mu}{k_{yy}}u_y+\mu\left[\frac{\partial^2 u_y}{\partial x^2}+\frac{\partial^2 u_y}{\partial y^2}+\frac{\partial^2 u_y}{\partial z^2}\right] \quad (3.17)$$

$$\rho_A\left(\frac{\partial u_z}{\partial t}\right)+\frac{\partial p}{\partial z}=-\frac{\mu}{k_{zz}}u_z+\mu\left[\frac{\partial^2 u_z}{\partial x^2}+\frac{\partial^2 u_z}{\partial y^2}+\frac{\partial^2 u_z}{\partial z^2}\right] \quad (3.18)$$

3.1.3 Convection-Dispersion-Reaction Equation

Fick's law states that

$$J=-D\frac{\partial C}{\partial x} \quad (3.19)$$

Where J is the molecular flux per unit time,

D is the molecular diffusivity measured in area per unit time,

$\partial C/\partial x$ is the concentration gradient.

In situations like the one we will be considering where, the diffusion coefficient is not constant, it is more appropriate to express it as:

$$J=-\frac{\partial(DC)}{\partial x} \quad (3.20)$$

Note that J is flux and hence, the rate of mass transfer is the product of J and the area

that is normal to the direction of x.

Using the same mass balance system (CONCENTRATION BALANCE)

During a period Δt,

$$Flux\ of\ fluid\ inflow\ into\ the\ element + Source$$
$$= Flux\ of\ fluid\ outflow\ from\ the\ element$$
$$+ Accumulated\ mass \tag{3.21}$$

$$Flux\ of\ fluid\ inflow\ into\ the\ element$$
$$= Flux\ inflow\ due\ to\ bulk\ fliud\ movement + Flux\ inflow\ due\ to\ dispersion$$
$$= \Delta t\left\{\left(\bar{C}u_x\Delta y\Delta z|_x + \bar{C}u_y\Delta x\Delta z\Big|_y + \bar{C}u_z\Delta x\Delta y|_z\right)\right.$$
$$-\left(\Delta y\Delta z\frac{\partial(D_x\bar{C})}{\partial x}\bigg|_x + \Delta x\Delta z\frac{\partial\left(D_y\bar{C}\right)}{\partial y}\bigg|_y\right.$$
$$\left.\left.+\Delta x\Delta y\frac{\partial(D_z\bar{C})}{\partial z}\bigg|_z\right)\right\} \tag{3.22}$$

$$Flux\ of\ fluid\ outflow\ from\ the\ element$$
$$= Flux\ outflow\ due\ to\ bulk\ fliud\ movement + Flux\ outflow\ due\ to\ dispersion$$
$$= \Delta t\left\{\left(\bar{C}u_x\Delta y\Delta z|_{x+\Delta x} + \bar{C}u_y\Delta x\Delta z\Big|_{y+\Delta y} + \bar{C}u_z\Delta x\Delta y|_{z+\Delta z}\right)\right.$$
$$-\left(\Delta y\Delta z\frac{\partial(D_x\bar{C})}{\partial x}\bigg|_{x+\Delta x} + \Delta x\Delta z\frac{\partial\left(D_y\bar{C}\right)}{\partial y}\bigg|_{y+\Delta y}\right.$$
$$\left.\left.+\Delta x\Delta y\frac{\partial(D_z\bar{C})}{\partial z}\bigg|_{z+\Delta z}\right)\right\} \tag{3.23}$$

$$Sink = -\Delta t(1-\emptyset)V_b v_f S^* E\bar{C}_s \quad \rightarrow \ (Order\ of\ the\ reaction = 1) \tag{3.24}$$

Where,

v_f is the fraction of carbonate mineral by volume in the formation,

E is the reaction rate constant and

S^* is the specific surface area in squared meter by cubic meter of the mineral.

$\bar{C}$ is the concentration of the acid (Cup mixing concentration) in the bulk of the fluid at location x, y, z

$\bar{C}_s$ is the concentration on the reaction surface

$$Accumulation = \Delta x \Delta y \Delta z((\bar{C}\emptyset)|_{t+\Delta t} - (\bar{C}\emptyset)|_t) \tag{3.25}$$

Combining this we have,

$$\begin{aligned}
\Delta t \Bigg\{ & \left(\bar{C}u_x \Delta y \Delta z|_x + \bar{C}u_y \Delta x \Delta z\Big|_y + \bar{C}u_z \Delta x \Delta y|_z \right) \\
& - \left(\Delta y \Delta z \frac{\partial (D_x \bar{C})}{\partial x}\bigg|_x + \Delta x \Delta z \frac{\partial (D_y \bar{C})}{\partial y}\bigg|_y + \Delta x \Delta y \frac{\partial (D_z \bar{C})}{\partial z}\bigg|_z \right) \Bigg\} \\
& - \Delta t \Bigg\{ \left(\bar{C}u_x \Delta y \Delta z|_{x+\Delta x} + \bar{C}u_y \Delta x \Delta z\Big|_{y+\Delta y} + \bar{C}u_z \Delta x \Delta y|_{z+\Delta z} \right) \\
& - \left(\Delta y \Delta z \frac{\partial (D_x \bar{C})}{\partial x}\bigg|_{x+\Delta x} + \Delta x \Delta z \frac{\partial (D_y \bar{C})}{\partial y}\bigg|_{y+\Delta y} \right. \\
& \left. + \Delta x \Delta y \frac{\partial (D_z \bar{C})}{\partial z}\bigg|_{z+\Delta z} \right) \Bigg\} - \Delta t (1 - \emptyset) V_b v_f S^* E \bar{C}_s \\
& = \Delta x \Delta y \Delta z((\bar{C}\emptyset)|_{t+\Delta t} - (\bar{C}\emptyset)|_t)
\end{aligned} \tag{3.26}$$

Rearranging, dividing the expression by $\Delta x \Delta y \Delta z \Delta t$ and taking limit as $\Delta x \to 0, \Delta y \to 0, \Delta z \to 0, \Delta t \to 0$ we have,

$$-\frac{\partial(\bar{C}u_x)}{\partial x}-\frac{\partial(\bar{C}u_y)}{\partial y}-\frac{\partial(\bar{C}u_z)}{\partial z}+\frac{\partial}{\partial x}\left(\frac{\partial(D_x\bar{C})}{\partial x}\right)+\frac{\partial}{\partial y}\left(\frac{\partial(D_y\bar{C})}{\partial y}\right)$$
$$+\frac{\partial}{\partial z}\left(\frac{\partial(D_z\bar{C})}{\partial z}\right)-(1-\emptyset)v_f\widetilde{S^*E\bar{C}_s}$$
$$=\frac{\partial(\bar{C}\emptyset)}{\partial t} \tag{3.27}$$

$\widetilde{S^*E\bar{C}_s}$ is the rate of consumption of the acid per unit bulk volume per unit time

If the diffusion coefficient is constant, then

$$-\frac{\partial(\bar{C}u_x)}{\partial x}-\frac{\partial(\bar{C}u_y)}{\partial y}-\frac{\partial(\bar{C}u_z)}{\partial z}+D\frac{\partial}{\partial x}\left(\frac{\partial\bar{C}}{\partial x}\right)+D\frac{\partial}{\partial y}\left(\frac{\partial\bar{C}}{\partial y}\right)+D\frac{\partial}{\partial z}\left(\frac{\partial\bar{C}}{\partial z}\right)$$
$$-\widetilde{S^*E\bar{C}_s}$$
$$=\frac{\partial(\bar{C}\emptyset)}{\partial t} \tag{3.28}$$

$$-\nabla\cdot(\bar{C}\vec{u})+D\nabla^2\bar{C}-(1-\emptyset)v_fS^*E\bar{C}_s=\frac{\partial(\bar{C}\emptyset)}{\partial t} \tag{3.29}$$

Experimental study has shown that the diffusion coefficient is partly constant and partly proportional to the speed of the fluid, so we have $D=D_m+\alpha|u|$,

Where α is a physical constant with dimension [L] and typical value of $2\times 10^{-6}meters$ while D_m has a typical value of $3.6\times 10^{-9}m^2/s$ [22].

Using this we get

$$-\nabla\cdot(\bar{C}\vec{u})+\frac{\partial}{\partial x}\left((D_m+\alpha_x|u_x|)\frac{\partial\bar{C}}{\partial x}\right)+\frac{\partial}{\partial y}\left(\left(D_m+\alpha_y|u_y|\right)\frac{\partial\bar{C}}{\partial y}\right)$$
$$+\frac{\partial}{\partial z}\left((D_m+\alpha_z|u_z|)\frac{\partial\bar{C}}{\partial z}\right)-(1-\emptyset)v_fS^*E\bar{C}_s$$
$$=\frac{\partial(\bar{C}\emptyset)}{\partial t} \tag{3.30}$$

3.1.3.1 Divergence versus Gradient.

The advection- dispersion equation has the first term containing divergence of the product of velocity and concentration while the term on the right is the time derivative of the product of concentration and porosity. We can simplify this as follows:

Since our porosity is not constant in time, we express the right hand side as

$$\frac{\partial(\bar{C}\emptyset)}{\partial t} = \emptyset\frac{\partial\bar{C}}{\partial t} + \bar{C}\frac{\partial\emptyset}{\partial t} \tag{3.31}$$

And continuity equation provides that,

$$\frac{\partial\emptyset}{\partial t} = -\nabla\cdot\vec{u} \tag{3.32}$$

so

$$-\nabla\cdot(\bar{C}\vec{u}) = -\nabla\bar{C}\cdot\vec{u} - \bar{C}\nabla\cdot\vec{u} = -\nabla\bar{C}\cdot\vec{u} + \bar{C}\frac{\partial\emptyset}{\partial t} \tag{3.33}$$

Using this in the equation, we have

$$-\nabla\bar{C}\cdot\vec{u} + \bar{C}\frac{\partial\emptyset}{\partial t} + \frac{\partial}{\partial x}\left((D_m + \alpha_x|u_x|)\frac{\partial\bar{C}}{\partial x}\right) + \frac{\partial}{\partial y}\left(\left(D_m + \alpha_y|u_y|\right)\frac{\partial\bar{C}}{\partial y}\right)$$

$$+\frac{\partial}{\partial z}\left((D_m + \alpha_z|u_z|)\frac{\partial\bar{C}}{\partial z}\right) - (1-\emptyset)v_f S^* E\bar{C}_s$$

$$= \emptyset\frac{\partial\bar{C}}{\partial t} + \bar{C}\frac{\partial\emptyset}{\partial t} \tag{3.34}$$

So the new equation comes down to

$$-\nabla\bar{C}\cdot\vec{u}+\frac{\partial}{\partial x}\left((D_m+\alpha_x|u_x|)\frac{\partial\bar{C}}{\partial x}\right)+\frac{\partial}{\partial y}\left(\left(D_m+\alpha_y|u_y|\right)\frac{\partial\bar{C}}{\partial y}\right)$$
$$+\frac{\partial}{\partial z}\left((D_m+\alpha_z|u_z|)\frac{\partial\bar{C}}{\partial z}\right)-(1-\emptyset)v_f S^* E\bar{C}_s=\emptyset\frac{\partial\bar{C}}{\partial t} \qquad (3.35)$$

3.1.4 Porosity-Mineral Volume-Permeability Equations

Considering the grid cell Figure **3-1** with volume

$$\Delta x\Delta y\Delta z=V_b \qquad (3.36)$$

The initial volume of the mineral

$$(1-\emptyset_0)V_b \qquad (3.37)$$

A fraction of this is carbonate, hence the volume of carbonate V_c is

$$V_c=(1-\emptyset_0)V_b v_f \qquad (3.38)$$

Where v_f is the volume fraction of carbonate.

We can calculate the area available for acid carbonate reaction thus gives:

$$(1-\emptyset_0)V_b v_f S^* \qquad (3.39)$$

Hence the rate of reaction or consumption of the acid (of acid-kmole/sec) is thus:

$$(1-\emptyset_0)V_b v_f S^* E\bar{C}_s \qquad (3.40)$$

Rate of dissolution of mineral is then (cubic meters/sec)

$$\frac{dV_c}{dt}=-(1-\emptyset_0)V_b v_f S^* E\bar{C}_s\left(\frac{n_M}{n_A}\right)\frac{M_M}{\rho} \qquad (3.41)$$

Where

$$\left(\frac{n_M}{n_A}\right) = stoichometric\ ratio\ of\ acid - mineral\ reaction$$

$$M_M = molar\ mass\ of\ the\ mineral\ in\ kg/mole$$

$$\rho = density\ of\ the\ mineral\ in\ kg/m^3$$

$$V_c = Volume\ of\ carbonate = (1 - \emptyset_0)V_b v_f$$

Using the fact that

$$Bulk\ Volume = Pore\ Volume\ (V_p) + Volume\ of\ Carbonate\ (V_c) + Volume\ of\ Quartz\ (V_q) \quad (3.42)$$

$$V_b = V_p + V_c + V_q \quad (3.43)$$

By taking the differentiation with respect to t

$$\frac{dV_b}{dt} = \frac{dV_p}{dt} + \frac{dV_c}{dt} + \frac{dV_q}{dt} \quad (3.44)$$

But

$$V_p = \emptyset V_b \quad (3.46)$$

And

$$\frac{dV_b}{dt} = 0 \quad (3.47)$$

Because the bulk volume is constant and

$$\frac{dV_q}{dt} = 0 \quad (3.48)$$

Because the quartz is not reacting

$$0 = V_b \frac{d\emptyset}{dt} - (1 - \emptyset_0) V_b v_f S^* E \bar{C}_s \left(\frac{n_M}{n_A}\right) \frac{M_M}{\rho} \tag{3.49}$$

Hence

$$\frac{d\emptyset}{dt} = (1 - \emptyset_0) v_f S^* E \bar{C}_s \left(\frac{n_M}{n_A}\right) \frac{M_M}{\rho} \tag{3.50}$$

The continuity equation thus becomes

$$\frac{\partial u_x}{\partial x} + \frac{\partial u_y}{\partial y} + \frac{\partial u_z}{\partial z} = -(1 - \emptyset_0) v_f S^* E \bar{C}_s \left(\frac{n_M}{n_A}\right) \frac{M_M}{\rho} \tag{3.51}$$

We can solve for porosity as thus

$$d\emptyset = (1 - \emptyset_0) v_f S^* E \bar{C}_s \left(\frac{n_M}{n_A}\right) \frac{M_M}{\rho} dt \tag{3.52}$$

$$\Delta\emptyset = (1 - \emptyset_0) v_f S^* E \bar{C}_s \left(\frac{n_M}{n_A}\right) \frac{M_M}{\rho} \Delta t \tag{3.53}$$

In an event where there is no change in time, or when the concentration is zero, we expect the porosity to remain the same

$$\frac{d\emptyset}{dt} = 0$$

$$\emptyset = 1 - (1 - \emptyset_0) \equiv \emptyset = \emptyset_0 \qquad as\ expected$$

The volume fraction is also not a constant. So we have

$$(1 - \emptyset_0) V_b \frac{dv_f}{dt} = -(1 - \emptyset_0) V_b v_f S^* E \bar{C}_s \left(\frac{n_M}{n_A}\right) \frac{M_M}{\rho} \tag{3.54}$$

$$\frac{dv_f}{dt} = -v_f S^* E \bar{C}_s \left(\frac{n_M}{n_A}\right) \frac{M_M}{\rho} \tag{3.55}$$

Just like we did for porosity, we have:

$$v_f = v_{f0} e^{-S^* E \bar{C}_s \left(\frac{n_M}{n_A}\right) \frac{M_M}{\rho} \Delta t} \tag{3.56}$$

Considering the Taylor expansions:

$$e^{-x} = 1 - \frac{x}{1!} + \frac{x^2}{2!} - \frac{x^3}{3!} + \frac{x^4}{4!} - \frac{x^5}{5!} + \frac{x^6}{6!} \dots \dots \tag{3.57}$$

And

$$\frac{1}{1+x} = 1 - x + x^2 - x^3 + x^4 - x^5 + x^6 \dots \dots \tag{3.58}$$

Hence when x is sufficiently small, we can neglect the second and higher powers of x to have:

$$e^{-x} \approx 1 - x \approx \frac{1}{1+x} \tag{3.59}$$

Using this transformation we have:

$$v_f = \frac{v_{f0}}{\left[1 + S^* E \bar{C}_s \left(\frac{n_M}{n_A}\right) \frac{M_M}{\rho} \Delta t\right]} \tag{3.60}$$

When the new porosity has been evaluated we can calculate the new permeability for the next of the system using

$$k = \alpha_k \exp\left(M(\emptyset - \emptyset_0)\right) \tag{3.61}$$

Where M and n are empirically determined constants that depend on the cementation, packing and shapes of the grains of the formation

3.1.5 Concentration at the Reacting Surface

The competition between the reaction and mass transfer is further influenced by diffusion of the acid molecule from the bulk of the fluid to the reacting surface via local mass transfer.

At steady state, the rate of consumption of the acid at the reacting surface equals the rate of transfer of acid molecules from the bulk of the fluid to the reacting surface.

$$k_c(\bar{C} - \bar{C}_s) = k_s\bar{C}_s \tag{3.62}$$

$k_s = (1 - \emptyset_0)V_b v_f S^* E$ is the local rate of constant for consumption of the acid

k_c is the local acid mass transfer rate

We have

$$\bar{C}_s = \frac{k_c\bar{C}}{k_c + k_s} = \frac{k_c\bar{C}}{k_c + (1 - \emptyset_0)V_b v_f S^* E} \tag{3.63}$$

Hence the advective, dispersive, reactive equation can thus be written as

$$\begin{aligned} -\nabla\bar{C}\cdot\vec{u} + \frac{\partial}{\partial x}\left((D_m + \alpha_x|u_x|)\frac{\partial\bar{C}}{\partial x}\right) + \frac{\partial}{\partial y}\left(\left(D_m + \alpha_y|u_y|\right)\frac{\partial\bar{C}}{\partial y}\right) \\ + \frac{\partial}{\partial z}\left((D_m + \alpha_z|u_z|)\frac{\partial\bar{C}}{\partial z}\right) - \left(\frac{k_c(1-\emptyset)v_f S^* E}{k_c + (1-\emptyset)V_b v_f S^* E}\right)\bar{C} \\ = \emptyset\frac{\partial\bar{C}}{\partial t} \end{aligned} \tag{3.64}$$

And the continuity equation

$$\frac{\partial u_x}{\partial x} + \frac{\partial u_y}{\partial y} + \frac{\partial u_z}{\partial z} = -\left(\frac{k_c(1-\emptyset)v_f S^* E\bar{C}}{k_c + (1-\emptyset)V_b v_f S^* E}\right)\left(\frac{n_M}{n_A}\right)\frac{M_M}{\rho} \tag{3.65}$$

3.2 Boundary Conditions and initial conditions

Figure 3-2 shows 26 special grids for which the boundary conditions has to be considered. The initial and boundary conditions are:

Velocities

$$\iint u_x(x=0,y,z,t)dydz = q \tag{3.66}$$

$$u_y(x,y=0,z,t) = 0 \tag{3.67}$$

$$u_y(x,y=w,z,t) = 0 \tag{3.68}$$

$$u_z(x,y,z=0,t) = 0 \tag{3.69}$$

$$u_z(x,y,z=h,t) = 0 \tag{3.70}$$

Pressure

$$P(x=L,y,z,t) = P_{out} \tag{3.71}$$

$$P(x,y,z,t=0) = P_{out} \tag{3.72}$$

Concentration

$$C(x=0,y,z,t) = C_{inj} \tag{3.73}$$

$$C(x,y,z,t=0) = 0 \tag{3.74}$$

Volume Fraction

$$v_f(x,y,z,t=0) = v_{f0} \tag{3.75}$$

Porosity

$$\emptyset(x,y,z,t=0) = \emptyset_i \tag{3.76}$$

Permeability

$$k(x,y,z,t=0) = \alpha_k \exp\big(M(\emptyset_i - \emptyset_0)\big) \tag{3.77}$$

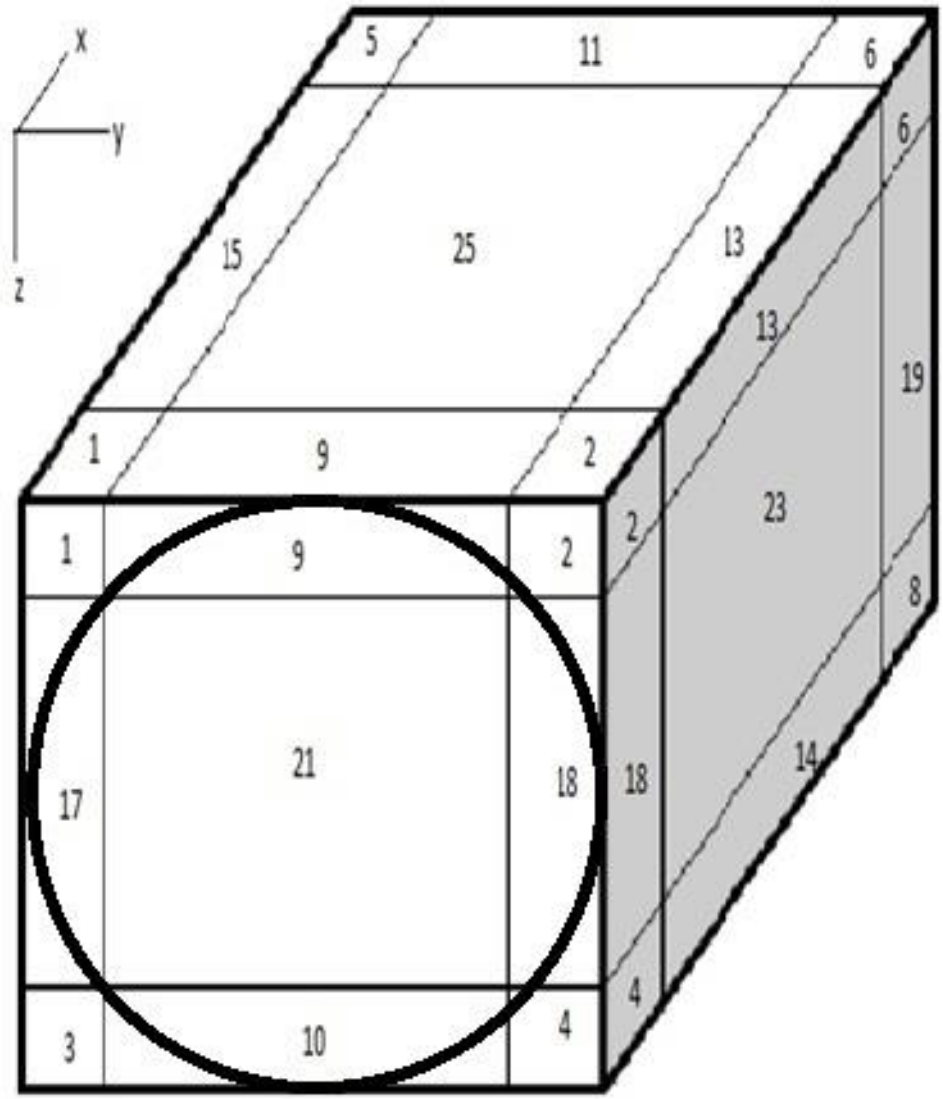

Figure 3-2: 3D rectangular core showing 26 boundary cells and the interior cells

3.3 Choice of coordinate system

We elect the rectangular coordinate system over the cylindrical coordinate system even if the later fits the geometry of the problem. This is based on two reasons:

- ✓ The radial discretization in cylindrical system is logarithmic and increases outwards as we move away from the center, this will lead to increase in the size of the bulk volume of each grid and so an equal amount of mineral dissolution in the grids will not amount to the same amount of porosity change. This will make tracking the wormholes very difficult.
- ✓ The diffusivity equation, as well and the convection advection equation in the cylindrical coordinate will be extremely complex to solve giving the interdependency of parameters in the radial and theta direction.

Now we have the challenge of describing a circular boundary in a rectangular system. Since the curved surface area of the core is to experience a No-flow condition during the stimulation, then we use the equation of a circle to determine grids that lies outside the circular boundary and allocate very small permeability values to them to prevent fluids from going into those grids.

This screening inequality is given as

$$\sqrt{(y-r)^2+(z-r)^2} \leq r \tag{3.78}$$

The Figure 3-3 shows circle made of square grids generated by using this method

The number of grids on the cross section is not arbitrary. The need to have acid injection via the center of the front end of the core constrains the number of grid we can use to only odd numbers.

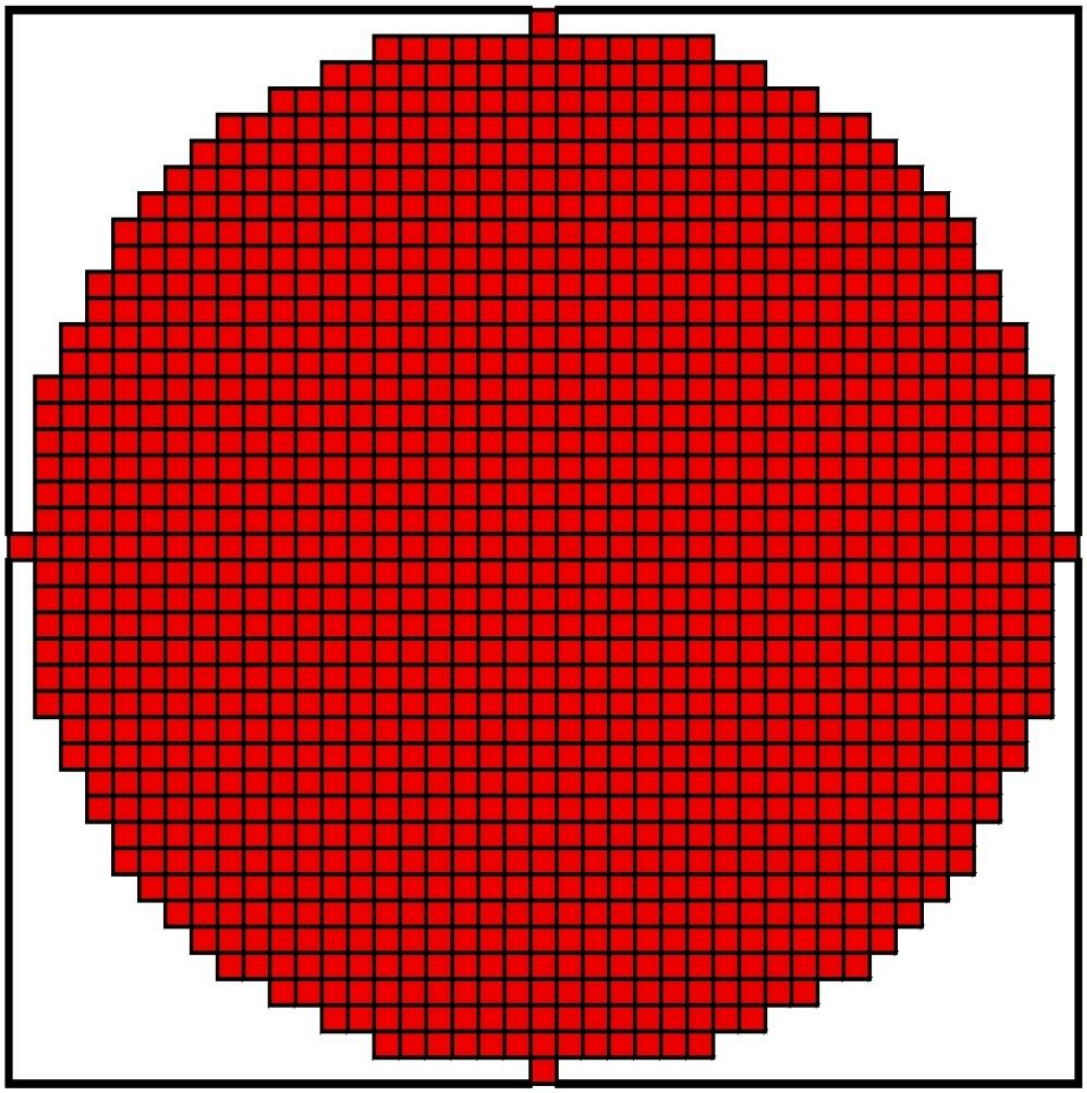

Figure 3-3: Discretization of front end of the core in a rectangular system

3.4 Development of coupled system of differential equations

The system of coupled differential equations always arises in the situation where the problems are nonlinear. This is the case when the coefficients of the sort variables or their derivatives are actually dependent on the variables themselves. In this problem, the concentration distribution affects the volume fraction, which in turn affect he porosity. The porosity determines the permeability, which will then determine the pressure distribution. The pressure distribution then determines the convective velocity field which then determines the concentration. This cycle of dependency of the variables (workflow of the solution of the systems of equations) is shown in figure below.

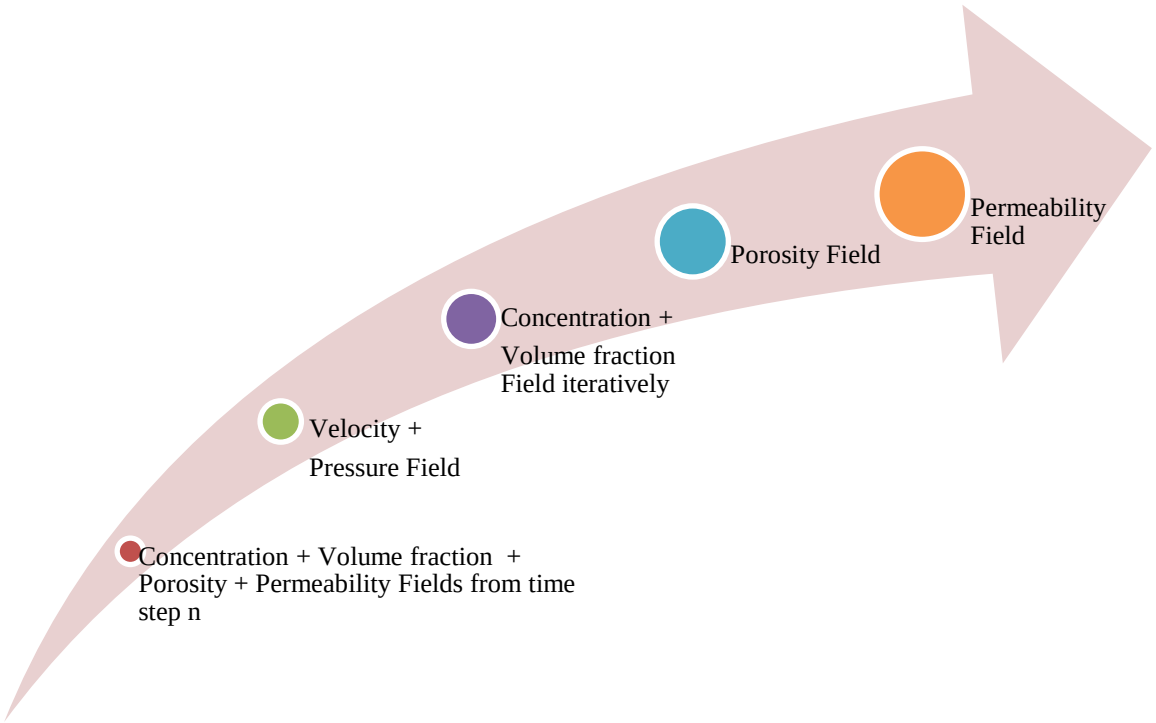

Figure 3-4: The dependency cycle of the primary variables of the system

We solve the coupled equation of motion and the continuity equation with the rate of change of porosity evaluated with the porosity value at the beginning of the time step. This velocity and pressure fields is then used to solve the convective-dispersion reaction and mineral equations iteratively for concentration and volume fraction and then we update the porosity and permeability when the convergence has been achieved. We will then express the error within each iteration as the difference between the assumed volume fraction and final estimated [24, 25].

$$\bar{\boldsymbol{E}} = \boldsymbol{v}^{\gamma+1} - \boldsymbol{v}^{\gamma} \tag{3.79}$$

$$\boldsymbol{error} = |\bar{\boldsymbol{E}}| \tag{3.80}$$

Continuity Equation

$$\frac{\partial u_x}{\partial x} + \frac{\partial u_y}{\partial y} + \frac{\partial u_z}{\partial z} = -\left(\frac{k_c(1-\emptyset)v_f S^* E\bar{C}}{k_c + (1-\emptyset)V_b v_f S^* E}\right)\left(\frac{n_M}{n_A}\right)\frac{M_M}{\rho} \tag{3.81}$$

Equation of Motion (Darcy-Stokes)

$$\rho_A\left(\frac{\partial u_x}{\partial t}\right) + \frac{\partial p}{\partial x} = -\frac{\mu}{k_{xx}}u_x + \mu\left[\frac{\partial^2 u_x}{\partial x^2} + \frac{\partial^2 u_x}{\partial y^2} + \frac{\partial^2 u_x}{\partial z^2}\right] \tag{3.82}$$

$$\rho_A\left(\frac{\partial u_y}{\partial t}\right) + \frac{\partial p}{\partial y} = -\frac{\mu}{k_{yy}}u_y + \mu\left[\frac{\partial^2 u_y}{\partial x^2} + \frac{\partial^2 u_y}{\partial y^2} + \frac{\partial^2 u_y}{\partial z^2}\right] \tag{3.83}$$

$$\rho_A\left(\frac{\partial u_z}{\partial t}\right) + \frac{\partial p}{\partial z} = -\frac{\mu}{k_{zz}}u_z + \mu\left[\frac{\partial^2 u_z}{\partial x^2} + \frac{\partial^2 u_z}{\partial y^2} + \frac{\partial^2 u_z}{\partial z^2}\right] \tag{3.84}$$

Convection-Dispersion Equation

$$-\nabla\bar{C}\cdot\vec{u}+\frac{\partial}{\partial x}\left((D_m+\alpha_x|u_x|)\frac{\partial\bar{C}}{\partial x}\right)+\frac{\partial}{\partial y}\left(\left(D_m+\alpha_y|u_y|\right)\frac{\partial\bar{C}}{\partial y}\right)$$
$$+\frac{\partial}{\partial z}\left((D_m+\alpha_z|u_z|)\frac{\partial\bar{C}}{\partial z}\right)-\left(\frac{k_c(1-\emptyset)v_fS^*E}{k_c+(1-\emptyset)V_bv_fS^*E}\right)\bar{C}$$
$$=\emptyset\frac{\partial\bar{C}}{\partial t} \tag{3.85}$$

Mineral Volume Equation

$$\frac{dv_f}{dt}=-\left(\frac{k_cS^*E\bar{C}}{k_c+(1-\emptyset)V_bv_fS^*E}\right)\left(\frac{n_M}{n_A}\right)\frac{M_M}{\rho} \tag{3.86}$$

Porosity Equation

$$\frac{d\emptyset}{dt}=\left(\frac{k_c(1-\emptyset)v_fS^*E\bar{C}}{k_c+(1-\emptyset)V_bv_fS^*E}\right)\left(\frac{n_M}{n_A}\right)\frac{M_M}{\rho} \tag{3.87}$$

Permeability Equation

$$k=\alpha_k\exp\left(M(\emptyset-\emptyset_0)\right) \tag{3.88}$$

3.5 Discretization of the equations

Using natural indexing with the z direction first then followed by y and then x and neglecting gravity, we discretized the equations with central differencing in the direction of y and z while using backward differencing for pressure and forward differencing for velocity in the direction of x

Continuity Equation

$$\frac{u_{x,m}^{n+1} - u_{x,m-NyNz}^{n+1}}{\Delta x} + \frac{u_{y,m+Nz}^{n+1} - u_{y,m-Nz}^{n+1}}{2\Delta y} + \frac{u_{z,+1}^{n+1} - u_{z,m-1}^{n+1}}{2\Delta z}$$

$$= -\left(\frac{k_c(1-\emptyset_m^{n+1})v_{f,m}^{n+1}S^*EC_m^{n+1}}{k_c + (1-\emptyset_m^{n+1})V_b v_{f,m}^{n+1}S^*E}\right)\left(\frac{n_M}{n_A}\right)\frac{M_M}{\rho} \tag{3.89}$$

Equation of Motion (Darcy-Stokes)

$$\rho_A\left(\frac{u_{x,m}^{n+1} - u_{x,m}^{n}}{\Delta t}\right) + \frac{p_{m+NyNz}^{n+1} - p_m^{n+1}}{\Delta x} + \frac{\mu}{k_{xx,m}^{n+1}}u_{x,m}^{n+1}$$

$$= \mu\left[\frac{u_{x,m+NyNz}^{n+1} - 2u_{x,m}^{n+1} + u_{x,m-NyNz}^{n+1}}{(\Delta x)^2} + \frac{u_{x,m+Nz}^{n+1} - 2u_{x,m}^{n+1} + u_{x,m-Nz}^{n+1}}{(\Delta y)^2}\right.$$

$$\left. + \frac{u_{x,m+1}^{n+1} - 2u_{x,m}^{n+1} + u_{x,m-1}^{n+1}}{(\Delta z)^2}\right] \tag{3.90}$$

$$\rho_A\left(\frac{u_{y,m}^{n+1} - u_{y,m}^{n}}{\Delta t}\right) + \frac{p_{m+Nz}^{n+1} - p_{m-Nz}^{n+1}}{2\Delta y} + \frac{\mu}{k_{yy,m}^{n+1}}u_{y,m}^{n+1}$$

$$= \mu\left[\frac{u_{y,m+NyNz}^{n+1} - 2u_{y,m}^{n+1} + u_{y,m-NyNz}^{n+1}}{(\Delta x)^2} + \frac{u_{y,m+Nz}^{n+1} - 2u_{y,m}^{n+1} + u_{y,m-Nz}^{n+1}}{(\Delta y)^2}\right.$$

$$\left. + \frac{u_{y,m+1}^{n+1} - 2u_{y,m}^{n+1} + u_{y,m-1}^{n+1}}{(\Delta z)^2}\right] \tag{3.91}$$

$$\rho_A\left(\frac{u_{z,m}^{n+1}-u_{z,m}^{n}}{\Delta t}\right)+\frac{p_{m+1}^{n+1}-p_{m-1}^{n+1}}{2\Delta z}+\frac{\mu}{k_{zz,m}^{n+1}}u_{z,m}^{n+1}$$

$$=\mu\left[\frac{u_{z,m+NyNz}^{n+1}-2u_{z,m}^{n+1}+u_{z,m-NyNz}^{n+1}}{(\Delta x)^2}+\frac{u_{z,m+Nz}^{n+1}-2u_{z,m}^{n+1}+u_{z,m-Nz}^{n+1}}{(\Delta y)^2}\right.$$

$$\left.+\frac{u_{z,m+1}^{n+1}-2u_{z,m}^{n+1}+u_{z,m-1}^{n+1}}{(\Delta z)^2}\right] \tag{3.92}$$

Convection-Dispersion Equation

$$-u_{x,m}^{n+1}\left(\frac{C_m^{n+1}-C_{m-NyNz}^{n+1}}{\Delta x}\right)-u_{y,m}^{n+1}\left(\frac{C_{m+Nz}^{n+1}-C_{m-Nz}^{n+1}}{2\Delta y}\right)-u_{z,m}^{n+1}\left(\frac{C_{m+1}^{n+1}-C_{m-1}^{n+1}}{2\Delta z}\right)$$

$$+\left(\left\{\frac{D_m}{(\Delta x)^2}+\alpha_x\left|\frac{u_{x,m+NyNz}^{n+1}+u_{x,m}^{n+1}}{2(\Delta x)^2}\right|\right\}\left(C_{m+NyNz}^{n+1}-C_m^{n+1}\right)\right.$$

$$\left.-\left\{\frac{D_m}{(\Delta x)^2}+\alpha_x\left|\frac{u_{x,m-NyNz}^{n+1}+u_{x,m}^{n+1}}{2(\Delta x)^2}\right|\right\}\left(C_m^{n+1}-C_{m-NyNz}^{n+1}\right)\right)$$

$$+\left(\left\{\frac{D_m}{(\Delta y)^2}+\alpha_y\left|\frac{u_{y,m+Nz}^{n+1}+u_{y,m}^{n+1}}{2(\Delta y)^2}\right|\right\}\left(C_{m+Nz}^{n+1}-C_m^{n+1}\right)\right.$$

$$\left.-\left\{\frac{D_m}{(\Delta y)^2}+\alpha_y\left|\frac{u_{y,m-Nz}^{n+1}+u_{y,m}^{n+1}}{2(\Delta y)^2}\right|\right\}\left(C_m^{n+1}-C_{m-Nz}^{n+1}\right)\right)$$

$$+\left(\left\{\frac{D_m}{(\Delta z)^2}+\alpha_z\left|\frac{u_{z,m+1}^{n+1}+u_{z,m}^{n+1}}{2(\Delta z)^2}\right|\right\}\left(C_{m+1}^{n+1}-C_m^{n+1}\right)\right.$$

$$\left.-\left\{\frac{D_m}{(\Delta z)^2}+\alpha_z\left|\frac{u_{z,m+1}^{n+1}+u_{z,m}^{n+1}}{2(\Delta z)^2}\right|\right\}\left(C_m^{n+1}-C_{m-1}^{n+1}\right)\right)$$

$$-\left(\frac{k_c(1-\emptyset_m^{n+1})v_{f,m}^{n+1}S^*E}{k_c+(1-\emptyset_m^{n+1})V_b v_{f,m}^{n+1}S^*E}\right)C_m^{n+1}$$

$$=\emptyset_m^{n+1}\left(\frac{C_m^{n+1}-C_m^{n}}{\Delta t}\right) \tag{3.93}$$

Mineral Volume Equation

$$\frac{v_{f,m}^{n+1} - v_{f,m}^{n}}{\Delta t} = -\left(\frac{k_c v_{f,m}^{n+1} S^* E C_m^{n+1}}{k_c + (1 - \emptyset_m^{n+1}) V_b v_{f,m}^{n+1} S^* E}\right)\left(\frac{n_M}{n_A}\right)\frac{M_M}{\rho_M} \tag{3.94}$$

Porosity Equation

$$\frac{\emptyset_m^{n+1} - \emptyset_m^{n}}{\Delta t} = \left(\frac{k_c (1 - \emptyset_m^{n+1}) v_{f,m}^{n+1} S^* E C_m^{n+1}}{k_c + (1 - \emptyset_m^{n+1}) V_b v_{f,m}^{n+1} S^* E}\right)\left(\frac{n_M}{n_A}\right)\frac{M_M}{\rho_M} \tag{3.95}$$

Permeability Equation

$$k_m^{n+1} = \alpha_k \exp\left(M(\emptyset_m^{n+1} - \emptyset_0)\right) \tag{3.96}$$

In order to allow for easy handling of the boundary conditions, we rewrite the discretized equations in terms of “transmissibilities”

Let,

$$T_{mm+NyNz} = T_{mm-NyNz} = \frac{1}{\Delta x}, \qquad T_{mm+Nz} = T_{mm-Nz} = \frac{1}{2\Delta y},$$
$$T_{mm+1} = T_{mm-1} = \frac{1}{2\Delta z}$$

So the continuity Equation

$$\frac{u_{x,m}^{n+1} - u_{x,m-NyNz}^{n+1}}{\Delta x} + \frac{u_{y,m+Nz}^{n+1} - u_{y,m-Nz}^{n+1}}{2\Delta y} + \frac{u_{z,m+1}^{n+1} - u_{z,m-1}^{n+1}}{2\Delta z}$$
$$= -\left(\frac{k_c (1 - \emptyset_m^{n+1}) v_{f,m}^{n+1} S^* E C_m^{n+1}}{k_c + (1 - \emptyset_m^{n+1}) V_b v_{f,m}^{n+1} S^* E}\right)\left(\frac{n_M}{n_A}\right)\frac{M_M}{\rho}$$

Becomes

$$\left[-T_{mm-NyNz}u_{x,m-NyNz}^{n+1}+T_{mm-NyNz}u_{x,m}^{n+1}\right]$$
$$+\left[-T_{mm-Nz}u_{y,m-Nz}^{n+1}-(T_{mm-Nz}-T_{mm+Nz})u_{y,m}^{n+1}+T_{mm+Nz}u_{y,m+Nz}^{n+1}\right]$$
$$+\left[-T_{mm-1}u_{z,m-1}^{n+1}-(T_{mm-1}-T_{mm+1})u_{z,m}^{n+1}+T_{mm+1}u_{z,m+1}^{n+1}\right]$$
$$=-\left(\frac{k_c(1-\emptyset_m^{n+1})v_{f,m}^{n+1}S^*EC_m^{n+1}}{k_c+(1-\emptyset_m^{n+1})V_bv_{f,m}^{n+1}S^*E}\right)\left(\frac{n_M}{n_A}\right)\frac{M_M}{\rho} \tag{3.97}$$

Equation of Motion (Darcy-Navier-Stokes)

$$\rho_A\left(\frac{u_{x,m}^{n+1}-u_{x,m}^{n}}{\Delta t}\right)+\frac{p_{m+NyNz}^{n+1}-p_m^{n+1}}{\Delta x}+\frac{\mu}{k_{xx,m}^{n+1}}u_{x,m}^{n+1}$$
$$=\mu\left[\frac{u_{x,m+NyNz}^{n+1}-2u_{x,m}^{n+1}+u_{x,m-NyNz}^{n+1}}{(\Delta x)^2}+\frac{u_{x,m+Nz}^{n+1}-2u_{x,m}^{n+1}+u_{x,m-Nz}^{n+1}}{(\Delta y)^2}\right.$$
$$\left.+\frac{u_{x,m+1}^{n+1}-2u_{x,m}^{n+1}+u_{x,m-1}^{n+1}}{(\Delta z)^2}\right]$$

Becomes

$$-\mu T_{mm-NyNz}^2u_{x,m-NyNz}^{n+1}-4\mu T_{mm-Nz}^2u_{x,m-Nz}^{n+1}-4\mu T_{mm-1}^2u_{x,m-1}^{n+1}$$
$$+\left(\mu T_{mm-NyNz}^2+4\mu T_{mm-Nz}^2+4\mu T_{mm-1}^2+4\mu T_{mm+1}^2+4\mu T_{mm+Nz}^2\right.$$
$$\left.+\mu T_{mm+NyNz}^2+\frac{\mu}{k_{xx,m}^{n+1}}+\frac{\rho_A}{\Delta t}\right)u_{x,m}^{n+1}-4\mu T_{mm+1}^2u_{x,m+1}^{n+1}$$
$$-4\mu T_{mm+Nz}^2u_{x,m+Nz}^{n+1}-\mu T_{mm+NyNz}^2u_{x,m+NyNz}^{n+1}-T_{mm+NyNz}p_m^{n+1}$$
$$+T_{mm+NyNz}p_{m+NyNz}^{n+1}=\left(\frac{\rho_A}{\Delta t}\right)u_{x,m}^{n} \tag{3.98}$$

$$\rho_A\left(\frac{u_{y,m}^{n+1}-u_{y,m}^{n}}{\Delta t}\right)+\frac{p_{m+Nz}^{n+1}-p_{m-Nz}^{n+1}}{2\Delta y}+\frac{\mu}{k_{yy,m}^{n+1}}u_{y,m}^{n+1}$$

$$=\mu\left[\frac{u_{y,m+NyNz}^{n+1}-2u_{y,m}^{n+1}+u_{y,m-NyNz}^{n+1}}{(\Delta x)^2}+\frac{u_{y,m+Nz}^{n+1}-2u_{y,m}^{n+1}+u_{y,m-Nz}^{n+1}}{(\Delta y)^2}\right.$$

$$\left.+\frac{u_{y,m+1}^{n+1}-2u_{y,m}^{n+1}+u_{y,m-1}^{n+1}}{(\Delta z)^2}\right]$$

Becomes

$$\begin{aligned}
&-\mu T_{mm-NyNz}^2 u_{y,m-NyNz}^{n+1}-4\mu T_{mm-Nz}^2 u_{y,m-Nz}^{n+1}-4\mu T_{mm-1}^2 u_{y,m-1}^{n+1}\\
&\quad+\left(\mu T_{mm-NyNz}^2+4\mu T_{mm-Nz}^2+4\mu T_{mm-1}^2+4\mu T_{mm+1}^2+4\mu T_{mm+Nz}^2\right.\\
&\quad\left.+\mu T_{mm+NyNz}^2+\frac{\mu}{k_{yy,m}^{n+1}}+\frac{\rho_A}{\Delta t}\right)u_{y,m}^{n+1}-4\mu T_{mm+1}^2 u_{y,m+1}^{n+1}\\
&\quad-4\mu T_{mm+Nz}^2 u_{y,m+Nz}^{n+1}-\mu T_{mm+NyNz}^2 u_{y,m+NyNz}^{n+1}-T_{mm-Nz}p_{m-Nz}^{n+1}\\
&\quad-(T_{mm-Nz}-T_{mm+Nz})p_m^{n+1}+T_{mm+Nz}p_{m+Nz}^{n+1}\\
&\quad=\left(\frac{\rho_A}{\Delta t}\right)u_{y,m}^{n}
\end{aligned}\tag{3.98}$$

$$\rho_A\left(\frac{u_{z,m}^{n+1}-u_{z,m}^{n}}{\Delta t}\right)+\frac{p_{m+1}^{n+1}-p_{m-1}^{n+1}}{2\Delta z}+\frac{\mu}{k_{zz,m}^{n+1}}u_{z,m}^{n+1}$$

$$=\mu\left[\frac{u_{z,m+NyNz}^{n+1}-2u_{z,m}^{n+1}+u_{z,m-NyNz}^{n+1}}{(\Delta x)^2}+\frac{u_{z,m+Nz}^{n+1}-2u_{z,m}^{n+1}+u_{z,m-Nz}^{n+1}}{(\Delta y)^2}\right.$$

$$\left.+\frac{u_{z,m+1}^{n+1}-2u_{z,m}^{n+1}+u_{z,m-1}^{n+1}}{(\Delta z)^2}\right]$$

Becomes

$$
\begin{aligned}
-\mu T^2_{mm-NyNz} u^{n+1}_{z,m-NyNz} - 4\mu T^2_{mm-Nz} u^{n+1}_{z,m-Nz} - 4\mu T^2_{mm-1} u^{n+1}_{z,m-1} \\
+ \Bigg(\mu T^2_{mm-NyNz} + 4\mu T^2_{mm-Nz} + 4\mu T^2_{mm-1} + 4\mu T^2_{mm+1} + 4\mu T^2_{mm+Nz} \\
+ \mu T^2_{mm+NyNz} + \frac{\mu}{k^{n+1}_{zz,m}} + \frac{\rho_A}{\Delta t} \Bigg) u^{n+1}_{z,m} - 4\mu T^2_{mm+1} u^{n+1}_{z,m+1} \\
- 4\mu T^2_{mm+Nz} u^{n+1}_{z,m+Nz} - \mu T^2_{mm+NyNz} u^{n+1}_{z,m+NyNz} - T_{mm-1} p^{n+1}_{m-1} \\
- (T_{mm-1} - T_{mm+1}) p^{n+1}_{m} + T_{mm+1} p^{n+1}_{m+1} \\
= \left(\frac{\rho_A}{\Delta t} \right) u^{n}_{z,m}
\end{aligned}
\tag{3.99}
$$

For Convection-Dispersion-Reaction Equation we defined mean velocities

$$
u^{n+1}_{xmm-NyNz} = \begin{cases} u^{n+1}_{xm-NyNz} & if \quad C^{n+1}_{m-NyNz} \geq C^{n+1}_{m} \\ u^{n+1}_{xm} & otherwise \end{cases},
$$

$$
u^{n+1}_{xmm+NyNz} = \begin{cases} u^{n+1}_{xm+NyNz} & if \quad C^{n+1}_{m+NyNz} \geq C^{n+1}_{m} \\ u^{n+1}_{xm} & otherwise \end{cases}
$$

$$
u^{n+1}_{ymm-Nz} = \begin{cases} u^{n+1}_{ym-Nz} & if \quad C^{n+1}_{m-Nz} \geq C^{n+1}_{m} \\ u^{n+1}_{ym} & otherwise \end{cases},
$$

$$
u^{n+1}_{ymm+Nz} = \begin{cases} u^{n+1}_{ym+Nz} & if \quad C^{n+1}_{m+Nz} \geq C^{n+1}_{m} \\ u^{n+1}_{ym} & otherwise \end{cases}
$$

$$
u^{n+1}_{zmm-1} = \begin{cases} u^{n+1}_{zm-1} & if \quad C^{n+1}_{m-1} \geq C^{n+1}_{m} \\ u^{n+1}_{zm} & otherwise \end{cases},
$$

$$
u^{n+1}_{zmm+1} = \begin{cases} u^{n+1}_{zm+1} & if \quad C^{n+1}_{m+1} \geq C^{n+1}_{m} \\ u^{n+1}_{zm} & otherwise \end{cases}
$$

Then we defined

$$
T_{mm-NyNz} = \frac{u^{n+1}_{x,m}}{\Delta x}, \qquad T_{mm+Nz} = T_{mm-Nz} = \frac{u^{n+1}_{y,m}}{2\Delta y}, \qquad T_{mm+1} = \ T_{mm-1} = \frac{u^{n+1}_{z,m}}{2\Delta z}
$$

$$
DT_{mm+NyNz} = \frac{D_m + \ \alpha_x \left| u^{n+1}_{xmm+NyNz} \right|}{(\Delta x)^2}, \qquad DT_{mm-NyNz} = \frac{D_m + \ \alpha_x \left| u^{n+1}_{xmm-NyNz} \right|}{(\Delta x)^2},
$$

$$DT_{mm+Nz} = \frac{D_m + \alpha_y \left|u_{ymm+Nz}^{n+1}\right|}{(\Delta y)^2}, \qquad DT_{mm-Nz} = \frac{D_m + \alpha_y \left|u_{ymm-Nz}^{n+1}\right|}{(\Delta y)^2},$$

$$DT_{mm+1} = \frac{D_m + \alpha_z |u_{zmm+1}^{n+1}|}{(\Delta z)^2}, \quad DT_{mm-1} = \frac{D_m + \alpha_z |u_{zmm-1}^{n+1}|}{(\Delta z)^2}$$

We have

$$\begin{aligned}
&-\left[-T_{mm-NyNz}C_{m-NyNz}^{n+1} + T_{mm-NyNz}C_m^{n+1}\right] \\
&\quad - \left[-T_{mm-Nz}C_{m-Nz}^{n+1} - (T_{mm-Nz} - T_{mm+Nz})C_m^{n+1} + T_{mm+Nz}C_{m+Nz}^{n+1}\right] \\
&\quad - \left[-T_{mm-1}C_{m-1}^{n+1} - (T_{mm-1} - T_{mm+1})C_m^{n+1} + T_{mm+1}C_{m+1}^{n+1}\right] \\
&\quad + DT_{mm-NyNz}C_{m-NyNz}^{n+1} + DT_{mm-Nz}C_{m-Nz}^{n+1} + DT_{mm-1}C_{m-1}^{n+1} \\
&\quad - \left(DT_{mm-NyNz} + DT_{mm-Nz} + DT_{mm-1} + DT_{mm+1} + DT_{mm+Nz}\right. \\
&\quad \left. + DT_{mm+NyNz}\right)C_m^{n+1} + DT_{mm+1}C_{m+1}^{n+1} + DT_{mm+Nz}C_{m+Nz}^{n+1} \\
&\quad + DT_{mm+NyNz}C_{m+NyNz}^{n+1} - \left(\frac{k_c(1-\emptyset_m^{n+1})v_{f,m}^{n+1}S^*E}{k_c + (1-\emptyset_m^{n+1})V_b v_{f,m}^{n+1}S^*E}\right)C_m^{n+1} \\
&\quad = \emptyset_m^{n+1}\left(\frac{C_m^{n+1} - C_m^n}{\Delta t}\right)
\end{aligned} \tag{3.100}$$

Mineral Volume Equation

$$\frac{v_{f,m}^{n+1} - v_{f,m}^n}{\Delta t} = -\left(\frac{k_c v_{f,m}^{n+1} S^* E C_m^{n+1}}{k_c + (1-\emptyset_m^{n+1})V_b v_{f,m}^{n+1} S^* E}\right)\left(\frac{n_M}{n_A}\right)\frac{M_M}{\rho_M} \tag{3.101}$$

Porosity Equation

$$\frac{\emptyset_m^{n+1} - \emptyset_m^n}{\Delta t} = \left(\frac{k_c(1-\emptyset_m^{n+1})v_{f,m}^{n+1} S^* E C_m^{n+1}}{k_c + (1-\emptyset_m^{n+1})V_b v_{f,m}^{n+1} S^* E}\right)\left(\frac{n_M}{n_A}\right)\frac{M_M}{\rho_M} \tag{3.102}$$

Permeability Equation

$$k_m^{n+1} = \alpha_k \exp\left(M(\emptyset_m^{n+1} - \emptyset_0)\right) \tag{3.103}$$

To simplify the computation, we maintain the porosity and permeability in the time step before the current one we are computing. Then we solve the Brinkman's equation for

pressure and velocity distribution. The fifth and sixth equations are then solved iteratively for the concentration and mineral volume distribution, then porosity and permeability field are solved for by simple vector operations.

We have 8 variables $(u_x, u_y, u_z, p, C, v_f, \emptyset, k)$ to be determined in each grid block, 4 (u_x, u_y, u_z, p) of which are to be determined simultaneously.

The system of equations thus become

$$\begin{aligned}
&\left[-T_{mm-NyNz}u_{x,m-NyNz}^{n+1} + T_{mm-NyNz}u_{x,m}^{n+1}\right] \\
&\qquad + \left[-T_{mm-Nz}u_{y,m-Nz}^{n+1} - (T_{mm-Nz} - T_{mm+Nz})u_{y,m}^{n+1} + T_{mm+Nz}u_{y,m+Nz}^{n+1}\right] \\
&\qquad + \left[-T_{mm-1}u_{z,m-1}^{n+1} - (T_{mm-1} - T_{mm+1})u_{z,m}^{n+1} + T_{mm+1}u_{z,m+1}^{n+1}\right] \\
&\qquad = -\left(\frac{k_c(1-\emptyset_m^n)v_{f,m}^n S^* E C_m^n}{k_c + (1-\emptyset_m^n)V_b v_{f,m}^n S^* E}\right)\left(\frac{n_M}{n_A}\right)\frac{M_M}{\rho} \qquad (3.104)
\end{aligned}$$

Equation of Motion (Darcy- Stokes)

$$\begin{aligned}
&-\mu T_{mm-NyNz}^2 u_{x,m-NyNz}^{n+1} - 4\mu T_{mm-Nz}^2 u_{x,m-Nz}^{n+1} - 4\mu T_{mm-1}^2 u_{x,m-1}^{n+1} \\
&\qquad + \left(\mu T_{mm-NyNz}^2 + 4\mu T_{mm-Nz}^2 + 4\mu T_{mm-1}^2 + 4\mu T_{mm+1}^2 + 4\mu T_{mm+Nz}^2\right. \\
&\qquad \left. + \mu T_{mm+NyNz}^2 + \frac{\mu}{k_{xx,m}^n} + \frac{\rho_A}{\Delta t}\right) u_{x,m}^{n+1} - 4\mu T_{mm+1}^2 u_{x,m+1}^{n+1} \\
&\qquad - 4\mu T_{mm+Nz}^2 u_{x,m+Nz}^{n+1} - \mu T_{mm+NyNz}^2 u_{x,m+NyNz}^{n+1} - T_{mm+NyNz} p_m^{n+1} \\
&\qquad + T_{mm+NyNz} p_{m+NyNz}^{n+1} = \left(\frac{\rho_A}{\Delta t}\right) u_{x,m}^n \qquad (3.105)
\end{aligned}$$

$$
\begin{aligned}
-\mu T^2_{mm-NyNz} u^{n+1}_{y,m-NyNz} - 4\mu T^2_{mm-Nz} u^{n+1}_{y,m-Nz} - 4\mu T^2_{mm-1} u^{n+1}_{y,m-1} \\
+ \Bigg(\mu T^2_{mm-NyNz} + 4\mu T^2_{mm-Nz} + 4\mu T^2_{mm-1} + 4\mu T^2_{mm+1} + 4\mu T^2_{mm+Nz} \\
+ \mu T^2_{mm+NyNz} + \frac{\mu}{k^n_{yy,m}} + \frac{\rho_A}{\Delta t} \Bigg) u^{n+1}_{y,m} - 4\mu T^2_{mm+1} u^{n+1}_{y,m+1} \\
- 4\mu T^2_{mm+Nz} u^{n+1}_{y,m+Nz} - \mu T^2_{mm+NyNz} u^{n+1}_{y,m+NyNz} - T_{mm-Nz} p^{n+1}_{m-Nz} \\
- (T_{mm-Nz} - T_{mm+Nz}) p^{n+1}_m + T_{mm+Nz} p^{n+1}_{m+Nz} \\
= \left(\frac{\rho_A}{\Delta t}\right) u^n_{y,m}
\end{aligned} \tag{3.106}
$$

$$
\begin{aligned}
-\mu T^2_{mm-NyNz} u^{n+1}_{z,m-NyNz} - 4\mu T^2_{mm-Nz} u^{n+1}_{z,m-Nz} - 4\mu T^2_{mm-1} u^{n+1}_{z,m-1} \\
+ \Bigg(\mu T^2_{mm-NyNz} + 4\mu T^2_{mm-Nz} + 4\mu T^2_{mm-1} + 4\mu T^2_{mm+1} + 4\mu T^2_{mm+Nz} \\
+ \mu T^2_{mm+NyNz} + \frac{\mu}{k^n_{zz,m}} + \frac{\rho_A}{\Delta t} \Bigg) u^{n+1}_{z,m} - 4\mu T^2_{mm+1} u^{n+1}_{z,m+1} \\
- 4\mu T^2_{mm+Nz} u^{n+1}_{z,m+Nz} - \mu T^2_{mm+NyNz} u^{n+1}_{z,m+NyNz} - T_{mm-1} p^{n+1}_{m-1} \\
- (T_{mm-1} - T_{mm+1}) p^{n+1}_m + T_{mm+1} p^{n+1}_{m+1} \\
= \left(\frac{\rho_A}{\Delta t}\right) u^n_{z,m}
\end{aligned} \tag{3.107}
$$

Incorporating the boundary conditions,

$(h\ countes\ in\ direction\ x,\ \ i\ countes\ in\ y\ and\ j\ countes\ in\ z)$

When $h = 1$

$u^{n+1}_{x,m-(NyNz)/2} = 0 \rightarrow u^{n+1}_{x,m} = -u^{n+1}_{x,m-NyNz}$, (No flow across)

$u^{n+1}_{y,m-(NyNz)/2} = 0 \rightarrow u^{n+1}_{y,m} = -u^{n+1}_{y,m-NyNz}$,

$u^{n+1}_{z,m-(NyNz)/2} = 0 \rightarrow u^{n+1}_{z,m} = -u^{n+1}_{z,m-NyNz}$ (No slip)

$$\left[2T_{mm-NyNz}u_{x,m}^{n+1}\right] + \left[-T_{mm-Nz}u_{y,m-Nz}^{n+1} - (T_{mm-Nz} - T_{mm+Nz})u_{y,m}^{n+1} + T_{mm+Nz}u_{y,m+Nz}^{n+1}\right] + \left[-T_{mm-1}u_{z,m-1}^{n+1} - (T_{mm-1} - T_{mm+1})u_{z,m}^{n+1} + T_{mm+1}u_{z,m+1}^{n+1}\right] = -\left(\frac{k_c(1-\emptyset_m^n)v_{f,m}^n S^* E C_m^n}{k_c + (1-\emptyset_m^n)V_b v_{f,m}^n S^* E}\right)\left(\frac{n_M}{n_A}\right)\frac{M_M}{\rho} \quad (3.108)$$

Equation of Motion (Darcy- Stokes)

$$\frac{\partial^2 u_x}{\partial x^2} = \frac{\frac{u_{x,m+NyNz}^{n+1} - u_{x,m}^{n+1}}{\Delta x} - \frac{u_{x,m}^{n+1} - u_{x,m-NyNz}^{n+1}}{\Delta x}}{\Delta x} = \frac{\frac{u_{x,m+NyNz}^{n+1} - u_{x,m}^{n+1}}{\Delta x} - \frac{2u_{x,m}^{n+1}}{\Delta x}}{\Delta x}$$

$$-\mu T_{mm-Nz}^2 u_{x,m-Nz}^{n+1} - \mu T_{mm-1}^2 u_{x,m-1}^{n+1} + \left(2\mu T_{mm-NyNz}^2 + \mu T_{mm-Nz}^2 + \mu T_{mm-1}^2 + \mu T_{mm+1}^2 + \mu T_{mm+Nz}^2 + \mu T_{mm+NyNz}^2 + \frac{\mu}{k_{xx,m}^n} + \frac{\rho_A}{\Delta t}\right)u_{x,m}^{n+1} - \mu T_{mm+1}^2 u_{x,m+1}^{n+1} - \mu T_{mm+Nz}^2 u_{x,m+Nz}^{n+1} - \mu T_{mm+NyNz}^2 u_{x,m+NyNz}^{n+1} - T_{mm+NyNz}p_m^{n+1} + T_{mm+NyNz}p_{m+NyNz}^{n+1} = \left(\frac{\rho_A}{\Delta t}\right)u_{x,m}^n \quad (3.109)$$

Similarly for the directions of y and z we have:

$$-4\mu T_{mm-Nz}^2 u_{y,m-Nz}^{n+1} - 4\mu T_{mm-1}^2 u_{y,m-1}^{n+1} + \left(2\mu T_{mm-NyNz}^2 + 4\mu T_{mm-Nz}^2 + 4\mu T_{mm-1}^2 + 4\mu T_{mm+1}^2 + 4\mu T_{mm+Nz}^2 + \mu T_{mm+NyNz}^2 + \frac{\mu}{k_{yy,m}^n} + \frac{\rho_A}{\Delta t}\right)u_{y,m}^{n+1} - 4\mu T_{mm+1}^2 u_{y,m+1}^{n+1} - 4\mu T_{mm+Nz}^2 u_{y,m+Nz}^{n+1} - \mu T_{mm+NyNz}^2 u_{y,m+NyNz}^{n+1} - T_{mm-Nz}p_{m-Nz}^{n+1} - (T_{mm-Nz} - T_{mm+Nz})p_m^{n+1} + T_{mm+Nz}p_{m+Nz}^{n+1} = \left(\frac{\rho_A}{\Delta t}\right)u_{y,m}^n \quad (3.110)$$

$$
\begin{aligned}
&-4\mu T^2_{mm-Nz}u^{n+1}_{z,m-Nz} - 4\mu T^2_{mm-1}u^{n+1}_{z,m-1} \\
&\quad + \Big(2\mu T^2_{mm-NyNz} + 4\mu T^2_{mm-Nz} + 4\mu T^2_{mm-1} + 4\mu T^2_{mm+1} + 4\mu T^2_{mm+Nz} \\
&\quad + \mu T^2_{mm+NyNz} + \frac{\mu}{k^n_{zz,m}} + \frac{\rho_A}{\Delta t}\Big)u^{n+1}_{z,m} - 4\mu T^2_{mm+1}u^{n+1}_{z,m+1} \\
&\quad - 4\mu T^2_{mm+Nz}u^{n+1}_{z,m+Nz} - \mu T^2_{mm+NyNz}u^{n+1}_{z,m+NyNz} - T_{mm-1}p^{n+1}_{m-1} \\
&\quad - (T_{mm-1} - T_{mm+1})p^{n+1}_{m} + T_{mm+1}p^{n+1}_{m+1} \\
&\quad = \left(\frac{\rho_A}{\Delta t}\right)u^n_{z,m} \qquad (3.111)
\end{aligned}
$$

Similarly for $i = 1, i = Ny, j = 1\ and\ j = Nz$

Hence to impose a no flow and no slip condition across all boundaries we only need to switch of the T(s) and switch on the BT(s) in the equations in the form:

$$
\begin{aligned}
&\left[-T_{mm-NyNz}u^{n+1}_{x,m-NyNz} + \left(T_{mm-NyNz} + BT_{mm-NyNz}\right)u^{n+1}_{x,m}\right] \\
&\quad + \left[-T_{mm-Nz}u^{n+1}_{y,m-Nz} - (T_{mm-Nz} - T_{mm+Nz})u^{n+1}_{y,m} + T_{mm+Nz}u^{n+1}_{y,m+Nz}\right] \\
&\quad + \left[-T_{mm-1}u^{n+1}_{z,m-1} - (T_{mm-1} - T_{mm+1})u^{n+1}_{z,m} + T_{mm+1}u^{n+1}_{z,m+1}\right] \\
&\quad = -\left(\frac{k_c(1-\emptyset^n_m)v^n_{f,m}S^*EC^n_m}{k_c + (1-\emptyset^n_m)V_b v^n_{f,m}S^*E}\right)\left(\frac{n_M}{n_A}\right)\frac{M_M}{\rho} \qquad (3.112)
\end{aligned}
$$

Equation of Motion (Darcy- Stokes)

$$
\begin{aligned}
&-\mu T^2_{mm-NyNz}u^{n+1}_{x,m-NyNz} - 4\mu T^2_{mm-Nz}u^{n+1}_{x,m-Nz} - 4\mu T^2_{mm-1}u^{n+1}_{x,m-1} \\
&\quad + \left(\mu\left(T^2_{mm-NyNz} + \frac{BT^2_{mm-NyNz}}{2}\right) + \mu\left(4T^2_{mm-Nz} + \frac{BT^2_{mm-Nz}}{2}\right)\right. \\
&\quad + \mu\left(4T^2_{mm-1} + \frac{BT^2_{mm-1}}{2}\right) + \mu\left(4T^2_{mm+1} + \frac{BT^2_{mm+1}}{2}\right) \\
&\quad + \mu\left(4T^2_{mm+Nz} + \frac{BT^2_{mm+Nz}}{2}\right) + \mu\left(T^2_{mm+NyNz} + \frac{BT^2_{mm+NyNz}}{2}\right) + \frac{\mu}{k^n_{xx,m}} \\
&\quad \left. + \frac{\rho_A}{\Delta t}\right)u^{n+1}_{x,m} - 4\mu T^2_{mm+1}u^{n+1}_{x,m+1} - 4\mu T^2_{mm+Nz}u^{n+1}_{x,m+Nz} \\
&\quad - \mu T^2_{mm+NyNz}u^{n+1}_{x,m+NyNz} - T_{mm+NyNz}p^{n+1}_{m} + T_{mm+NyNz}p^{n+1}_{m+NyNz} \\
&\quad = \left(\frac{\rho_A}{\Delta t}\right)u^n_{x,m} \qquad (3.113)
\end{aligned}
$$

$$
\begin{aligned}
&-\mu T_{mm-NyNz}^{2} u_{y,m-NyNz}^{n+1} - 4\mu T_{mm-Nz}^{2} u_{y,m-Nz}^{n+1} - 4\mu T_{mm-1}^{2} u_{y,m-1}^{n+1} \\
&\quad + \left(\mu\left(T_{mm-NyNz}^{2} + \frac{BT_{mm-NyNz}^{2}}{2}\right) + \mu\left(4T_{mm-Nz}^{2} + \frac{BT_{mm-Nz}^{2}}{2}\right)\right. \\
&\quad + \mu\left(4T_{mm-1}^{2} + \frac{BT_{mm-1}^{2}}{2}\right) + \mu\left(4T_{mm+1}^{2} + \frac{BT_{mm+1}^{2}}{2}\right) \\
&\quad + \mu\left(4T_{mm+Nz}^{2} + \frac{BT_{mm+Nz}^{2}}{2}\right) + \mu\left(T_{mm+NyNz}^{2} + \frac{BT_{mm+NyNz}^{2}}{2}\right) + \frac{\mu}{k_{yy,m}^{n}} \\
&\quad \left. + \frac{\rho_A}{\Delta t}\right) u_{y,m}^{n+1} - 4\mu T_{mm+1}^{2} u_{y,m+1}^{n+1} - 4\mu T_{mm+Nz}^{2} u_{y,m+Nz}^{n+1} \\
&\quad - \mu T_{mm+NyNz}^{2} u_{y,m+NyNz}^{n+1} - T_{mm-Nz} p_{m-Nz}^{n+1} - (T_{mm-Nz} - T_{mm+Nz}) p_{m}^{n+1} \\
&\quad + T_{mm+Nz} p_{m+Nz}^{n+1} = \left(\frac{\rho_A}{\Delta t}\right) u_{y,m}^{n} \qquad (3.114)
\end{aligned}
$$

$$
\begin{aligned}
&-\mu T_{mm-NyNz}^{2} u_{z,m-NyNz}^{n+1} - 4\mu T_{mm-Nz}^{2} u_{z,m-Nz}^{n+1} - 4\mu T_{mm-1}^{2} u_{z,m-1}^{n+1} \\
&\quad + \left(\mu\left(T_{mm-NyNz}^{2} + \frac{BT_{mm-NyNz}^{2}}{2}\right) + \mu\left(4T_{mm-Nz}^{2} + \frac{BT_{mm-Nz}^{2}}{2}\right)\right. \\
&\quad + \mu\left(4T_{mm-1}^{2} + \frac{BT_{mm-1}^{2}}{2}\right) + \mu\left(4T_{mm+1}^{2} + \frac{BT_{mm+1}^{2}}{2}\right) \\
&\quad + \mu\left(4T_{mm+Nz}^{2} + \frac{BT_{mm+Nz}^{2}}{2}\right) + \mu\left(T_{mm+NyNz}^{2} + \frac{BT_{mm+NyNz}^{2}}{2}\right) + \frac{\mu}{k_{zz,m}^{n}} \\
&\quad \left. + \frac{\rho_A}{\Delta t}\right) u_{z,m}^{n+1} - 4\mu T_{mm+1}^{2} u_{z,m+1}^{n+1} - 4\mu T_{mm+Nz}^{2} u_{z,m+Nz}^{n+1} \\
&\quad - \mu T_{mm+NyNz}^{2} u_{z,m+NyNz}^{n+1} - T_{mm-1} p_{m-1}^{n+1} - (T_{mm-1} - T_{mm+1}) p_{m}^{n+1} \\
&\quad + T_{mm+1} p_{m+1}^{n+1} = \left(\frac{\rho_A}{\Delta t}\right) u_{z,m}^{n} \qquad (3.115)
\end{aligned}
$$

With

$$
T_{mm-NyNz}^{n+1} = \begin{cases} \dfrac{1}{\Delta x}\ ; & h \neq 1 \\ 0; & otherwise \end{cases}, \qquad T_{mm+NyNz}^{n+1} = \begin{cases} \dfrac{1}{\Delta x}\ ; & h \neq Nx \\ 0; & otherwise \end{cases}
$$

$$
T_{mm-Nz}^{n+1} = \begin{cases} \dfrac{1}{2\Delta y}\ ; & i \neq 1 \\ 0; & otherwise \end{cases}, \qquad T_{mm+Nz}^{n+1} = \begin{cases} \dfrac{1}{2\Delta y}\ ; & i \neq Ny \\ 0; & otherwise \end{cases}
$$

$$T_{mm-1}^{n+1} = \begin{cases} \frac{1}{2\Delta z}\ ;\ j \neq 1 \\ 0;\quad otherwise \end{cases}, \qquad T_{mm+1}^{n+1} = \begin{cases} \frac{1}{2\Delta z}\ ;\ j \neq Nz \\ 0;\quad otherwise \end{cases}$$

$$BT_{mm-NyNz}^{n+1} = \begin{cases} \frac{2}{\Delta x}\ ;\ h = 1 \\ 0;\quad otherwise \end{cases}, \qquad BT_{mm+NyNz}^{n+1} = \begin{cases} \frac{2}{\Delta x}\ ;\ h = Nx \\ 0;\quad otherwise \end{cases}$$

$$BT_{mm-Nz}^{n+1} = \begin{cases} \frac{2}{\Delta y}\ ;\ i = 1 \\ 0;\quad otherwise \end{cases}, \qquad BT_{mm+Nz}^{n+1} = \begin{cases} \frac{2}{\Delta y}\ ;\ i = Ny \\ 0;\quad otherwise \end{cases}$$

$$BT_{mm-1}^{n+1} = \begin{cases} \frac{2}{\Delta z}\ ;\ j = 1 \\ 0;\quad otherwise \end{cases}, \qquad BT_{mm+1}^{n+1} = \begin{cases} \frac{2}{\Delta z}\ ;\ j = Nz \\ 0;\quad otherwise \end{cases}$$

But the at $h = Nx$ we have a constant pressure boundary

$$\frac{\partial p}{\partial x} = \frac{Pout - p_m^{n+1}}{\left(\frac{1}{2}\right)\Delta x}$$

Hence we have

$$\begin{aligned} &\left[-T_{mm-NyNz}u_{x,m-NyNz}^{n+1} + \left(T_{mm-NyNz} + BT_{mm-NyNz}\right)u_{x,m}^{n+1}\right] \\ &\quad + \left[-T_{mm-Nz}u_{y,m-Nz}^{n+1} - (T_{mm-Nz} - T_{mm+Nz})u_{y,m}^{n+1} + T_{mm+Nz}u_{y,m+Nz}^{n+1}\right] \\ &\quad + \left[-T_{mm-1}u_{z,m-1}^{n+1} - (T_{mm-1} - T_{mm+1})u_{z,m}^{n+1} + T_{mm+1}u_{z,m+1}^{n+1}\right] \\ &\quad = -\left(\frac{k_c(1-\emptyset_m^n)v_{f,m}^n S^* E C_m^n}{k_c + (1-\emptyset_m^n)V_b v_{f,m}^n S^* E}\right)\left(\frac{n_M}{n_A}\right)\frac{M_M}{\rho} \end{aligned} \tag{3.116}$$

Equation of Motion (Darcy- Stokes)

$$
\begin{aligned}
&-\mu T_{mm-NyNz}^{2} u_{x,m-NyNz}^{n+1} - 4\mu T_{mm-Nz}^{2} u_{x,m-Nz}^{n+1} - 4\mu T_{mm-1}^{2} u_{x,m-1}^{n+1} \\
&\quad + \left(\mu\left(T_{mm-NyNz}^{2} + \frac{BT_{mm-NyNz}^{2}}{2}\right) + \mu\left(4T_{mm-Nz}^{2} + \frac{BT_{mm-Nz}^{2}}{2}\right)\right. \\
&\quad + \mu\left(4T_{mm-1}^{2} + \frac{BT_{mm-1}^{2}}{2}\right) + \mu\left(4T_{mm+1}^{2} + \frac{BT_{mm+1}^{2}}{2}\right) \\
&\quad + \mu\left(4T_{mm+Nz}^{2} + \frac{BT_{mm+Nz}^{2}}{2}\right) + \mu\left(T_{mm+NyNz}^{2} + \frac{BT_{mm+NyNz}^{2}}{2}\right) + \frac{\mu}{k_{xx,m}^{n}} \\
&\quad \left. + \frac{\rho_A}{\Delta t}\right) u_{x,m}^{n+1} - 4\mu T_{mm+1}^{2} u_{x,m+1}^{n+1} - 4\mu T_{mm+Nz}^{2} u_{x,m+Nz}^{n+1} \\
&\quad - \mu T_{mm+NyNz}^{2} u_{x,m+NyNz}^{n+1} - \left(\frac{2}{\Delta x}\right) p_{m}^{n+1} \\
&\quad = \left(\frac{\rho_A}{\Delta t}\right) u_{x,m}^{n} - \left(\frac{2}{\Delta x}\right) Pout
\end{aligned}
\tag{3.117}
$$

$$
\begin{aligned}
&-\mu T_{mm-NyNz}^{2} u_{y,m-NyNz}^{n+1} - 4\mu T_{mm-Nz}^{2} u_{y,m-Nz}^{n+1} - 4\mu T_{mm-1}^{2} u_{y,m-1}^{n+1} \\
&\quad + \left(\mu\left(T_{mm-NyNz}^{2} + \frac{BT_{mm-NyNz}^{2}}{2}\right) + \mu\left(4T_{mm-Nz}^{2} + \frac{BT_{mm-Nz}^{2}}{2}\right)\right. \\
&\quad + \mu\left(4T_{mm-1}^{2} + \frac{BT_{mm-1}^{2}}{2}\right) + \mu\left(4T_{mm+1}^{2} + \frac{BT_{mm+1}^{2}}{2}\right) \\
&\quad + \mu\left(4T_{mm+Nz}^{2} + \frac{BT_{mm+Nz}^{2}}{2}\right) + \mu\left(T_{mm+NyNz}^{2} + \frac{BT_{mm+NyNz}^{2}}{2}\right) + \frac{\mu}{k_{yy,m}^{n}} \\
&\quad \left. + \frac{\rho_A}{\Delta t}\right) u_{y,m}^{n+1} - 4\mu T_{mm+1}^{2} u_{y,m+1}^{n+1} - 4\mu T_{mm+Nz}^{2} u_{y,m+Nz}^{n+1} \\
&\quad - \mu T_{mm+NyNz}^{2} u_{y,m+NyNz}^{n+1} - T_{mm-Nz} p_{m-Nz}^{n+1} - (T_{mm-Nz} - T_{mm+Nz}) p_{m}^{n+1} \\
&\quad + T_{mm+Nz} p_{m+Nz}^{n+1} = \left(\frac{\rho_A}{\Delta t}\right) u_{y,m}^{n}
\end{aligned}
\tag{3.118}
$$

$$
\begin{aligned}
&-\mu T_{mm-NyNz}^{2} u_{z,m-NyNz}^{n+1} - 4\mu T_{mm-Nz}^{2} u_{z,m-Nz}^{n+1} - 4\mu T_{mm-1}^{2} u_{z,m-1}^{n+1} \\
&\quad + \left(\mu\left(T_{mm-NyNz}^{2} + \frac{BT_{mm-NyNz}^{2}}{2}\right) + \mu\left(4T_{mm-Nz}^{2} + \frac{BT_{mm-Nz}^{2}}{2}\right)\right. \\
&\quad + \mu\left(4T_{mm-1}^{2} + \frac{BT_{mm-1}^{2}}{2}\right) + \mu\left(4T_{mm+1}^{2} + \frac{BT_{mm+1}^{2}}{2}\right) \\
&\quad + \mu\left(4T_{mm+Nz}^{2} + \frac{BT_{mm+Nz}^{2}}{2}\right) + \mu\left(T_{mm+NyNz}^{2} + \frac{BT_{mm+NyNz}^{2}}{2}\right) + \frac{\mu}{k_{zz,m}^{n}} \\
&\quad \left. + \frac{\rho_A}{\Delta t}\right) u_{z,m}^{n+1} - 4\mu T_{mm+1}^{2} u_{z,m+1}^{n+1} - 4\mu T_{mm+Nz}^{2} u_{z,m+Nz}^{n+1} \\
&\quad - \mu T_{mm+NyNz}^{2} u_{z,m+NyNz}^{n+1} - T_{mm-1} p_{m-1}^{n+1} - (T_{mm-1} - T_{mm+1}) p_{m}^{n+1} \\
&\quad + T_{mm+1} p_{m+1}^{n+1} = \left(\frac{\rho_A}{\Delta t}\right) u_{z,m}^{n} \qquad (3.119)
\end{aligned}
$$

A single equation for the 5 boundary conditions is thus gives

$$
\begin{aligned}
&\left[-T_{mm-NyNz} u_{x,m-NyNz}^{n+1} + \left(T_{mm-NyNz} + BT_{mm-NyNz}\right) u_{x,m}^{n+1}\right] \\
&\quad + \left[-T_{mm-Nz} u_{y,m-Nz}^{n+1} - (T_{mm-Nz} - T_{mm+Nz}) u_{y,m}^{n+1} + T_{mm+Nz} u_{y,m+Nz}^{n+1}\right] \\
&\quad + \left[-T_{mm-1} u_{z,m-1}^{n+1} - (T_{mm-1} - T_{mm+1}) u_{z,m}^{n+1} + T_{mm+1} u_{z,m+1}^{n+1}\right] \\
&\quad = -\left(\frac{k_c (1 - \emptyset_m^n) v_{f,m}^n S^* E C_m^n}{k_c + (1 - \emptyset_m^n) V_b v_{f,m}^n S^* E}\right)\left(\frac{n_M}{n_A}\right)\frac{M_M}{\rho} \qquad (3.120)
\end{aligned}
$$

Equation of Motion (Darcy- Stokes)

$$
\begin{aligned}
-\mu T^2_{mm-NyNz} u^{n+1}_{x,m-NyNz} - 4\mu T^2_{mm-Nz} u^{n+1}_{x,m-Nz} - 4\mu T^2_{mm-1} u^{n+1}_{x,m-1} \\
+ \left(\mu\left(T^2_{mm-NyNz} + \frac{BT^2_{mm-NyNz}}{2}\right) + \mu\left(4T^2_{mm-Nz} + \frac{BT^2_{mm-Nz}}{2}\right)\right. \\
+ \mu\left(4T^2_{mm-1} + \frac{BT^2_{mm-1}}{2}\right) + \mu\left(4T^2_{mm+1} + \frac{BT^2_{mm+1}}{2}\right) \\
+ \mu\left(4T^2_{mm+Nz} + \frac{BT^2_{mm+Nz}}{2}\right) + \mu\left(T^2_{mm+NyNz} + \frac{BT^2_{mm+NyNz}}{2}\right) + \frac{\mu}{k^n_{xx,m}} \\
\left. + \frac{\rho_A}{\Delta t}\right) u^{n+1}_{x,m} - 4\mu T^2_{mm+1} u^{n+1}_{x,m+1} - 4\mu T^2_{mm+Nz} u^{n+1}_{x,m+Nz} \\
- \mu T^2_{mm+NyNz} u^{n+1}_{x,m+NyNz} - \left(T_{mm+NyNz} + BT_{mm+NyNz}\right) p^{n+1}_m \\
+ T_{mm+NyNz} p^{n+1}_{m+NyNz} \\
= \left(\frac{\rho_A}{\Delta t}\right) u^n_{x,m} - BT_{mm+NyNz} Pout
\end{aligned}
\tag{3.121}
$$

$$
\begin{aligned}
-\mu T^2_{mm-NyNz} u^{n+1}_{y,m-NyNz} - 4\mu T^2_{mm-Nz} u^{n+1}_{y,m-Nz} - 4\mu T^2_{mm-1} u^{n+1}_{y,m-1} \\
+ \left(\mu\left(T^2_{mm-NyNz} + \frac{BT^2_{mm-NyNz}}{2}\right) + \mu\left(4T^2_{mm-Nz} + \frac{BT^2_{mm-Nz}}{2}\right)\right. \\
+ \mu\left(4T^2_{mm-1} + \frac{BT^2_{mm-1}}{2}\right) + \mu\left(4T^2_{mm+1} + \frac{BT^2_{mm+1}}{2}\right) \\
+ \mu\left(4T^2_{mm+Nz} + \frac{BT^2_{mm+Nz}}{2}\right) + \mu\left(T^2_{mm+NyNz} + \frac{BT^2_{mm+NyNz}}{2}\right) + \frac{\mu}{k^n_{yy,m}} \\
\left. + \frac{\rho_A}{\Delta t}\right) u^{n+1}_{y,m} - 4\mu T^2_{mm+1} u^{n+1}_{y,m+1} - 4\mu T^2_{mm+Nz} u^{n+1}_{y,m+Nz} \\
- \mu T^2_{mm+NyNz} u^{n+1}_{y,m+NyNz} - T_{mm-Nz} p^{n+1}_{m-Nz} - (T_{mm-Nz} - T_{mm+Nz}) p^{n+1}_m \\
+ T_{mm+Nz} p^{n+1}_{m+Nz} = \left(\frac{\rho_A}{\Delta t}\right) u^n_{y,m}
\end{aligned}
\tag{3.122}
$$

$$
\begin{aligned}
&-\mu T_{mm-NyNz}^{2} u_{z,m-NyNz}^{n+1} - 4\mu T_{mm-Nz}^{2} u_{z,m-Nz}^{n+1} - 4\mu T_{mm-1}^{2} u_{z,m-1}^{n+1} \\
&\quad + \left(\mu\left(T_{mm-NyNz}^{2} + \frac{BT_{mm-NyNz}^{2}}{2}\right) + \mu\left(4T_{mm-Nz}^{2} + \frac{BT_{mm-Nz}^{2}}{2}\right)\right. \\
&\quad + \mu\left(4T_{mm-1}^{2} + \frac{BT_{mm-1}^{2}}{2}\right) + \mu\left(4T_{mm+1}^{2} + \frac{BT_{mm+1}^{2}}{2}\right) \\
&\quad + \mu\left(4T_{mm+Nz}^{2} + \frac{BT_{mm+Nz}^{2}}{2}\right) + \mu\left(T_{mm+NyNz}^{2} + \frac{BT_{mm+NyNz}^{2}}{2}\right) + \frac{\mu}{k_{zz,m}^{n}} \\
&\quad \left. + \frac{\rho_A}{\Delta t}\right) u_{z,m}^{n+1} - 4\mu T_{mm+1}^{2} u_{z,m+1}^{n+1} - 4\mu T_{mm+Nz}^{2} u_{z,m+Nz}^{n+1} \\
&\quad - \mu T_{mm+NyNz}^{2} u_{z,m+NyNz}^{n+1} - T_{mm-1} p_{m-1}^{n+1} - (T_{mm-1} - T_{mm+1}) p_{m}^{n+1} \\
&\quad + T_{mm+1} p_{m+1}^{n+1} = \left(\frac{\rho_A}{\Delta t}\right) u_{z,m}^{n} \qquad (3.123)
\end{aligned}
$$

For the Injection Point

$$
u_{x,m-(NyNz)/2}^{n+1} \approx \left(\frac{k_{xx,m}^{n}}{\mu}\right)\left(\frac{Pinj - p_{m}^{n+1}}{\frac{1}{2}\Delta x}\right)
$$

We have

$$
\begin{aligned}
&\left[BT_{mm-NyNz} u_{x,m}^{n+1}\right] \\
&\quad + \left[-T_{mm-Nz} u_{y,m-Nz}^{n+1} - (T_{mm-Nz} - T_{mm+Nz}) u_{y,m}^{n+1} + T_{mm+Nz} u_{y,m+Nz}^{n+1}\right] \\
&\quad + \left[-T_{mm-1} u_{z,m-1}^{n+1} - (T_{mm-1} - T_{mm+1}) u_{z,m}^{n+1} + T_{mm+1} u_{z,m+1}^{n+1}\right] \\
&\quad + \left(\frac{k_{xx,m}^{n}}{\mu}\right) BT_{mm-NyNz}^{2} p_{m}^{n+1} - \left(\frac{k_{xx,m}^{n}}{\mu}\right) BT_{mm-NyNz}^{2} Pinj \\
&\quad = -\left(\frac{k_c (1 - \emptyset_m^n) v_{f,m}^{n} S^* E C_m^n}{k_c + (1 - \emptyset_m^n) V_b v_{f,m}^{n} S^* E}\right)\left(\frac{n_M}{n_A}\right)\frac{M_M}{\rho} \qquad (3.124)
\end{aligned}
$$

And

$$
\frac{\partial^2 u_x}{\partial x^2} = \frac{\dfrac{u_{x,m+NyNz}^{n+1} - u_{x,m}^{n+1}}{\Delta x} - \dfrac{u_{x,m}^{n+1} - u_{x,m-NyNz}^{n+1}}{\Delta x}}{\Delta x}
$$

Will be approximated as

$$\frac{\dfrac{u_{x,m+NyNz}^{n+1}-u_{x,m}^{n+1}}{\Delta x}-\dfrac{u_{x,m}^{n+1}-\left(\dfrac{k_{xx,m}^{n}}{\mu}\right)\left(\dfrac{Pinj-p_{m}^{n+1}}{\frac{1}{2}\Delta x}\right)}{\frac{1}{2}\Delta x}}{\Delta x}$$

$$=\frac{\dfrac{u_{x,m+NyNz}^{n+1}-u_{x,m}^{n+1}}{\Delta x}-\dfrac{2u_{x,m}^{n+1}}{\Delta x}}{\Delta x}+\left(\frac{2}{\Delta x}\right)^{2}\left(\frac{k_{xx,m}^{n}}{\mu\Delta x}\right)(Pinj-p_{m}^{n+1})$$

This is just as the case of No-flow boundary where we had

$$\frac{\dfrac{u_{x,m+NyNz}^{n+1}-u_{x,m}^{n+1}}{\Delta x}-\dfrac{2u_{x,m}^{n+1}}{\Delta x}}{\Delta x}$$

Here we just have the addition of

$$\left(\frac{2}{\Delta x}\right)^{2}\left(\frac{k_{xx,m}^{n}}{\mu\Delta x}\right)(Pinj-p_{m}^{n+1})$$

Then we have

$$\begin{aligned}
&-4\mu T_{mm-Nz}^{2}u_{x,m-Nz}^{n+1}-4\mu T_{mm-1}^{2}u_{x,m-1}^{n+1}\\
&\quad+\Bigg(2\mu T_{mm-NyNz}^{2}+4\mu T_{mm-Nz}^{2}+4\mu T_{mm-1}^{2}+4\mu T_{mm+1}^{2}+4\mu T_{mm+Nz}^{2}\\
&\quad+\mu T_{mm+NyNz}^{2}+\frac{\mu}{k_{xx,m}^{n}}+\frac{\rho_{A}}{\Delta t}\Bigg)u_{x,m}^{n+1}-4\mu T_{mm+1}^{2}u_{x,m+1}^{n+1}\\
&\quad-4\mu T_{mm+Nz}^{2}u_{x,m+Nz}^{n+1}-\mu T_{mm+NyNz}^{2}u_{x,m+NyNz}^{n+1}\\
&\quad-\left(T_{mm+NyNz}-BT_{mm-NyNz}^{2}\left(\frac{k_{xx,m}^{n}}{\Delta x}\right)\right)p_{m}^{n+1}+T_{mm+NyNz}p_{m+NyNz}^{n+1}\\
&\quad-BT_{mm-NyNz}^{2}\left(\frac{k_{xx,m}^{n}}{\Delta x}\right)Pinj=\left(\frac{\rho_{A}}{\Delta t}\right)u_{x,m}^{n}
\end{aligned}\tag{3.125}$$

We can write a final equation with an injection switch in the form

$$\begin{aligned}
&\left[-T_{mm-NyNz}u_{x,m-NyNz}^{n+1} + \left(T_{mm-NyNz} + BT_{mm-NyNz}\right)u_{x,m}^{n+1}\right] \\
&\quad + \left[-T_{mm-Nz}u_{y,m-Nz}^{n+1} - (T_{mm-Nz} - T_{mm+Nz})u_{y,m}^{n+1} + T_{mm+Nz}u_{y,m+Nz}^{n+1}\right] \\
&\quad + \left[-T_{mm-1}u_{z,m-1}^{n+1} - (T_{mm-1} - T_{mm+1})u_{z,m}^{n+1} + T_{mm+1}u_{z,m+1}^{n+1}\right] + INJS \\
&\quad \cdot \left(\frac{k_{xx,m}^{n}}{\mu}\right) BT_{mm-NyNz}^{2} p_{m}^{n+1} - INJS \cdot \left(\frac{k_{xx,m}^{n}}{\mu}\right) BT_{mm-NyNz}^{2} Pinj \\
&\quad = -\left(\frac{k_c(1-\emptyset_m^n)v_{f,m}^n S^* E C_m^n}{k_c + (1-\emptyset_m^n)V_b v_{f,m}^n S^* E}\right)\left(\frac{n_M}{n_A}\right)\frac{M_M}{\rho} \qquad (3.126)
\end{aligned}$$

Equation of Motion (Darcy- Stokes)

$$\begin{aligned}
&-\mu T_{mm-NyNz}^{2} u_{x,m-NyNz}^{n+1} - 4\mu T_{mm-Nz}^{2} u_{x,m-Nz}^{n+1} - 4\mu T_{mm-1}^{2} u_{x,m-1}^{n+1} \\
&\quad + \left(\mu\left(T_{mm-NyNz}^{2} + \frac{BT_{mm-NyNz}^{2}}{2}\right) + \mu\left(4T_{mm-Nz}^{2} + \frac{BT_{mm-Nz}^{2}}{2}\right)\right. \\
&\quad + \mu\left(4T_{mm-1}^{2} + \frac{BT_{mm-1}^{2}}{2}\right) + \mu\left(4T_{mm+1}^{2} + \frac{BT_{mm+1}^{2}}{2}\right) \\
&\quad + \mu\left(4T_{mm+Nz}^{2} + \frac{BT_{mm+Nz}^{2}}{2}\right) + \mu\left(T_{mm+NyNz}^{2} + \frac{BT_{mm+NyNz}^{2}}{2}\right) + \frac{\mu}{k_{xx,m}^{n}} \\
&\quad \left. + \frac{\rho_A}{\Delta t}\right) u_{x,m}^{n+1} - 4\mu T_{mm+1}^{2} u_{x,m+1}^{n+1} - 4\mu T_{mm+Nz}^{2} u_{x,m+Nz}^{n+1} \\
&\quad - \mu T_{mm+NyNz}^{2} u_{x,m+NyNz}^{n+1} \\
&\quad - \left(T_{mm+NyNz} + BT_{mm+NyNz} - INJS \cdot BT_{mm-NyNz}^{2}\left(\frac{k_{xx,m}^{n}}{\Delta x}\right)\right) p_{m}^{n+1} \\
&\quad + T_{mm+NyNz} p_{m+NyNz}^{n+1} - INJS \cdot BT_{mm-NyNz}^{2}\left(\frac{k_{xx,m}^{n}}{\Delta x}\right) Pinj \\
&\quad = \left(\frac{\rho_A}{\Delta t}\right) u_{x,m}^{n} - BT_{mm+NyNz} Pout \qquad (3.127)
\end{aligned}$$

$$
\begin{aligned}
&-\mu T_{mm-NyNz}^{2} u_{y,m-NyNz}^{n+1} - 4\mu T_{mm-Nz}^{2} u_{y,m-Nz}^{n+1} - 4\mu T_{mm-1}^{2} u_{y,m-1}^{n+1} \\
&\quad + \left(\mu\left(T_{mm-NyNz}^{2} + \frac{BT_{mm-NyNz}^{2}}{2}\right) + \mu\left(4T_{mm-Nz}^{2} + \frac{BT_{mm-Nz}^{2}}{2}\right)\right. \\
&\quad + \mu\left(4T_{mm-1}^{2} + \frac{BT_{mm-1}^{2}}{2}\right) + \mu\left(4T_{mm+1}^{2} + \frac{BT_{mm+1}^{2}}{2}\right) \\
&\quad + \mu\left(4T_{mm+Nz}^{2} + \frac{BT_{mm+Nz}^{2}}{2}\right) + \mu\left(T_{mm+NyNz}^{2} + \frac{BT_{mm+NyNz}^{2}}{2}\right) + \frac{\mu}{k_{yy,m}^{n}} \\
&\quad \left. + \frac{\rho_A}{\Delta t}\right) u_{y,m}^{n+1} - 4\mu T_{mm+1}^{2} u_{y,m+1}^{n+1} - 4\mu T_{mm+Nz}^{2} u_{y,m+Nz}^{n+1} \\
&\quad - \mu T_{mm+NyNz}^{2} u_{y,m+NyNz}^{n+1} - T_{mm-Nz} p_{m-Nz}^{n+1} - (T_{mm-Nz} - T_{mm+Nz}) p_{m}^{n+1} \\
&\quad + T_{mm+Nz} p_{m+Nz}^{n+1} = \left(\frac{\rho_A}{\Delta t}\right) u_{y,m}^{n} \qquad (3.128)
\end{aligned}
$$

$$
\begin{aligned}
&-\mu T_{mm-NyNz}^{2} u_{z,m-NyNz}^{n+1} - 4\mu T_{mm-Nz}^{2} u_{z,m-Nz}^{n+1} - 4\mu T_{mm-1}^{2} u_{z,m-1}^{n+1} \\
&\quad + \left(\mu\left(T_{mm-NyNz}^{2} + \frac{BT_{mm-NyNz}^{2}}{2}\right) + \mu\left(4T_{mm-Nz}^{2} + \frac{BT_{mm-Nz}^{2}}{2}\right)\right. \\
&\quad + \mu\left(4T_{mm-1}^{2} + \frac{BT_{mm-1}^{2}}{2}\right) + \mu\left(4T_{mm+1}^{2} + \frac{BT_{mm+1}^{2}}{2}\right) \\
&\quad + \mu\left(4T_{mm+Nz}^{2} + \frac{BT_{mm+Nz}^{2}}{2}\right) + \mu\left(T_{mm+NyNz}^{2} + \frac{BT_{mm+NyNz}^{2}}{2}\right) + \frac{\mu}{k_{zz,m}^{n}} \\
&\quad \left. + \frac{\rho_A}{\Delta t}\right) u_{z,m}^{n+1} - 4\mu T_{mm+1}^{2} u_{z,m+1}^{n+1} - 4\mu T_{mm+Nz}^{2} u_{z,m+Nz}^{n+1} \\
&\quad - \mu T_{mm+NyNz}^{2} u_{z,m+NyNz}^{n+1} - T_{mm-1} p_{m-1}^{n+1} - (T_{mm-1} - T_{mm+1}) p_{m}^{n+1} \\
&\quad + T_{mm+1} p_{m+1}^{n+1} = \left(\frac{\rho_A}{\Delta t}\right) u_{z,m}^{n} \qquad (3.129)
\end{aligned}
$$

Where

$$T_{mm-NyNz}^{n+1} = \begin{cases} \frac{1}{\Delta x}\ ;\ \ h \neq 1 \\ 0;\quad otherwise \end{cases}, \qquad T_{mm+NyNz}^{n+1} = \begin{cases} \frac{1}{\Delta x}\ ;\ \ h \neq Nx \\ 0;\quad otherwise \end{cases}$$

$$T_{mm-Nz}^{n+1} = \begin{cases} \frac{1}{\Delta y}\ ;\ \ i \neq 1 \\ 0;\quad otherwise \end{cases}, \qquad T_{mm+Nz}^{n+1} = \begin{cases} \frac{1}{\Delta y}\ ;\ \ i \neq Ny \\ 0;\quad otherwise \end{cases}$$

$$T_{mm-1}^{n+1} = \begin{cases} \frac{1}{\Delta z}\ ;\ \ j \neq 1 \\ 0;\quad otherwise \end{cases}, \qquad T_{mm+1}^{n+1} = \begin{cases} \frac{1}{\Delta z}\ ;\ \ j \neq Nz \\ 0;\quad otherwise \end{cases}$$

$$BT_{mm-NyNz}^{n+1} = \left(\frac{2}{\Delta x}\right)\delta_k(h-1), \qquad BT_{mm+NyNz}^{n+1} = \left(\frac{2}{\Delta x}\right)\delta_k(h-Nx),$$

$$BT_{mm-Nz}^{n+1} = \left(\frac{2}{\Delta y}\right)\delta_k(i-1),$$

$$BT_{mm+Nz}^{n+1} = \left(\frac{2}{\Delta y}\right)\delta_k(i-Ny), \qquad BT_{mm-1}^{n+1} = \left(\frac{2}{\Delta z}\right)\delta_k(j-1),$$

$$BT_{mm+1}^{n+1} = \left(\frac{2}{\Delta z}\right)\delta_k(j-Nz)$$

$$INJS = \delta_k(h-1)$$

Convection-Dispersion-Reaction Equation

$$
\begin{aligned}
&-\left[-T_{mm-NyNz}C_{m-NyNz}^{n+1} + T_{mm-NyNz}C_{m}^{n+1}\right] \\
&\quad - \left[-T_{mm-Nz}C_{m-Nz}^{n+1} - (T_{mm-Nz} - T_{mm+Nz})C_{m}^{n+1} + T_{mm+Nz}C_{m+Nz}^{n+1}\right] \\
&\quad - \left[-T_{mm-1}C_{m-1}^{n+1} - (T_{mm-1} - T_{mm+1})C_{m}^{n+1} + T_{mm+1}C_{m+1}^{n+1}\right] \\
&\quad + DT_{mm-NyNz}C_{m-NyNz}^{n+1} + DT_{mm-Nz}C_{m-Nz}^{n+1} + DT_{mm-1}C_{m-1}^{n+1} \\
&\quad - \left(DT_{mm-NyNz} + DT_{mm-Nz} + DT_{mm-1} + DT_{mm+1} + DT_{mm+Nz}\right. \\
&\quad \left. + DT_{mm+NyNz}\right)C_{m}^{n+1} + DT_{mm+1}C_{m+1}^{n+1} + DT_{mm+Nz}C_{m+Nz}^{n+1} \\
&\quad + DT_{mm+NyNz}C_{m+NyNz}^{n+1} - \left(\frac{k_c(1-\emptyset_m^{n+1})v_{f,m}^{n+1}S^*E}{k_c + (1-\emptyset_m^{n+1})V_b v_{f,m}^{n+1}S^*E}\right)C_m^{n+1} \\
&\quad = \emptyset_m^{n+1}\left(\frac{C_m^{n+1} - C_m^n}{\Delta t}\right) \qquad (3.130)
\end{aligned}
$$

At $h = 1$,

$$
\begin{aligned}
&-\left[2T_{mm-NyNz}C_{m}^{n+1}\right] \\
&\quad - \left[-T_{mm-Nz}C_{m-Nz}^{n+1} - (T_{mm-Nz} - T_{mm+Nz})C_{m}^{n+1} + T_{mm+Nz}C_{m+Nz}^{n+1}\right] \\
&\quad - \left[-T_{mm-1}C_{m-1}^{n+1} - (T_{mm-1} - T_{mm+1})C_{m}^{n+1} + T_{mm+1}C_{m+1}^{n+1}\right] \\
&\quad + DT_{mm-Nz}C_{m-Nz}^{n+1} + DT_{mm-1}C_{m-1}^{n+1} \\
&\quad - \left(2DT_{mm-NyNz} + DT_{mm-Nz} + DT_{mm-1} + DT_{mm+1} + DT_{mm+Nz}\right. \\
&\quad \left. + DT_{mm+NyNz}\right)C_{m}^{n+1} + DT_{mm+1}C_{m+1}^{n+1} + DT_{mm+Nz}C_{m+Nz}^{n+1} \\
&\quad + DT_{mm+NyNz}C_{m+NyNz}^{n+1} - \left(\frac{k_c(1-\emptyset_m^{n+1})v_{f,m}^{n+1}S^*E}{k_c + (1-\emptyset_m^{n+1})V_b v_{f,m}^{n+1}S^*E}\right)C_m^{n+1} \\
&\quad = \emptyset_m^{n+1}\left(\frac{C_m^{n+1} - C_m^n}{\Delta t}\right) - \left(2T_{mm-NyNz} + 2DT_{mm-NyNz}\right)Cinj \qquad (3.131)
\end{aligned}
$$

So we define

$$BT_{mm-NyNz} = \frac{2u_{x,m}^{n+1}}{\Delta x},$$

$$BDT_{mm-NyNz} = 2\left(\frac{D_m + \alpha_x \left|u_{xmm-NyNz}^{n+1}\right|}{(\Delta x)^2}\right),$$

Hence, to impose no-flow boundaries on all four faces ($y = 0,\ y = w,\ z = 0,\ z = H$), we set:

$$T_{mm-Nz} = 0, \qquad T_{mm+Nz} = 0$$

$$T_{mm-1} = 0, \qquad T_{mm+1} = 0$$

$$DT_{mm-Nz} = 0, \qquad DT_{mm+Nz} = 0$$

$$DT_{mm-1} = 0, \qquad DT_{mm+1} = 0$$

$$BT_{mm-Nz} = \frac{2u_{y,m}^{n+1}}{\Delta y}, \qquad BT_{mm+Nz} = \frac{2u_{y,m}^{n+1}}{\Delta y},$$

$$BT_{mm-1} = \frac{2u_{z,m}^{n+1}}{\Delta z}, \qquad BT_{mm+1} = \frac{2u_{z,m}^{n+1}}{\Delta z}$$

$$-\left[-T_{mm-NyNz}C_{m-NyNz}^{n+1}+\left(T_{mm-NyNz}+BT_{mm-NyNz}\right)C_{m}^{n+1}\right]$$

$$-\left[-T_{mm-Nz}C_{m-Nz}^{n+1}\right.$$

$$-\left(\left(T_{mm-Nz}+BT_{mm-Nz}\right)-\left(T_{mm+Nz}+BT_{mm+Nz}\right)\right)C_{m}^{n+1}$$

$$\left.+T_{mm+Nz}C_{m+Nz}^{n+1}\right]$$

$$-\left[-T_{mm-1}C_{m-1}^{n+1}-\left(\left(T_{mm-1}+BT_{mm-1}\right)-\left(T_{mm+1}+BT_{mm+1}\right)\right)C_{m}^{n+1}\right.$$

$$\left.+T_{mm+1}C_{m+1}^{n+1}\right]+DT_{mm-NyNz}C_{m-NyNz}^{n+1}+DT_{mm-Nz}C_{m-Nz}^{n+1}$$

$$+DT_{mm-1}C_{m-1}^{n+1}$$

$$-\left(\left(DT_{mm-NyNz}+BDT_{mm-NyNz}\right)+DT_{mm-Nz}+DT_{mm-1}+DT_{mm+1}\right.$$

$$\left.+DT_{mm+Nz}+DT_{mm+NyNz}\right)C_{m}^{n+1}+DT_{mm+1}C_{m+1}^{n+1}+DT_{mm+Nz}C_{m+Nz}^{n+1}$$

$$+DT_{mm+NyNz}C_{m+NyNz}^{n+1}-\left(\frac{k_c(1-\emptyset_m^{n+1})v_{f,m}^{n+1}S^{*}E}{k_c+(1-\emptyset_m^{n+1})V_b v_{f,m}^{n+1}S^{*}E}\right)C_{m}^{n+1}$$

$$=\emptyset_m^{n+1}\left(\frac{C_m^{n+1}-C_m^{n}}{\Delta t}\right)-\left(BT_{mm-NyNz}+BDT_{mm-NyNz}\right)Cinj \qquad (3.132)$$

Where,

$$T_{mm-NyNz}=\begin{cases}0 & if\ h=1\\ \dfrac{u_{x,m}^{n+1}}{\Delta x} & otherwise\end{cases},$$

$$T_{mm+Nz}=\begin{cases}0 & if\ i=Ny\\ \dfrac{u_{y,m}^{n+1}}{\Delta y} & otherwise\end{cases}$$

$$T_{mm-Nz}=\begin{cases}0 & if\ i=1\\ \dfrac{u_{y,m}^{n+1}}{\Delta y} & otherwise\end{cases},$$

$$T_{mm+1}=\begin{cases}0 & if\ j=Nz\\ \dfrac{u_{z,m}^{n+1}}{2\Delta z} & otherwise\end{cases}$$

$$T_{mm-1} = \begin{cases} 0 & if\ j = 1 \\ \dfrac{u_{z,m}^{n+1}}{2\Delta z} & otherwise \end{cases}$$

$$DT_{mm+NyNz} = \begin{cases} 0 & if\ h = Nx \\ \dfrac{D_m + \alpha_x \left| u_{xmm+NyNz}^{n+1} \right|}{(\Delta x)^2} & otherwise \end{cases},$$

$$DT_{mm-NyNz} = \begin{cases} 0 & if\ h = 1 \\ \dfrac{D_m + \alpha_x \left| u_{xmm-NyNz}^{n+1} \right|}{(\Delta x)^2} & otherwise \end{cases},$$

$$DT_{mm+Nz} = \begin{cases} 0 & if\ i = Ny \\ \dfrac{D_m + \alpha_y \left| u_{ymm+Nz}^{n+1} \right|}{(\Delta y)^2} & otherwise \end{cases},$$

$$DT_{mm-Nz} = \begin{cases} 0 & if\ i = 1 \\ \dfrac{D_m + \alpha_y \left| u_{ymm-Nz}^{n+1} \right|}{(\Delta y)^2} & otherwise \end{cases},$$

$$DT_{mm+1} = \begin{cases} 0 & if\ j = Nz \\ \dfrac{D_m + \alpha_z \left| u_{zmm+1}^{n+1} \right|}{(\Delta z)^2} & otherwise \end{cases},$$

$$DT_{mm-1} = \begin{cases} 0 & if\ j = 1 \\ \dfrac{D_m + \alpha_z \left| u_{zmm-1}^{n+1} \right|}{(\Delta z)^2} & otherwise \end{cases}$$

$$BT_{mm-NyNz} = \begin{cases} \dfrac{2u_{x,m}^{n+1}}{\Delta x} & if\ h = 1 \\ 0 & otherwise \end{cases},$$

$$BT_{mm-Nz} = \begin{cases} \dfrac{2u_{y,m}^{n+1}}{\Delta y} & if\ i = 1 \\ 0 & otherwise \end{cases}, \quad BT_{mm+Nz} = \begin{cases} \dfrac{2u_{y,m}^{n+1}}{\Delta y} & if\ i = Ny \\ 0 & otherwise \end{cases},$$

$$BT_{mm-1} = \begin{cases} \dfrac{2u_{z,m}^{n+1}}{\Delta z} & if\ j = 1 \\ 0 & otherwise \end{cases}, \quad BT_{mm+1} = \begin{cases} \dfrac{2u_{z,m}^{n+1}}{\Delta z} & if\ j = Nz \\ 0 & otherwise \end{cases}$$

Then we consider that at $h = Nx$ we have a constant pressure boundary

$$C_m^{n+1} = C_{m+NyNz}^{n+1}$$

This condition has no effect on the advection part of the equation and can be incorporated in the dispersion by setting $DT_{mm+NyNz} = 0$

$$\begin{aligned}
&-\left[-T_{mm-NyNz}C_{m-NyNz}^{n+1} + \left(T_{mm-NyNz} + BT_{mm-NyNz}\right)C_m^{n+1}\right] \\
&\quad - \left[-T_{mm-Nz}C_{m-Nz}^{n+1}\right. \\
&\quad - \left(\left(T_{mm-Nz} + BT_{mm-Nz}\right) - \left(T_{mm+Nz} + BT_{mm+Nz}\right)\right)C_m^{n+1} \\
&\quad \left. + T_{mm+Nz}C_{m+Nz}^{n+1}\right] \\
&\quad - \left[-T_{mm-1}C_{m-1}^{n+1} - \left(\left(T_{mm-1} + BT_{mm-1}\right) - \left(T_{mm+1} + BT_{mm+1}\right)\right)C_m^{n+1}\right. \\
&\quad \left. + T_{mm+1}C_{m+1}^{n+1}\right] + DT_{mm-NyNz}C_{m-NyNz}^{n+1} + DT_{mm-Nz}C_{m-Nz}^{n+1} \\
&\quad + DT_{mm-1}C_{m-1}^{n+1} \\
&\quad - \left(\left(DT_{mm-NyNz} + BDT_{mm-NyNz}\right) + DT_{mm-Nz} + DT_{mm-1} + DT_{mm+1}\right. \\
&\quad \left. + DT_{mm+Nz} + DT_{mm+NyNz}\right)C_m^{n+1} + DT_{mm+1}C_{m+1}^{n+1} + DT_{mm+Nz}C_{m+Nz}^{n+1} \\
&\quad + DT_{mm+NyNz}C_{m+NyNz}^{n+1} - \left(\frac{k_c(1-\emptyset_m^{n+1})v_{f,m}^{n+1}S^*E}{k_c + (1-\emptyset_m^{n+1})V_b v_{f,m}^{n+1}S^*E}\right)C_m^{n+1} \\
&\quad = \emptyset_m^{n+1}\left(\frac{C_m^{n+1} - C_m^n}{\Delta t}\right) - \left(BT_{mm-NyNz} + BDT_{mm-NyNz}\right)Cinj \qquad (3.133)
\end{aligned}$$

Finally, we write the discretized advection- dispersion-reaction equation in the form:

$$
\begin{aligned}
-\left(T_{mm-NyNz} + DT_{mm-NyNz}\right)C_{m-NyNz}^{n+1} - \ & (T_{mm-Nz} + DT_{mm-Nz})C_{m-Nz}^{n+1} \\
& - \ (T_{mm-1} + DT_{mm-1})C_{m-1}^{n+1} \\
& + \Bigg(\left(T_{mm-NyNz} + BT_{mm-NyNz}\right) \\
& - \left((T_{mm-Nz} + BT_{mm-Nz}) - (T_{mm+Nz} + BT_{mm+Nz})\right) \\
& - \left((T_{mm-1} + BT_{mm-1}) - (T_{mm+1} + BT_{mm+1})\right) \\
& + \left(DT_{mm-NyNz} + BDT_{mm-NyNz}\right) + \ DT_{mm-Nz} + \ DT_{mm-1} + \ DT_{mm+1} \\
& + \ DT_{mm+Nz} + DT_{mm+NyNz} + \left(\frac{k_c(1-\emptyset_m^{n+1})v_{f,m}^{n+1}S^*E}{k_c + (1-\emptyset_m^{n+1})V_b v_{f,m}^{n+1}S^*E}\right) \\
& + \frac{\emptyset_m^{n+1}}{\Delta t}\Bigg) C_m^{n+1} + \ (T_{mm+1} - DT_{mm+1})C_{m+1}^{n+1} \\
& + \ (T_{mm+Nz} - DT_{mm+Nz})C_{m+Nz}^{n+1} - DT_{mm+NyNz}C_{m+NyNz}^{n+1} \\
& = \frac{\emptyset_m^{n+1}}{\Delta t} C_m^n + \left(BT_{mm-NyNz} + BDT_{mm-NyNz}\right)Cinj \qquad (3.134)
\end{aligned}
$$

3.6 Development of Numerical Algorithm of coupled system of differential equations

The discretized coupled continuity and motion equation gives rise to the block hepta-diagonal matrix. The coefficient matrix for the system is expected to be as shown in Figure 3-5.

The content of the highlighted blocks from left to right is given below

$$\begin{bmatrix} -T_{mm-NyNz} & 0 & 0 & 0 \\ -\mu T^2_{mm-NyNz} & 0 & 0 & 0 \\ 0 & -\mu T^2_{mm-NyNz} & 0 & 0 \\ 0 & 0 & -\mu T^2_{mm-NyNz} & 0 \end{bmatrix}$$

$$\begin{bmatrix} 0 & -T_{mm-Nz} & 0 & 0 \\ -4\mu T^2_{mm-Nz} & 0 & 0 & 0 \\ 0 & -4\mu T^2_{mm-Nz} & 0 & -T_{mm+Nz} \\ 0 & 0 & -4\mu T^2_{mm-Nz} & 0 \end{bmatrix}$$

$$\begin{bmatrix} 0 & 0 & -T_{mm-1} & 0 \\ -4\mu T^2_{mm-1} & 0 & 0 & 0 \\ 0 & -4\mu T^2_{mm-1} & 0 & 0 \\ 0 & 0 & -4\mu T^2_{mm-1} & -T_{mm+1} \end{bmatrix}$$

$$[see\ the\ appendix\ for\ the\ content\ of\ the\ red\ box]$$

$$\begin{bmatrix} 0 & 0 & T_{mm-1} & 0 \\ -4\mu T^2_{mm+1} & -4\mu T^2_{mm+1} & 0 & 0 \\ 0 & 0 & 0 & 0 \\ 0 & & -4\mu T^2_{mm+1} & T_{mm+1} \end{bmatrix}$$

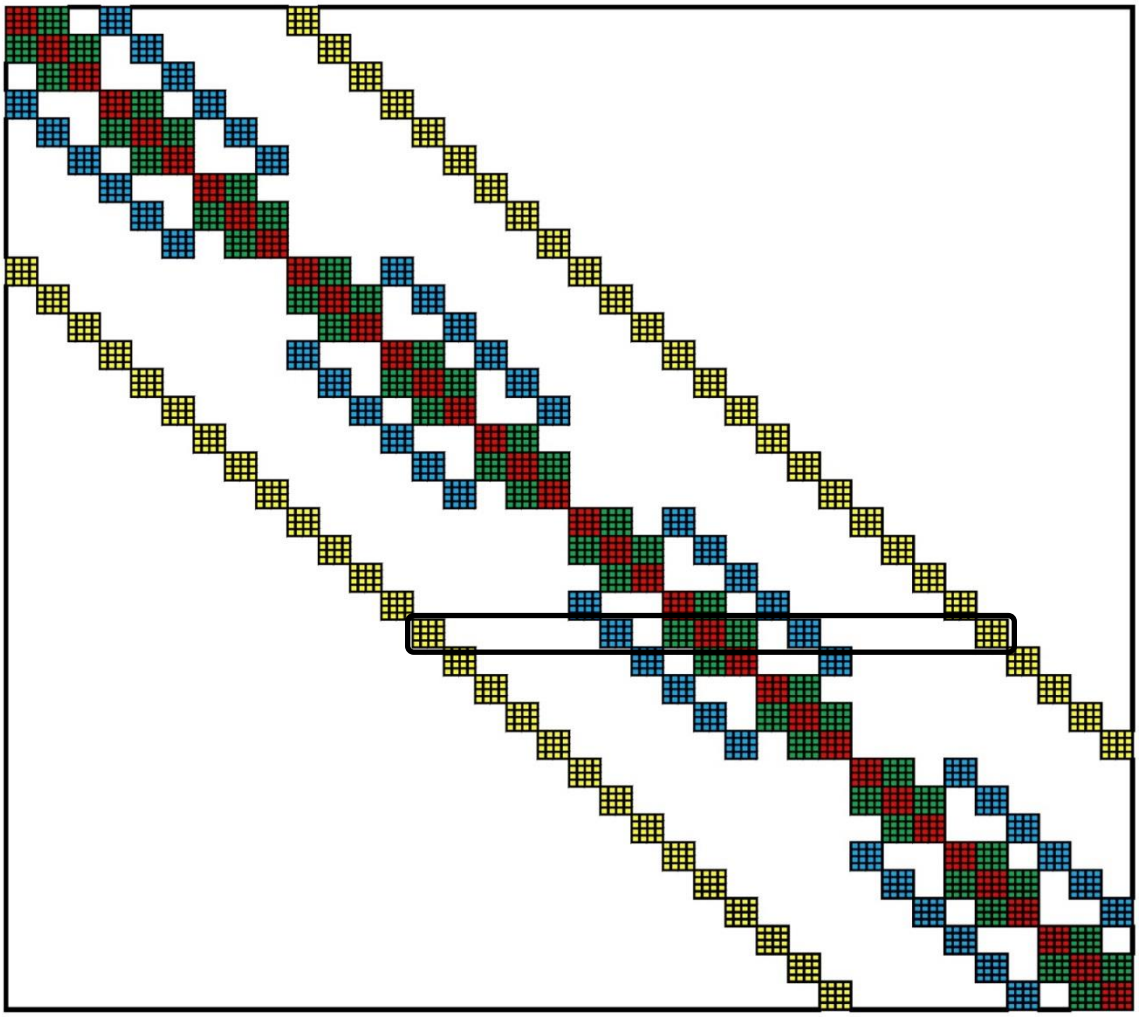

Figure 3-5: The block (4 by 4) hepta-diagonal coefficient matrix for the system of coupled continuity and brinkman flow equations

$$\begin{bmatrix} 0 & T_{mm-Nz} & 0 & 0 \\ -4\mu T_{mm+Nz}^2 & 0 & 0 & 0 \\ 0 & 0 & 0 & T_{mm+Nz} \\ 0 & -4\mu T_{mm+Nz}^2 & -4\mu T_{mm+Nz}^2 & 0 \\ 0 & 0 & & \end{bmatrix}$$

$$\begin{bmatrix} 0 & 0 & 0 & 0 \\ -\mu T_{mm+NyNz}^2 & 0 & 0 & T_{mm+NyNz} \\ 0 & -\mu T_{mm+NyNz}^2 & 0 & 0 \\ 0 & 0 & -\mu T_{mm+NyNz}^2 & 0 \end{bmatrix}$$

3.7 Development of Computational model (MATLAB Code) for the coupled system of differential equations

The benefit of computational power is to get the computer to solve our problem for us. To do that, we must be able to communicate with the computer in the language it understands. To do this, we convert the numerical scheme developed into MATLAB algorithm for the simulation. See the appendix for the MATLAB code for the problem.

The Generic structure of the code is summarized in the Figure 3-7 below

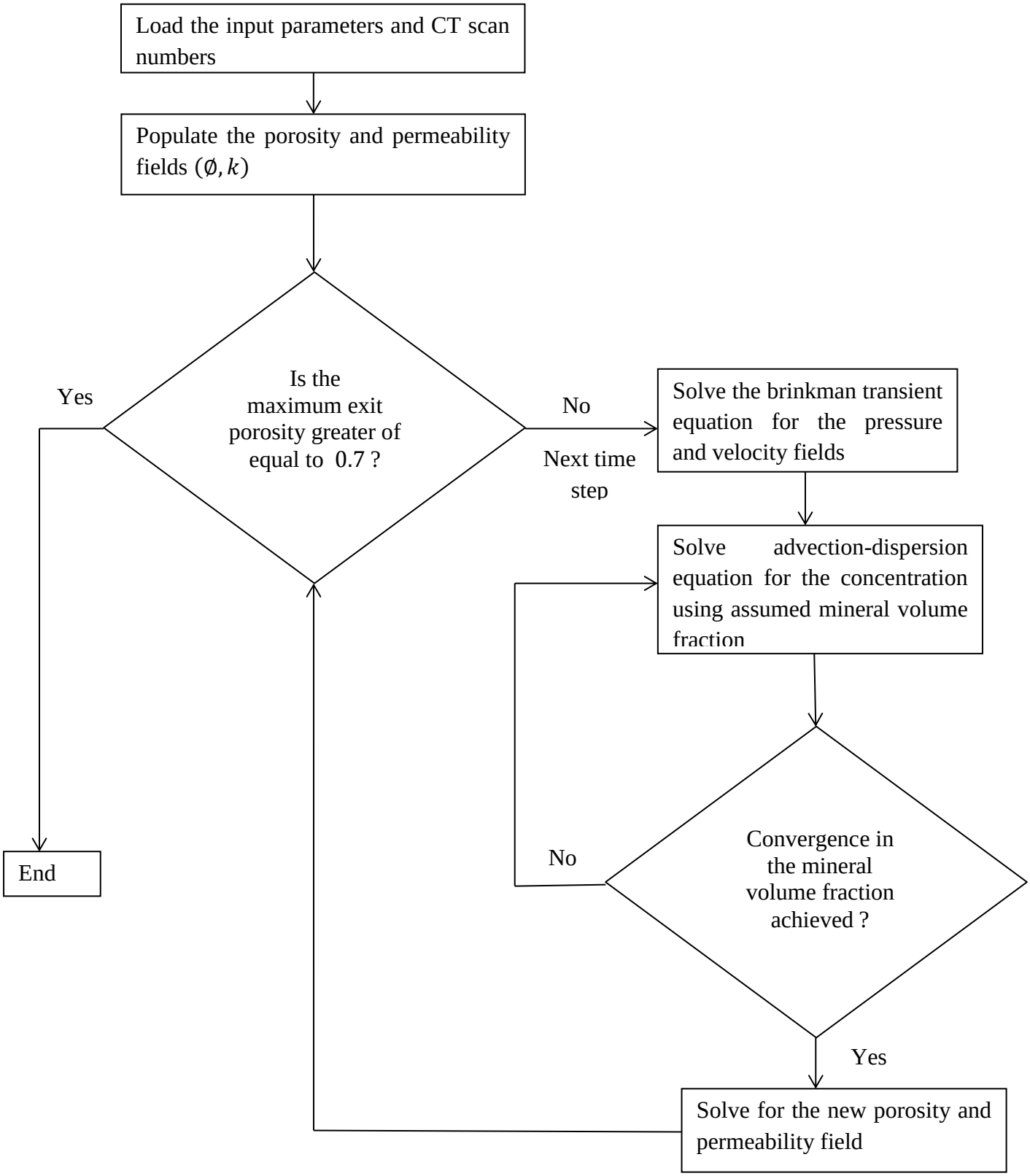

Figure 3-6: Flow chart of the MATLAB solution scheme

3.8 Data preparation for CT scan input

Experimental result is used validate the simulation. To compare the simulation result with that of the experiment, they must run on the same set of inputs. Every other input is readily available except the porosity and permeability fields. Therefore, this will require us to process images of CT scan of the core to determine the core porosity distribution.

3.8.1 Processing of CT Scan Images of Core

The CT scan images of the cores are available in the JPEG format. This has to be converted to the CT scan number which can be correlated with the porosity of the core.

3.8.1.1 RGB-CT scan Calibration

Image processing is any form of signal processing for which the input is an image, such as a photograph or video frame; the output of image processing may be either an image or a set of characteristics or parameters related to the image. Most image-processing techniques involve treating the image as a two-dimensional signal and applying standard signal-processing techniques to it. We develop an algorithm whose input files are series of CT scan images in jpeg format. This algorithm discretizes pictures according the number of grids we want for the simulation. It determines the mean red, green and blue numbers within each grid and converts those numbers to CT scan numbers. Doing this required us to pre-calibrate the algorithm with CT scan numbers generated by direct processing (or CT scan scale) with the CT scan machine. This calibration creates a set of

weights that applies to the red, green and blues numbers in other to convert them to CT scan numbers. We will then use the algorithm to generate the CT scan numbers and subsequently convert these into porosity and permeability fields.

The image of the CT scans of the core is read into the Matlab. This created and M by N by 3 block matrix. M and N represent the size (in pixels) of the picture and depth represent three layers of red, green and blue. The scale of CT-scan (see Figure 3-7) number provided with the picture is first processed to generate the correlation between RGB and the CT scan number.

Figure 3-7: CT-scan number scale

The combination of red, green and blue in every pixel of the scale is correlated with the CT scan number that ranges from -2000 to 3000 and this is validated in Figure 3-8 below.

$$CTscanNo = 51.8R + 5314.2G - 30.1B - 2046.4 \qquad (3.135)$$

R = red color scale of the scan read by MATLAB

G = green color scale of the scan read by MATLAB

B = blue color scale of the scan read by MATLAB

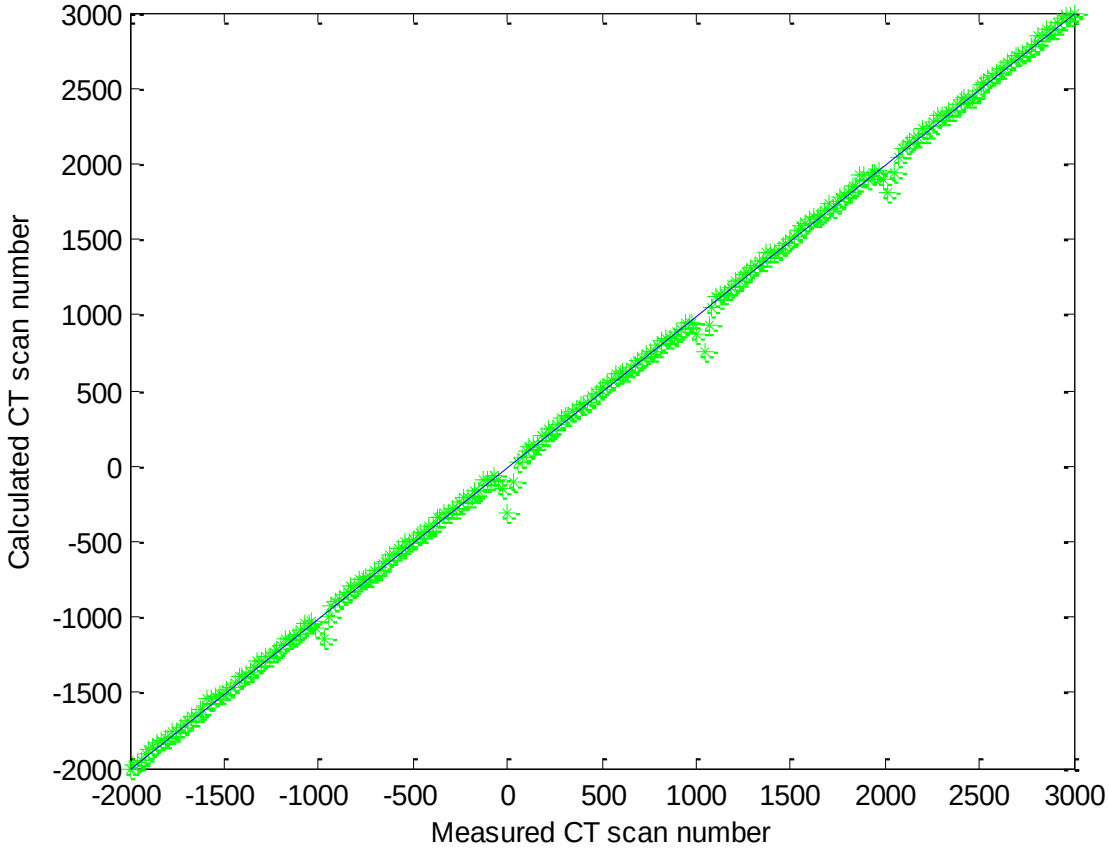

Figure 3-8: JPEG-CT-Scan number calibration validation graph

Note: the four even spaced depressions represent the white lines used in the graduation of the scale and are not part of the actual CT scan color variation.

3.8.1.2 JPEG-CT scan Conversion

The RGB-CT scan calibration is used to convert the entire pictures into mean CT scan numbers for each grid cell. First we develop a MATLAB code to identify the edges of the core in the CT scan images and then crop the images to a square shape that exactly encloses the circular cross section of the core see Figure 3-9 and Figure 3-10.

The cropped image is then discretized into 21 by 21 with the highest number of pixels in the middle and the lowest at the edge for cases where the number of pixels is not a multiple of 21.

The mean (2D) of the red, green and blue number is then evaluated and is used to evaluate the CT scan number for the grid. Since the grids that lie outside the circle are to be neglected we assign CT number of zero to those grids. And we evaluate the mean CT scan number for the porosity calibration as shown in Figure 3-11.

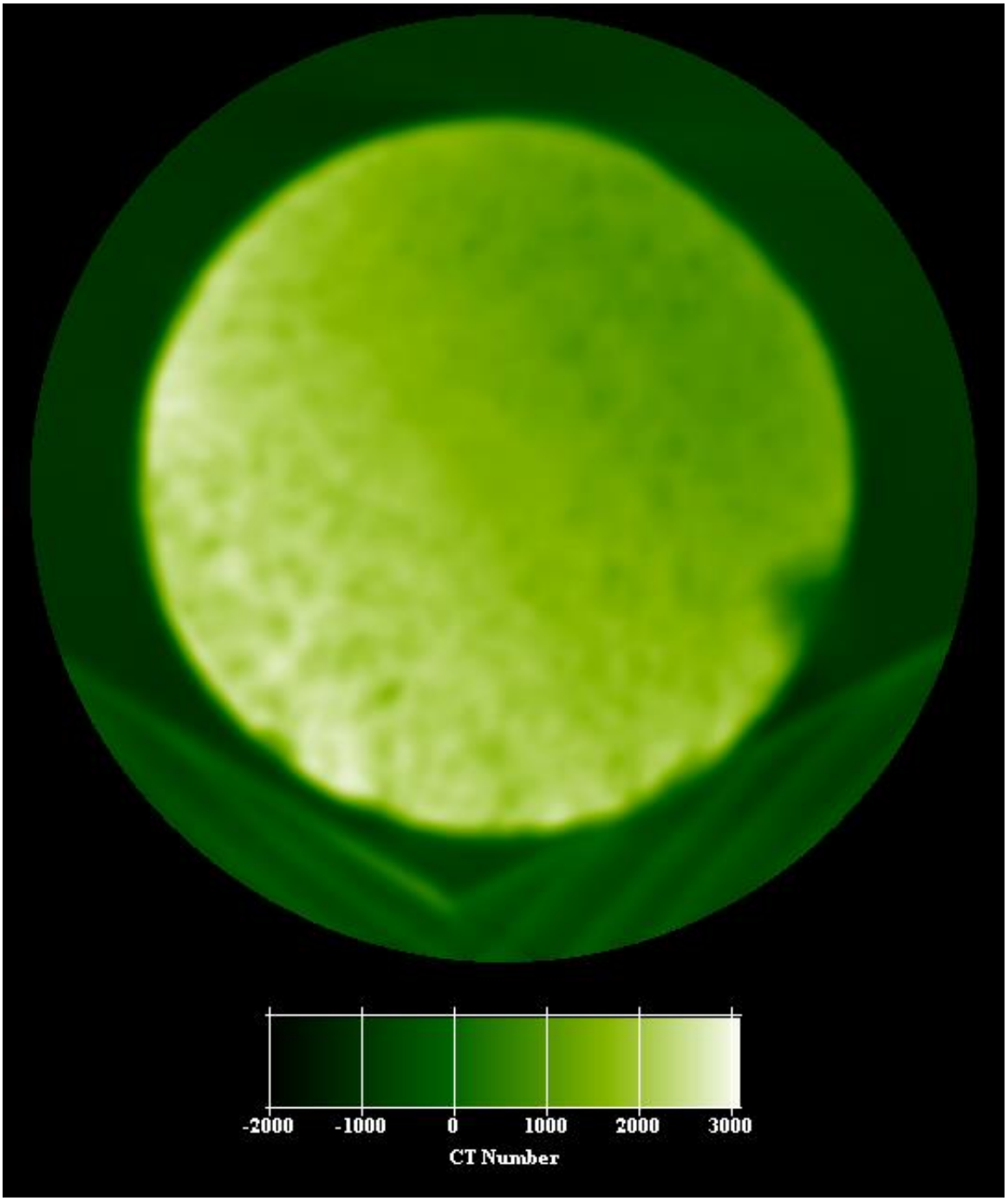

Figure 3-9: The CT scan image before cropping

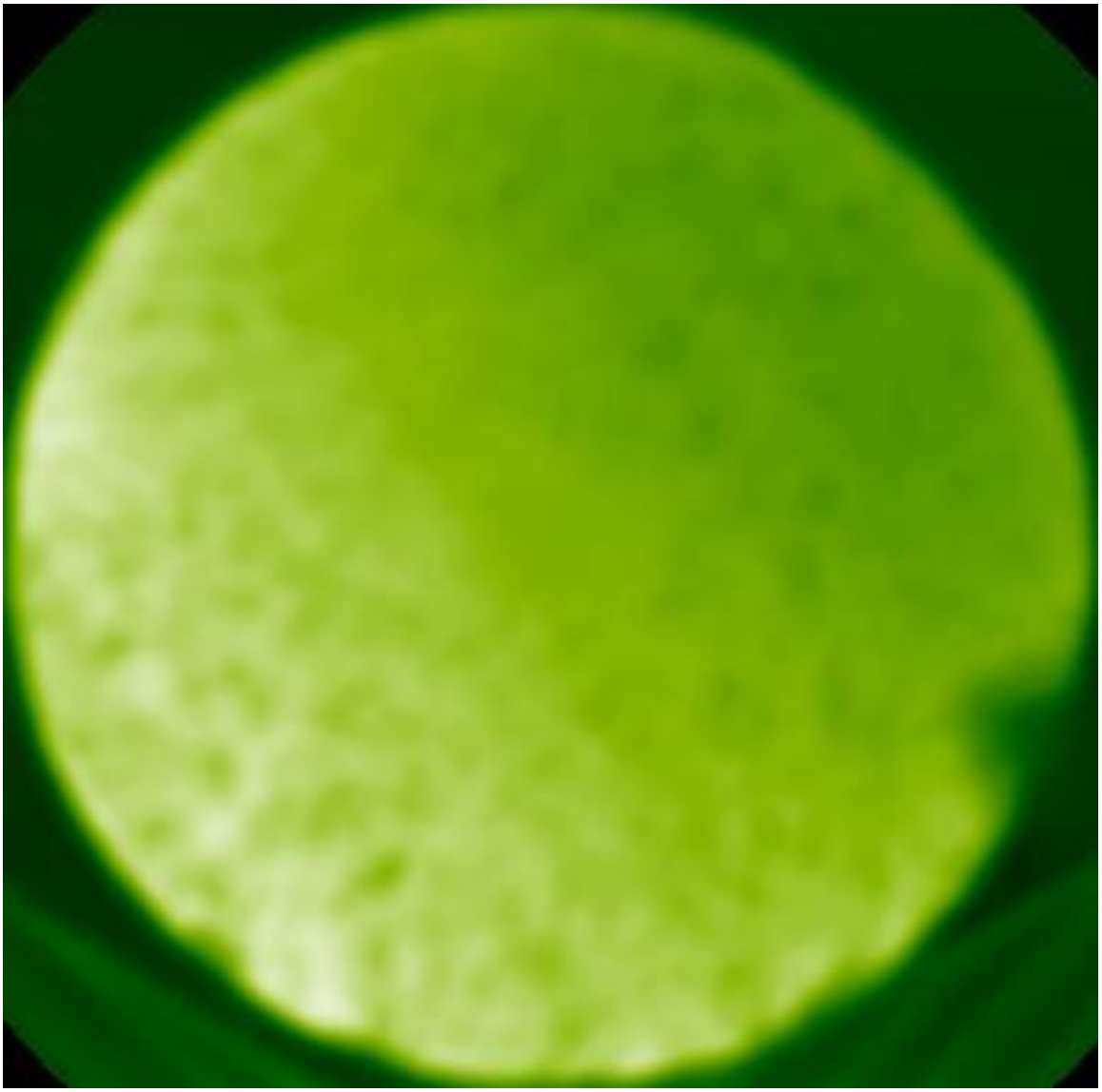

Figure 3-10: The cropped CT scan image

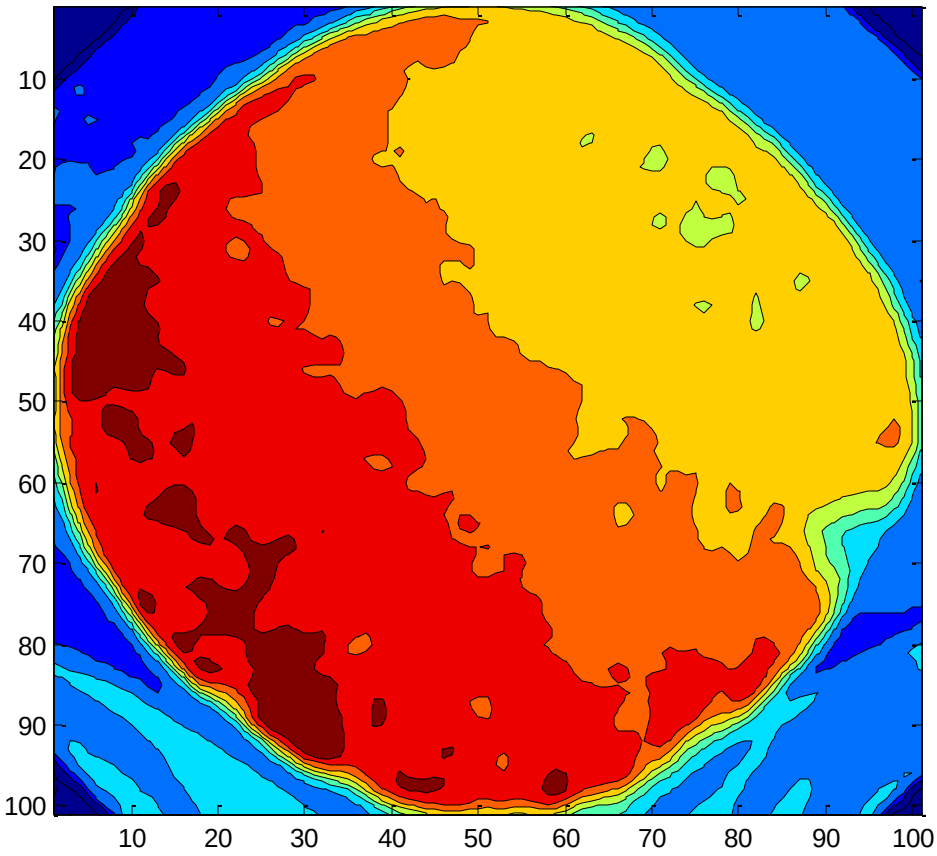

Figure 3-11: CT-scan number generated by the image processing algorithm (101 by 101)

3.8.1.3 CT scan number to porosity Calibration

To convert the CT scan number to porosity, we have to evaluate the constant of the linear relation for the core sample we are dealing with. The mean porosity and CT scan numbers for core are used.

$$\emptyset_i = a \times (CTscanNo)_i + b \tag{3.137}$$

The overall porosity for a core is thus

$$\emptyset = \frac{a}{N_g}\sum_{i=1}^{N_g}(CTscanNo)_i + b \tag{3.138}$$

Where

$$\frac{1}{N_g}\sum_{i=1}^{N_g}(CTscanNo)_i = mean\ CTscan\ number \tag{3.139}$$

Using the pre stimulation values of the CT-scans of core samples 10 11 12 13 14 and 15, we found

$$a = -0.000210687300734, \qquad b = 0.671525514086973$$

3.6.1.4 CT scan number to porosity Conversion

Initial porosity distribution each grid is calculated according the equation. Then we use the circular region criterion to ensure that the value for region outside the circle is set to 1

so that if any amount of acid gets outside, no reaction will occur since the value of $(1 - \emptyset)$ will be zero.

$$\emptyset = 0.671525514086973 - 0.000210687300734 \times CTscanNo \qquad (3.140)$$

An example of porosity distribution generated for the CT scan image of Figure 3-9 is shown in Figure 3-12 below.

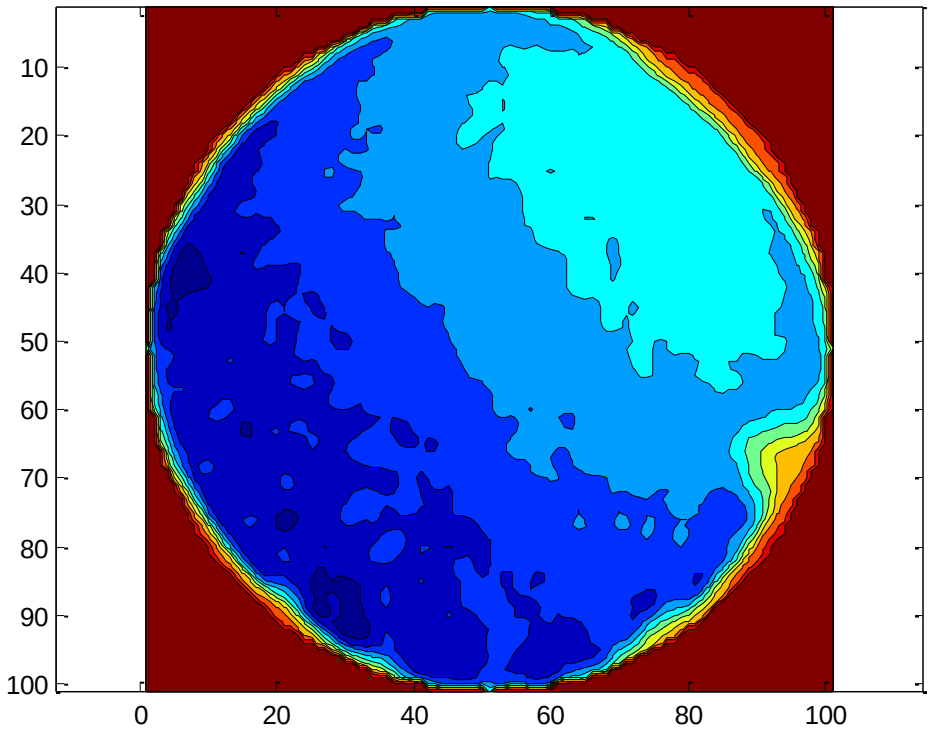

Figure 3-12: Porosity field generated using the calibration developed (101 by 101)

3.8.2 Re-characterization for initial permeability field.

There is no accurate means to predict the permeability distribution of the grids within the core. Hence to produce a permeability field with total permeability equal to that of the measured permeability of the core, we use the idea of congruent resistive networks shown in Figure 3-13. Two resistive networks are said to be congruent if the ratio of resistance of every resistor R_{Ai} in network A to that of a corresponding resistor R_{Bi}in network B is constant. For these networks, the potentials at any two corresponding nodes maintain the same ratio as the resistors as shown in Figure 3-14. This idea uses the fact that current through corresponding branches of two congruent networks are the same when the same amount of current is supplied from corresponding points even if the resistors on the corresponding branches are not the same.

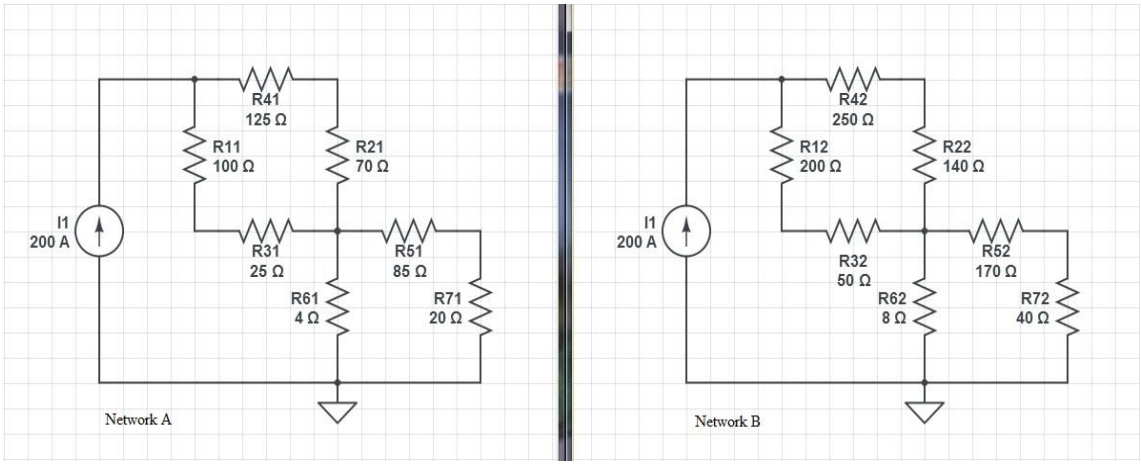

Figure 3-13: Two Congruent networks

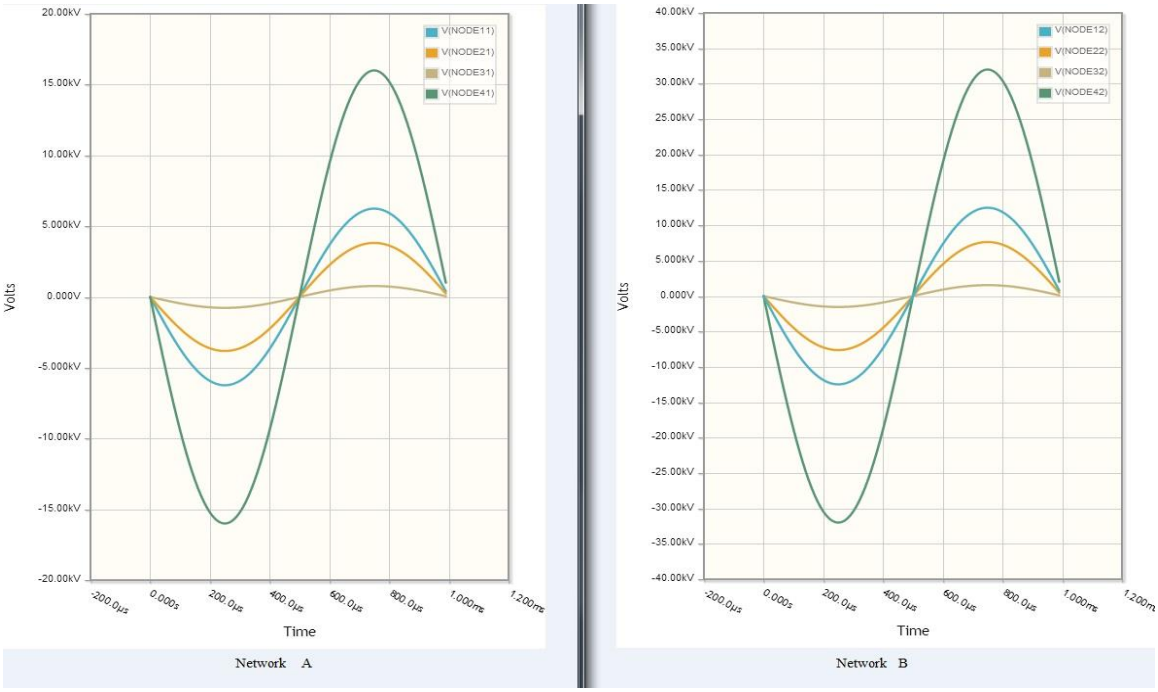

Figure 3-14: Potentials at the four identical locations on the two networks

To use this idea to populate the permeability field of the core, we use the following simple procedure;

1. Use a simple correlation to generate the permeability distribution.

$$k = \exp\big(M(\emptyset - \emptyset_0)\big) - \exp(-M\emptyset_0) \tag{3.141}$$

Where $\emptyset_0$ is the mean porosity and M is the connectivity-cementation constant for the core.

But since M is positive and reasonably large, we can neglect the second term, hence

$$k \approx \exp\big(M(\emptyset - \emptyset_0)\big) \tag{3.142}$$

The connectivity-cementation constant is a key parameter in determining the permeability field. It determines the order of the value of the permeability with is has a mean value of 10^4 millidarcy for the porous medium and 10^9 millidarcy for fracture or wormholes.

The grid transforms completely from conventional porous medium into a wormhole when the porosity hits the body center packing factor of $\pi/6$ or 0.5236, hence we evaluate M using the mean porosity of the core as

$$M = \begin{cases} \dfrac{\ln(10^4)}{(0.5236 - \emptyset_0)} & \emptyset < 0.5236 \qquad (porous\ medium) \\ \dfrac{\ln(10^9)}{(1.0000 - \emptyset_0)} & \emptyset \geq 0.5236\ (fracture\ or\ wormhole) \end{cases} \tag{3.143}$$

2. Run a single phase core flood simulation using the steady state diffusivity equation.
3. Evaluate the overall permeability using Darcy equation.
4. Evaluate the scale factor using

$$\alpha_k = \frac{Measured\ permeability}{Calculated\ permeability} \tag{3.143}$$

5. Correct the permeability field using

$$K = \alpha_k \times \exp\big(M(\emptyset - \emptyset_0)\big) \tag{3.144}$$

Note: This correction factor α_k is a geometrical parameter and is a function of grain size distribution and packing.

4. CHAPTER 4

RESULTS AND DISCUSSION

4.1 Wormhole from randomly generated porosity field input

The result of simulation for randomly generated porosity field with specific mean porosity and heterogeneity values is presented in **Error! Reference source not found.** hile that of porosity generated from CT scan number is shown in Figure 4-2 to Figure 4-8

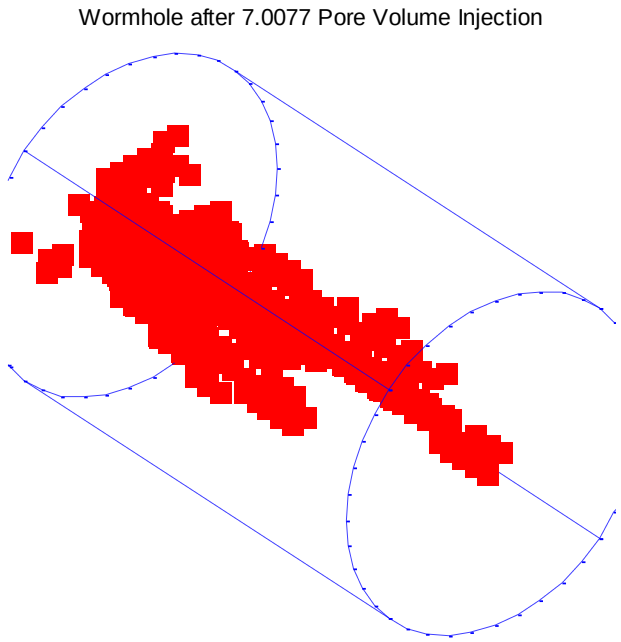

Figure 4-1: Wormhole generated at breakthrough for a randomly generated porosity distribution (1cc/min)

4.2 Results for porosity field generated from CTscan of core 15

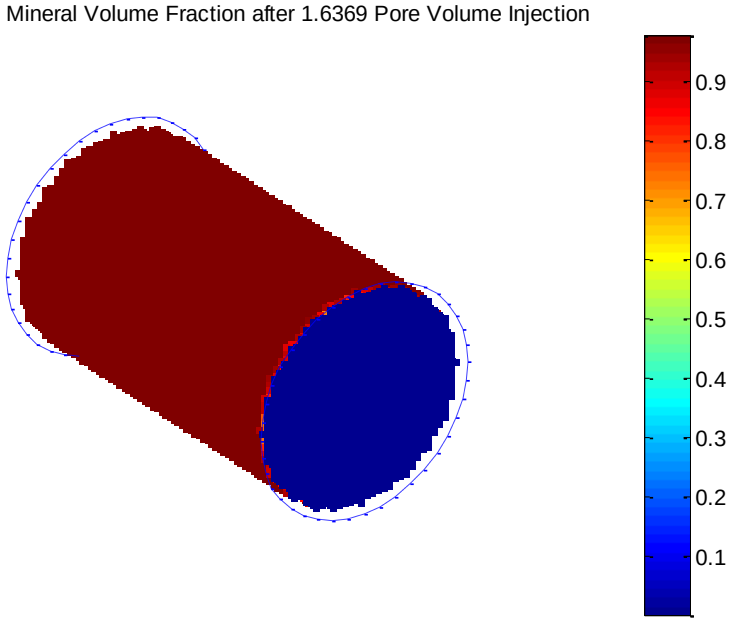

Figure 4-2: Mineral Volume Fraction distribution of core 15 at 1.6369 breakthrough pore volume injection (rate of injection 1 cc/min)

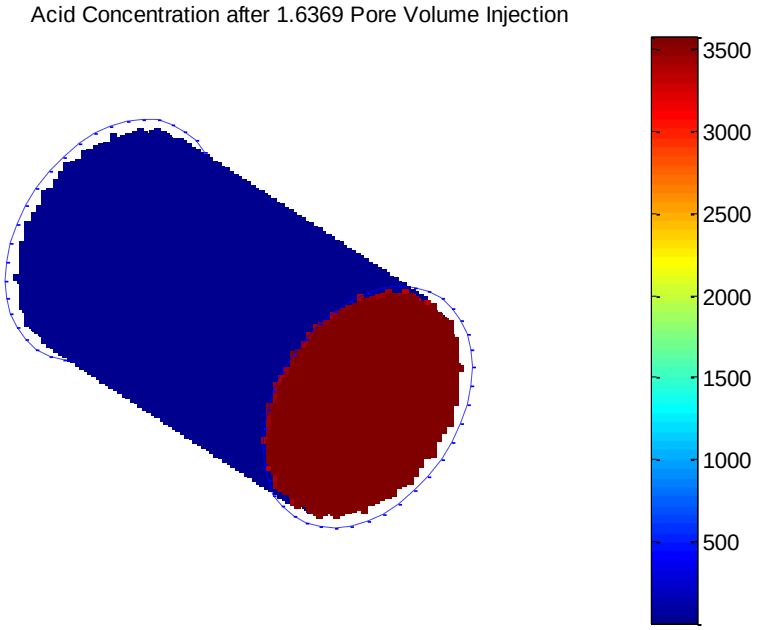

Figure 4-3: Acid Concentration distribution of core 15 at 1.6369 breakthrough pore volume injection (rate of injection 1 cc/min)

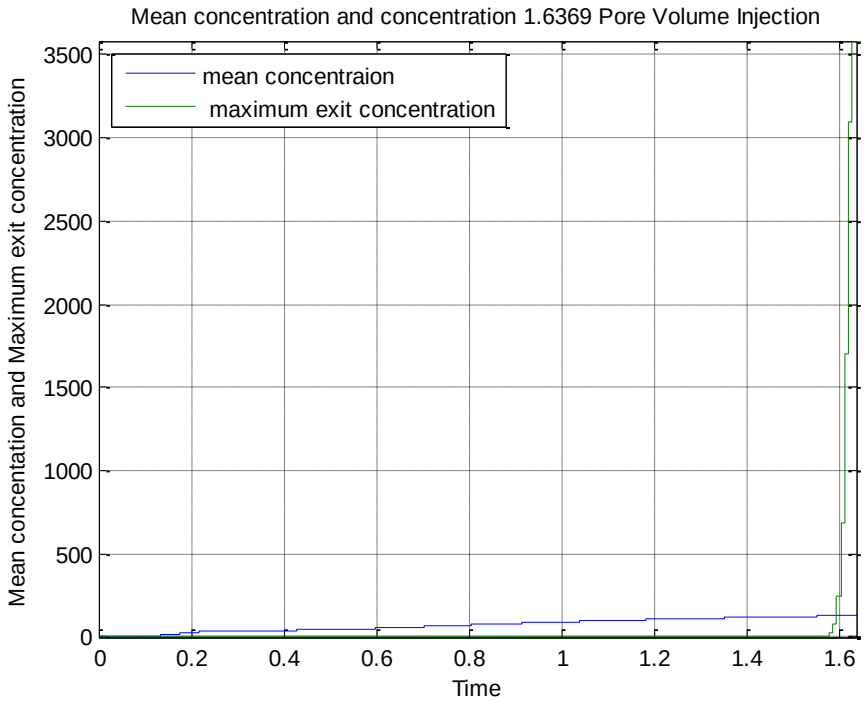

Figure 4-4: Mean acid concentration and maximum effluent concentration of core at 1.6369 breakthrough pore volume injection (rate of injection 1 cc/min)

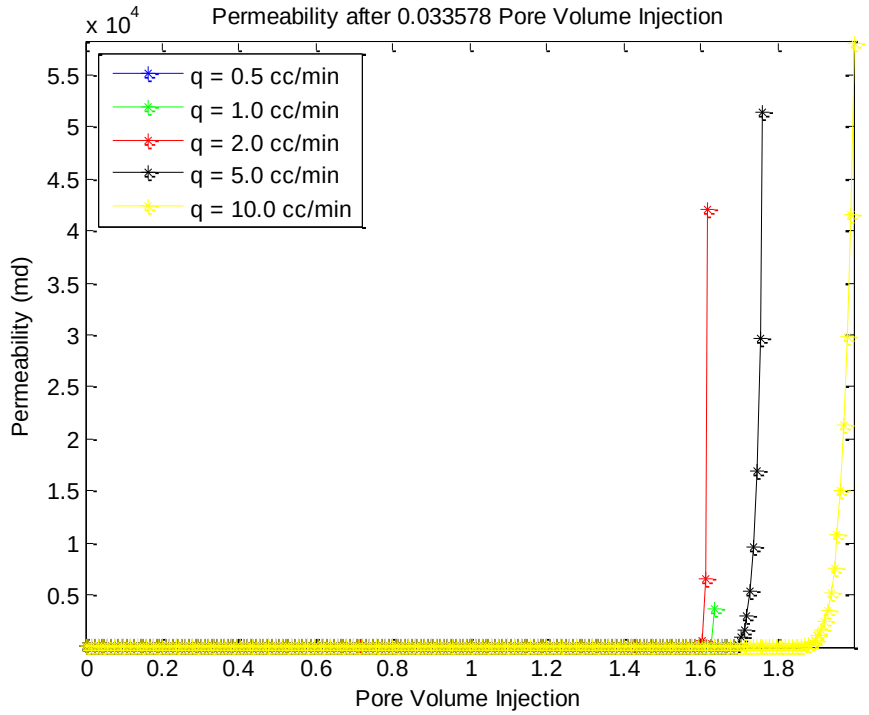

Figure 4-5: Permeability change of core 15 at different injection rates

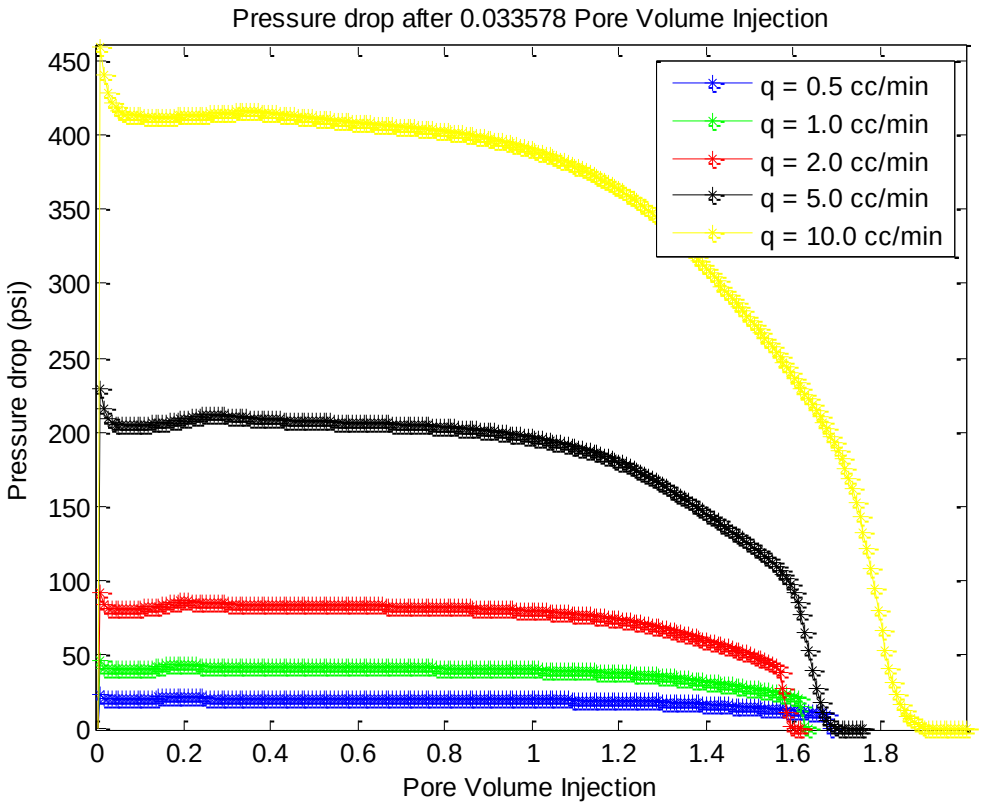

Figure 4-6: Pressure drop change of core 15 at different injection rates

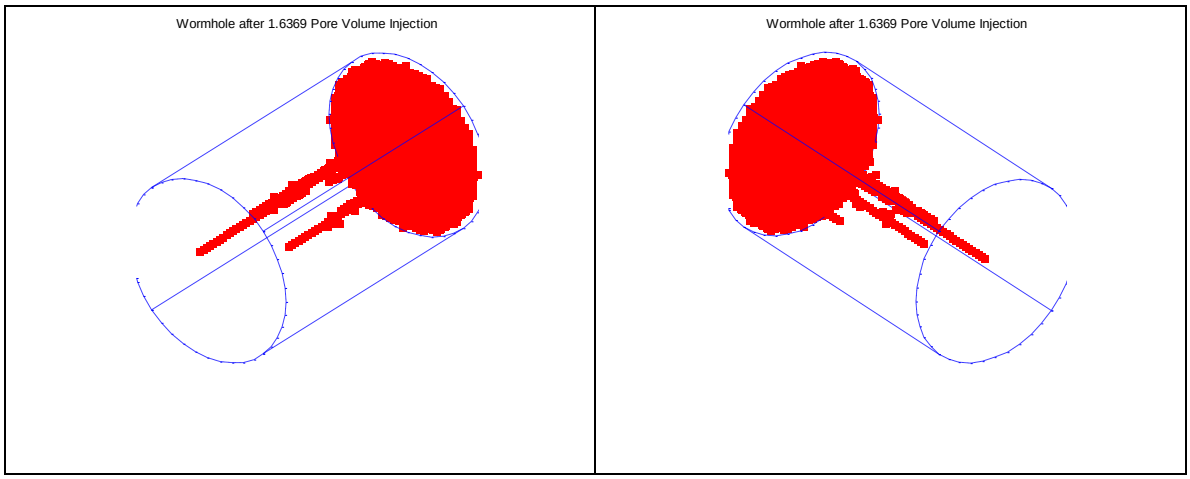

Figure 4-7: Two oblique views of wormhole at breakthrough for core 15 (1 cc/min)

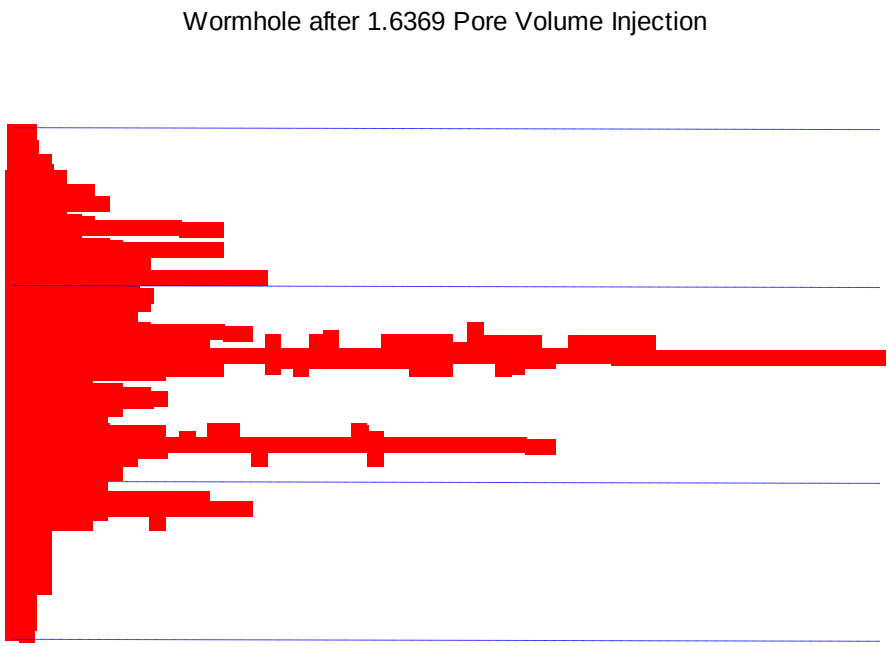

Figure 4-8: Side view of wormhole at breakthrough for core 15 (1 cc/min)

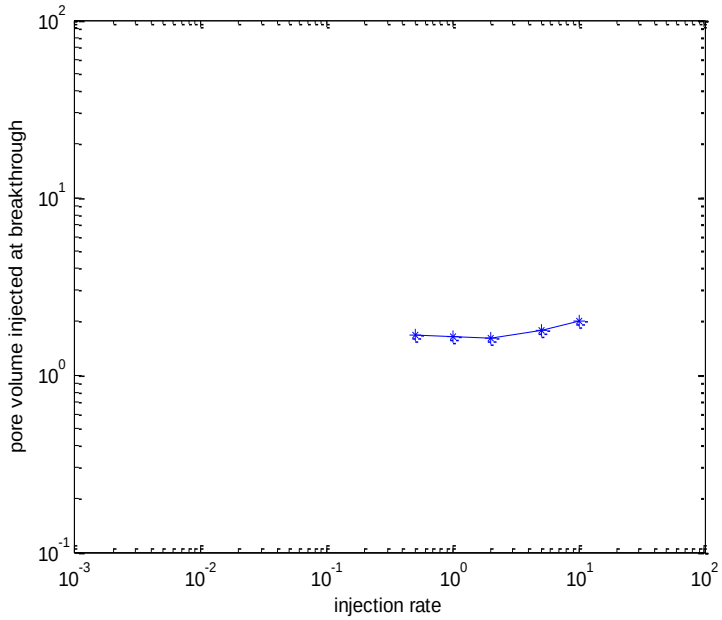

Figure 4-9: Acidization curve-Pore volume injected to breakthrough for core 15 at different injection rates (Simulation)

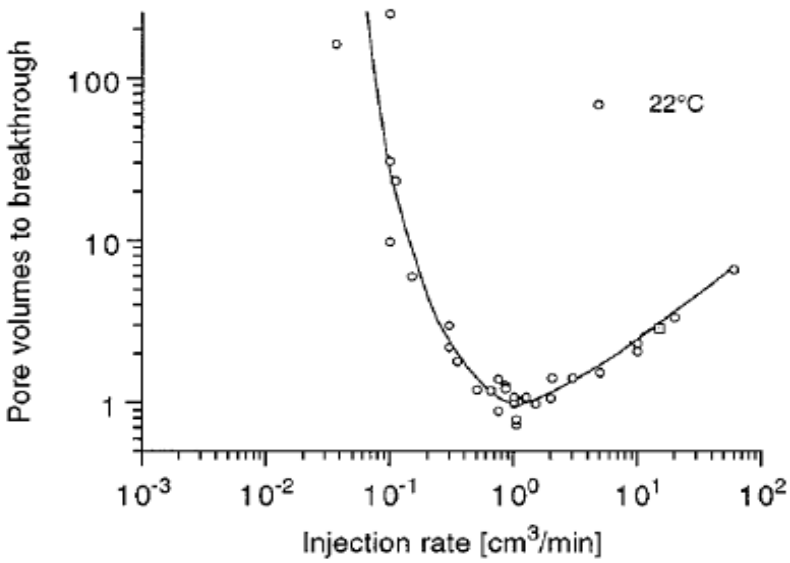

Figure 4-10: Acidization curve-Pore volume injected to breakthrough at different injection rates (Experiment) Fredd and Fogler [3]

Simulation of wormhole in a cylindrical core requires the use of grids that lies within the boundary of the circle of the cylinder. The rectangular grid size of 37 by 37 by 61 was used in the simulation. Taking out the high porosity grids on the boundaries of the circle translates to 901 cross sectional on the circular cross section, against 1369 grids on the square cross section. Hence a total of 54961 grids are used in the simulation.

The Figure 4-2 shows the mineral volume distribution of core 15 at breakthrough for 1 cc/min rate of injection. By comparing the mineral volume fraction distribution after the same pore volume injected for different rate of injection, it can be shown that there is reduction in the face dissolution with increased rate of injection (Damkholer number decrease). The plot of the pore volume injection to breakthrough in excellent agreement with experimental observation by Fredd and Fogler [3] shows the minimum pore volume injection (1.24) to breakthrough occurred at 2cc/min rate of injection for local transfer rate constant of $5 \times 10^{-10}/s$.

Figure 4-3 show the acid concentration distribution of core 15 at breakthrough for 1 cc/min rate of injection. The figures show low concentration at the locations having high mineral volume fraction which is in agreement with decrease in the rate of acid consumption with the mineral volume fraction.

Figure 4-4 shows the mean concentration in the core and maximum effluent concentration with time (pore volume injection). It is observed that the concentration is mass transfer controlled as the mean concentration remain virtually zero at high Damkholer number and gradually increases with injection rate (fall in Damkholer number). The maximum effluent concentration climbed suddenly at breakthrough for

high Damkholer numbers (low injection rate) while the rise was gradual in the case of high injection rate. Also the core at breakthrough is known to have some amount of life acid left in it at breakthrough, and hence the gradual rise of the mean acid concentration to the non-zero final value at breakthrough.

The permeability and pressure drop variation plots in Figure 4-5 and Figure 4-6 respectively show pressure drop remain literarily unchanged in during the first half of the simulation time, then falls gradually for some time before acceleration towards zero from about 90% of the simulation time until is almost zero at break through while the permeability remains virtually unchanged until it a sudden 100 folds jump at breakthrough. It can be seen that the red plot shows the earliest permeability jump which signals where the breakthrough occurred when we injected at a rate of 2 cc/min.

The Figure 4-7 and Figure 4-8 show different (2 isometric and one side views) of wormhole generated at breakthrough for the rate of injection used. By comparing with similar figure for other rate of injection we can show that the competition between the dominant wormhole and the second worm hole is less pronounced at low injection rate while the propagation of the second wormhole grows as the rate of injection increases above (or fall below) the optimum 2cc/min.

The breakthrough pore volume injected for the 5 rates of injection are compared with the experimental observation in Figure 4-9 and Figure 4-10 is in agreement with experimental observation. The deviation can be explained from the fact that in the experiment, it is impossible to use exactly the same core twice, and so the core used in

the experiments does not have exactly the same porosity distribution and permeability as used in the simulation.

4.3 Comparison of slices of simulated result with the corresponding experimental results

Table 4-1: Comparison of slices of simulated result with the corresponding experimental results

Distance from injection face (inches)	CT scan of specimen core 15	Simulation of core 15
0.24	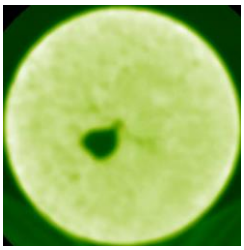	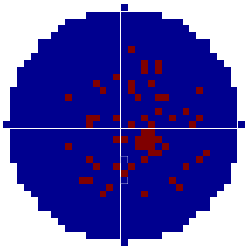
0.48	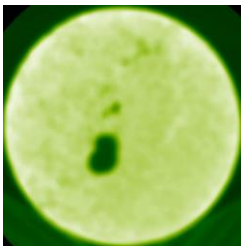	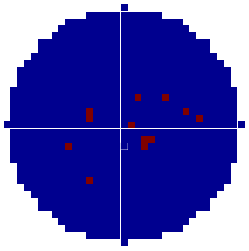
0.72	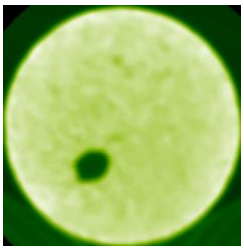	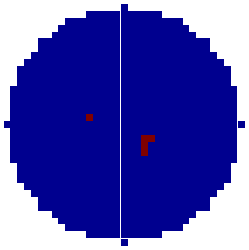

0.96	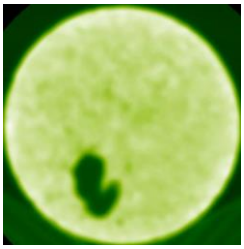	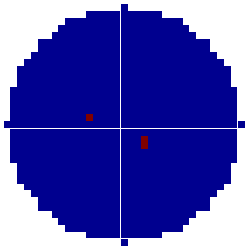
1.2	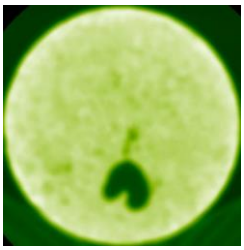	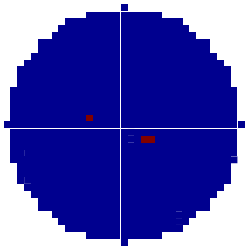
1.44	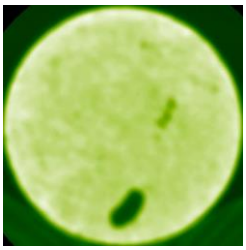	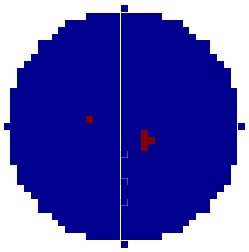
1.68	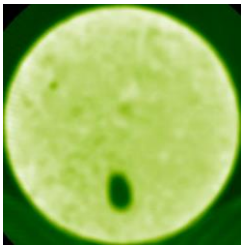	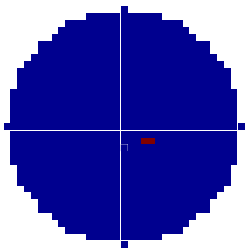
1.92	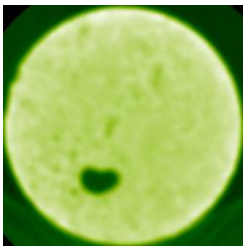	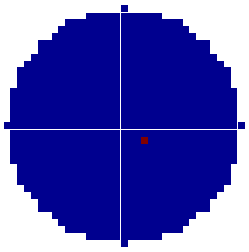

2.16	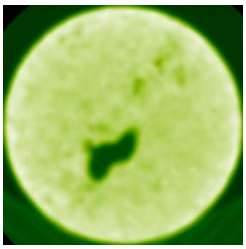	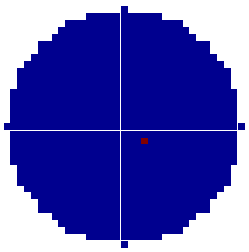
2.4	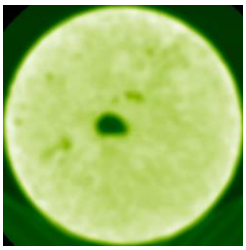	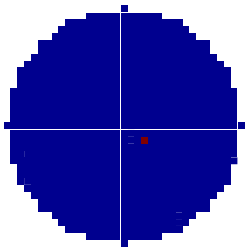

Error! Reference source not found. shows the comparison, between the sections of the ore generated by the simulation and the actual experiment. It should be noted however that seemingly bigger hole in the experiment is due to the fact that the experiment was not terminated exactly after breakthrough at 2.4 inches (as it is the case with the simulation) due to the longer length of the core (12 inches) used in the experiment. The difference in the orientation of core during pre-acidization and post acidization scan is also responsible for the mismatch of the simulation and experimental result. This is so because the pre stimulation scan of the core is the input that provided the porosity and permeability field used in the simulation.

4.4 Comparison of simulation with different local mass transfer coefficient results

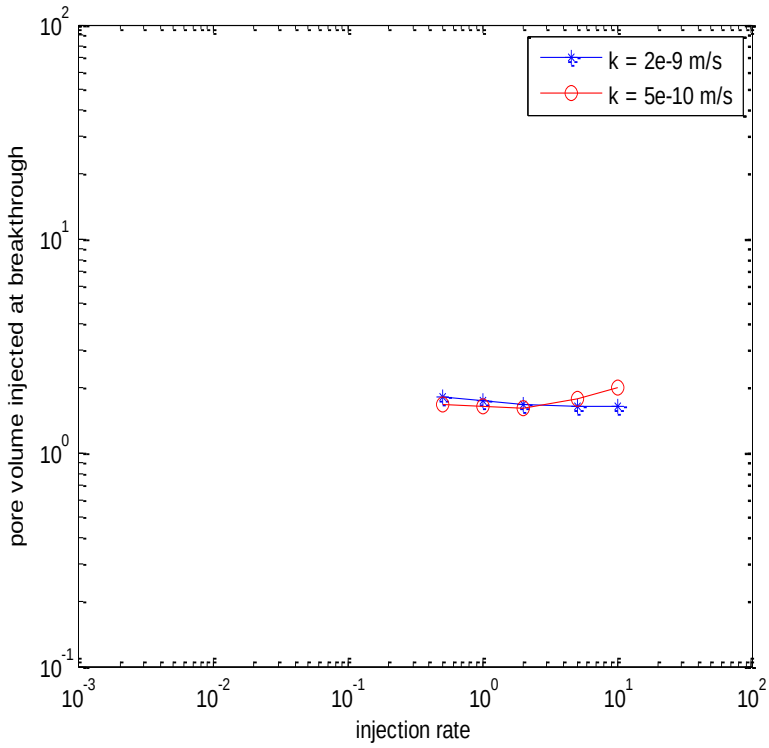

Figure 4-11: Portion of acidization curve for different local mass transfer coefficient

Figure 4-11 shows a partial acidization curve we got running the simulation with 300% increase in the local mass transfer coefficient $(2 \times 10^{-9}/s)$. A shift in the optimum injection rate for the lowest pore volume injection to breakthrough was observed. The increase in the optimum injection rate happened despite an almost constant pore volume injection to breakthrough. This result is interesting because it provides that at optimum injection rate, the path of the acid and the amount of mineral dissolved is the same even if the rate of dissolution as controlled by the mass transfer from the bulk of the acid to the surface for reaction is different.

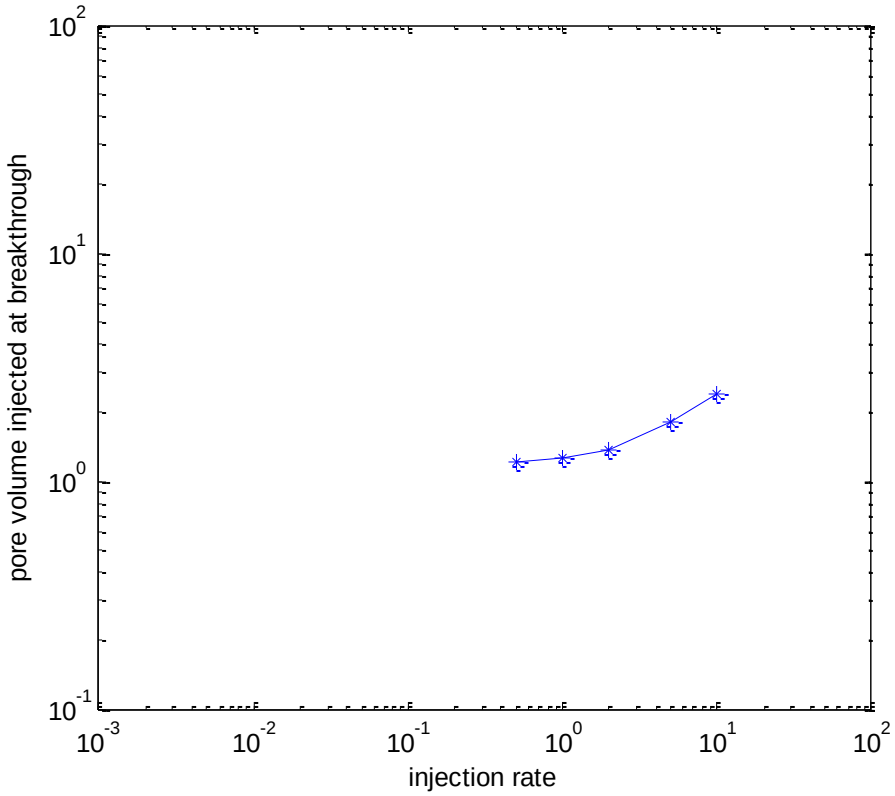

Figure 4-12: Acidization curve for core 12

Finally, looking the result (acidization curve-Figure 4-12) we obtained for core 12 which originally has a lower permeability than core 15, we can conclude that the breakthrough pore volume injection is also affected by the initial permeability of the core sample. The lower the original permeability of the sample, the higher the pore volume injection required to achieve breakthrough. It is also important to note that the optimum injection rate reduces with reduces original permeability of the sample.

5. CHAPTER 5

CONCLUSION

The main contributions of this work are:

1. The solution of transient brinkman equation for circular boundary in a rectangular coordinate system
2. The development of a 2 permeability function model for matrix and fracture permeability
    - The sudden rise in permeability or fall in the pressure drop observed at breakthrough is due to discontinuity in the permeability function. Hence the use of two different permeability functions
3. Permeability re-characterization for the grid permeability field for the core
    - The use of this method of generating the initial permeability field ensures that the overall permeability of the core being simulated is exactly the same as that of the real core.
4. Study of the pore volume injection to breakthrough for different injection rate
    - The breakthrough pore volume injection is proportional to the cube root of the injection rate when the rate is higher than the optimum and approaches and asymptote that corresponds to complete rock dissolution at very low injection rates
5. The use of the mean core acid concentration and maximum effluent acid concentration during stimulation.

- The mean concentration can be used to determine it the acid mineral interaction is reaction controlled of mass transferred controlled. It mass transfer controlled if the mean core and maximum effluent acid concentration remains very low throughout until breakthrough, but is reaction controlled if the two parameters are high.

6. Understanding of wormhole competition.

- It is observed that the competition between the dominant wormhole and the second worm hole is less pronounced at optimum injection rate while the propagation of the second wormhole grows as the rate of injection increases above (or fall below) the optimum 2cc/min.
- Once the breakthrough has occurred, the growth of the less dominant wormholes is stalled as all the acids continue to go through the dominant wormhole that has already broken through.
- It is also observed that a change in the local mass transfer coefficient result in a shift of the acidization curve but a change in the pore volume to breakthrough was not observed for the range of values of injection rates used in the simulation
- It is also found that the initial permeability affects the pore volume injection to breakthrough in an inverse relationship. The lower the initial permeability, the larger the pore volume injection required to breakthrough but the optimum occurred at a lower injection rate.

References

1. Hung, K.M., Hill, A.D.: A Mechanistic Model of Wormhole Growth in Carbonate Matric Acidizing and Acid Fracturing, (1989).

2. Economedes, M.: Petroleum Production Systems, (1994).

3. Fredd, C.N., Fogler, H.S., Michigan, U.: Optimum Conditions for Wormhole Formation in Carbonate Porous Media : Influence of Transport and Reaction. (1999).

4. Pichler, T., Frick, T.P., Economides, M.J., Leoben, M.U., Nittmann, J.: SPE 25004 Stochastic Modeling of Wormhole Growth in Carbonate Acidizing With Biased Randomness. (1992).

5. Gong, M.: SPE 52165 Quantitative Model of Wormholing Process in Carbonate Acidizing. (1999).

6. Jian-Yang, Y., Bernard, T., Alex, B.: A Wormhole Network Model of Cold Production in Heavy Oil. Proceedings of International Thermal Operations/Heavy Oil Symposium. (1999).

7. Fredd, C.N.: SPE 59537 Dynamic Model of Wormhole Formation Demonstrates Conditions for Effective Skin Reduction During Carbonate Matrix Acidizing. (2000).

8. Golfier, F., Bazin, B., Zarcone, C., Lernormand, R., Lasseux, D., Quintard, M.: Acidizing Carbonate Reservoirs: Numerical Modelling of Wormhole Propagation and Comparison to Experiments. Proceedings of SPE European Formation Damage Conference. 1–11 (2001).

9. Buijse, M., Glasbergen, G.: A Semiempirical Model To Calculate Wormhole Growth in Carbonate Acidizing. Proceedings of SPE Annual Technical Conference and Exhibition. (2005).

10. Gdanski, R.: SPE 54719 A Fundamentally New Model of Acid Wormholing in Carbonates. (1999).

11. Panga, M., Ziauddin, M., Gandikota, R., Balakotaiah, V.: A New Model for Predicting Wormhole Structure and Formation in Acid Stimulation of Carbonates. Proceedings of SPE International Symposium and Exhibition on Formation Damage Control. 1, 1–11 (2004).

12. Izgec, O., Zhu, D., Hill, A.D., Texas, A.: SPE 122357 Models and Methods for Understanding of Early Acid Breakthrough Observed in Acid Core-floods of Vuggy Carbonates. 1969, (2009).

13. Xiaogang, L., Jie, T., Zhaozhong, Y.: Simulation of Wormhole in Carbonate Acidizing Using a New Diffusion Limited Aggregation Model. 2010 International Conference on Computational and Information Sciences. 340–343 (2010).

14. Smirnov, a. S., Fedorov, K.M., Shevelev, a. P.: Modeling the acidizing of a carbonate formation. Fluid Dynamics. 45, 779–786 (2010).

15. Mcduff, D., Jackson, S., Shuchart, C., Postl, D., Upstream, E.: Understanding Wormholes in Carbonates : Unprecedented Experimental Scale and 3D Visualization. 78–81 (2010).

16. Huang, T., Hill, A.D., Schechter, R.S., Texas, U.: Reaction Rate and Fluid Loss : The Keys to Wormhole Initiation and Propagation in Carbonate Acidizing. 287–292 (2000).

17. Daccord, G., Touboul, E., Lenormand, R., Schlumberger, D.: Carbonate Acidizing : Toward a Quantitative Model of the Wormholing Phenomenon. 63–68 (1989).

18. Fredd, C.N., Miller, M.J.: Validation of Carbonate Matrix Stimulation Models. Proceedings of SPE International Symposium on Formation Damage Control. (2000).

19. Yuan, J., Babchin, a., Tremblay, B.: Modelling Wormhole Flow in Cold Production. Journal of Canadian Petroleum Technology. 39, (2000).

20. Istchenko, C.M., Gates, I.D.: The Well-Wormhole Model of Cold Production of Heavy Oil Reservoirs Cold Production Models. (2011).

21. Rege, S.D., Fogler, H.S.: Competition among flow, dissolution, and precipitation in porous media. AIChE Journal. 35, 1177–1185 (1989).

22. Maheshwari, P., Balakotaiah, V.: 3-D Simulation of Carbonate Acidization with HCl: Comparison with Experiments. (2013).

23. Panga, M., Balakotaiah, V., Ziauddin, M.: Modeling, Simulation and Comparison of Models for Wormhole Formation during Matrix Stimulation of Carbonates. Proceedings of SPE Annual Technical Conference and Exhibition. 2, 1–19 (2002).

24. Kale*, D., Mattar, L.: Solution of a Non-linear Gas Flow Equation By the Perturbation Technique. Journal of Canadian Petroleum Technology. 63–67 (1980).

25. Johnson, R.L.: Iterative Solution of Large Non linear Systems. Society for Industrial and Applied Mathematics. 5, 236–237 (1968).

Appendix

Content of the center grid block in the hepta-diagonal system

$T_{mm-NyNz} + BT_{mm-NyNz}$	$T_{mm-Nz} + BT_{mm-Nz}$	$T_{mm-1} + BT_{mm-1}$	0
$\mu\left(T^2_{mm-NyNz} + \frac{BT^2_{mm-NyNz}}{2}\right) + \mu\left(T^2_{mm-Nz} + \frac{BT^2_{mm-Nz}}{2}\right) + \mu\left(T^2_{mm-1} + \frac{BT^2_{mm-1}}{2}\right) + \mu\left(T^2_{mm+1} + \frac{BT^2_{mm+1}}{2}\right) + \mu\left(T^2_{mm+Nz} + \frac{BT^2_{mm+Nz}}{2}\right) + \mu\left(T^2_{mm+NyNz} + \frac{BT^2_{mm+NyNz}}{2}\right) + \frac{\mu}{k^n_{xx,m}} + \frac{\rho_A}{\Delta t}$	0	0	$-T_{mm-NyNz} - BT_{mm-NyNz}$
0	$\mu\left(T^2_{mm-NyNz} + \frac{BT^2_{mm-NyNz}}{2}\right) + \mu\left(T^2_{mm-Nz} + \frac{BT^2_{mm-Nz}}{2}\right) + \mu\left(T^2_{mm-1} + \frac{BT^2_{mm-1}}{2}\right) + \mu\left(T^2_{mm+1} + \frac{BT^2_{mm+1}}{2}\right) + \mu\left(T^2_{mm+Nz} + \frac{BT^2_{mm+Nz}}{2}\right) + \mu\left(T^2_{mm+NyNz} + \frac{BT^2_{mm+NyNz}}{2}\right) + \frac{\mu}{k^n_{yy,m}} + \frac{\rho_A}{\Delta t}$	0	$-T_{mm-Nz} - BT_{mm-Nz}$
0	0	$\mu\left(T^2_{mm-NyNz} + \frac{BT^2_{mm-NyNz}}{2}\right) + \mu\left(T^2_{mm-Nz} + \frac{BT^2_{mm-Nz}}{2}\right) + \mu\left(T^2_{mm-1} + \frac{BT^2_{mm-1}}{2}\right) + \mu\left(T^2_{mm+1} + \frac{BT^2_{mm+1}}{2}\right) + \mu\left(T^2_{mm+Nz} + \frac{BT^2_{mm+Nz}}{2}\right) + \mu\left(T^2_{mm+NyNz} + \frac{BT^2_{mm+NyNz}}{2}\right) + \frac{\mu}{k^n_{zz,m}} + \frac{\rho_A}{\Delta t}$	$-T_{mm-1} - BT_{mm-1}$

Vitae

Name	:Lateef A. Kareem
Nationality	:Nigerian
Date of Birth	:11/17/1985
Email	:talk2laton@gmail.com
Permanent Address	:9 Coker Street Mosafejo Amukoko, Lagos, Nigeria
Academic Background	:BSc (2007) Petroleum Engineering, FUTO, Nigeria